Pacific Northwest
NATIONAL LABORATORY

PNNL-39858

Site-Specific Design Case Study for Municipal Solid Waste (MSW) to Sustainable Aviation Fuel (SAF) via Plasma Gasification and Olefin Oligomerization

October 2026

Francesca Pierobon
Dilara Göreke
Shuang Xu
Yuan Jiang
Steven Phillips
Udishnu Sanyal
Karthi Ramasamy

U.S. DEPARTMENT of ENERGY

Prepared for the U.S. Department of Energy
under Contract DE-AC05-76RL01830

DISCLAIMER

This report was prepared as an account of work sponsored by an agency of the United States Government. Neither the United States Government nor any agency thereof, nor Battelle Memorial Institute, nor any of their employees, makes **any warranty, express or implied, or assumes any legal liability or responsibility for the accuracy, completeness, or usefulness of any information, apparatus, product, or process disclosed, or represents that its use would not infringe privately owned rights**. Reference herein to any specific commercial product, process, or service by trade name, trademark, manufacturer, or otherwise does not necessarily constitute or imply its endorsement, recommendation, or favoring by the United States Government or any agency thereof, or Battelle Memorial Institute. The views and opinions of authors expressed herein do not necessarily state or reflect those of the United States Government or any agency thereof.

PACIFIC NORTHWEST NATIONAL LABORATORY
operated by
BATTELLE
for the
UNITED STATES DEPARTMENT OF ENERGY
under Contract DE-AC05-76RL01830

Printed in the United States of America

Available to DOE and DOE contractors from
the Office of Scientific and Technical Information,
P.O. Box 62, Oak Ridge, TN 37831-0062
www.osti.gov
ph: (865) 576-8401
fax: (865) 576-5728
email: reports@osti.gov

Available to the public from the National Technical Information Service
5301 Shawnee Rd., Alexandria, VA 22312
ph: (800) 553-NTIS (6847)
or (703) 605-6000
email: info@ntis.gov
Online ordering: http://www.ntis.gov

PNNL-39858

Site-Specific Design Case Study for Municipal Solid Waste (MSW) to Sustainable Aviation Fuel (SAF) via Plasma Gasification and Olefin Oligomerization

October 2026

Francesca Pierobon
Dilara Göreke
Shuang Xu
Yuan Jiang
Steven Phillips
Udishnu Sanyal
Karthi Ramasamy

Prepared for
the U.S. Department of Energy
under Contract DE-AC05-76RL01830

Pacific Northwest National Laboratory
Richland, Washington 99354

Executive Summary

The use of municipal solid waste (MSW) for synthetic aviation fuel (SAF) production represents an economically attractive opportunity that can simultaneously reduce waste accumulation in landfills, avoid methane emissions from waste decaying in landfills, and expand U.S. supply chains to meet growing jet fuel demand. MSW consists of any household, commercial, or institutional waste, such as product packaging, food scraps, newspapers, bottles, grass clippings, furniture, clothing, appliances, paint, and batteries. Previous research has focused on thermochemical processes for MSW-to-SAF conversion, including the use of direct and indirect gasifiers to convert MSW into syngas and syngas into fuels via Fischer–Tropsch synthesis, or via the production of oxygenated intermediates followed by upgrading to fuel. Because the product distribution of hydrocarbons from Fischer–Tropsch synthesis follows the Anderson–Schulz–Flory distribution, the SAF selectivity usually cannot exceed 40 percent. On the other hand, routes via oxygenated intermediates, such as methanol, can potentially achieve higher SAF selectivity. Historically, oxygenated intermediate upgrading pathways focus on ethanol, 2,3-butanediol, and methanol.

This design case study presents a route for MSW-to-SAF production through a methanol-to-olefins and olefin oligomerization pathway. The pathway, shown in Figure ES-1, includes preprocessing of MSW into refuse-derived fuel (RDF),[1] conversion of RDF into syngas via plasma-enhanced gasification, production of methanol from syngas, conversion of methanol into olefins, subsequent oligomerization of olefins, olefin hydroprocessing, and separation of the final products. Compared with other gasification technologies, plasma/plasma-enhanced gasifiers are more suitable for treating MSW, given their greater feedstock flexibility, higher rate of conversion of organic matter to syngas, and limited or nonexistent tar production. Methanol can be directly used as solvent, extraction agent, antifreeze fluid additive, alternative marine fuel, gasoline blendstocks, or versatile intermediate for producing various chemicals, such as olefins, formaldehyde, or acetic acid. It is typically produced from syngas via a commercially available catalyst and process. The proposed pathway uses a new catalytic approach, developed at Pacific Northwest National Laboratory, that is characterized by a bifunctional Ni/SiO_2-Al_2O_3 (metal)/zeolites (acid) catalyst for single-step co-oligomerization of C_2 and C_{3+} olefins, with a bench-scale-demonstrated single-pass conversion of approximately 92 percent for C_2 and over 97 percent for ≥C_3 olefins and a selectivity of approximately 74 percent toward the production of jet-range products.

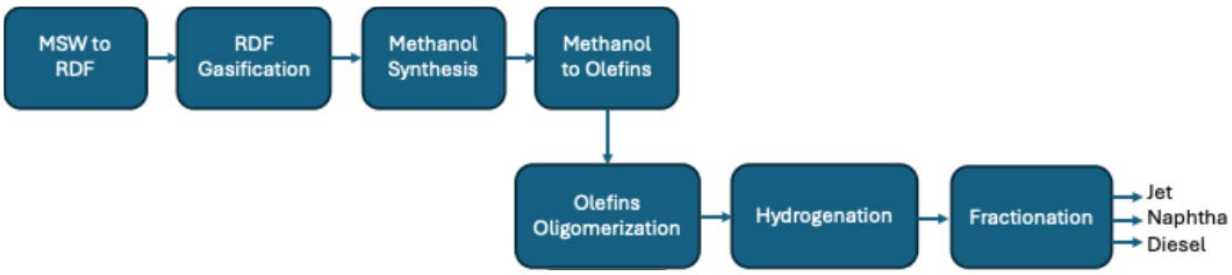


Figure ES-1. Block flow diagram of the municipal solid waste (MSW)-to-jet pathway.

This design case study aims to bridge research gaps by providing deeper analyses and information that are relevant for waste-to-energy and alcohol-to-jet industry stakeholders and

[1] Refuse-derived fuel (RDF) refers to sorted and treated municipal solid waste (MSW) that is ready to be fed to the gasification reactor.

other SAF producers. This research included specific siting, regional waste resource inventory and transportation cost analyses, gathering of fuel market information, evaluation of sustainable fuel incentive impacts, net present value (NPV) and internal rate of return, carbon dioxide equivalent ($CO_{2,eq}$), and statistical analysis of cost and technical uncertainties of the MSW-to-SAF plant design. A chemical process simulation, techno-economic analysis, and life cycle assessment were performed to evaluate the technical, economic, and environmental feasibility of the proposed process. Future work may analyze the feasibility and trade-offs of separating plastics from MSW in the MSW-to-SAF process. The key findings are summarized in Table ES-1.

Market drivers and incentive programs: Converting MSW into SAF can simultaneously reduce waste accumulation in landfills and expand U.S. supply chains to meet growing jet fuel demand. Federal- and state-level programs are available to provide economic support and incentives, including the Renewable Fuel Standard (RFS), California's Low Carbon Fuel Standard (LCFS), and other comparable state-level programs. The RFS and LCFS programs consider specifically the biogenic fraction of MSW feedstocks, which this study accounts for. Additionally, MSW tipping fees are a critical component of current waste management economics. Diverting MSW from landfills reduces national waste disposal costs.

Region selection and resource assessment: MSW is particularly advantageous as a feedstock because of its large-scale availability and existing collection infrastructure. Unlike other feedstock types, MSW is already collected and processed at waste processing facilities nationwide, with the majority of it ultimately being disposed of in landfills. California alone contributes an estimated 11.7 percent of solid waste disposed of annually across U.S. landfills,[1] making it a promising potential location for implementing plants for producing SAF from MSW feedstock. Furthermore, California's existing LCFS program can provide additional financial incentives for a renewable plant located in the region. This study involved a regional feedstock resource assessment for MSW based on the State of California's waste characterization studies.

Plant siting and logistics: This study targeted a specific location near a landfill in Los Angeles County, California, that contains the largest landfill and waste transfer stations in the area. Potential regions with adequate MSW feedstock supply, according to the locations of landfills and waste collection points, were identified to ensure cost-effective waste transportation. The selected region can supply MSW feedstock for the SAF plant up to a rate of 7,100 dry short tons per day (TPD) at an approximate distance of 14.7 miles. This translates into a waste delivery cost of around $5.55 per ton of unsorted MSW ($6.35 per ton of RDF at the reactor throat). The baseline plant scale was set to 1,000 TPD, a decision based on the local availability of MSW and the size of existing MSW gasification plants.

Technology selections: The review of MSW gasification plants and their main characteristics identified high-temperature plasma-enhanced gasification as a promising technology for waste management, offering solutions to reduce MSW volume and generate renewable energy or chemicals like methanol or transportation fuels, showcasing its potential in the nation's waste handling and resource recovery ecosystem. Plasma technology offers advantages like lower environmental impact and greater flexibility in treating complex feedstocks like unprocessed MSW.

Design cases: This design case study considered two cases. Case 1 maximizes the SAF production from MSW, where all syngas produced from gasification is sent to methanol

[1] Data source detailed in Section 5.0.

production. This case only leverages waste heat and light gases generated during conversion for steam and power production, while 73.3 percent of total electricity consumed is purchased from the grid to meet the energy requirements. Case 2 is a self-powered process that maximizes the life cycle emissions reduction, where a portion of syngas is used to generate power and steam on-site, creating a self-sufficient energy system. Case 2 does not require grid electricity, but its SAF production rate is lower than that of Case 1 because a portion of syngas produced from MSW is not used for fuel production.

Minimum fuel selling price: For a 1,000 TPD MSW-to-SAF plant, without any MSW tipping fee credits or incentive programs (i.e., RFS, LCFS), the modeled minimum fuel selling prices (MFSPs) were $5.49 and $7.75 per gasoline gallon equivalent (gge) for Base Case 1 and Base Case 2, respectively. Without incentives, the estimated MFSP of Case 2 is expected to be higher than that of Case 1 because of its reduced fuel yield. A targeted MFSP of $2.50/gge can potentially be achieved with MSW tipping fee credits and/or fuel incentives.

Life cycle carbon dioxide equivalent ($CO_{2,eq}$) emissions: $CO_{2,eq}$ emissions were 37.9 gCO_{2e}/MJ fuel for Case 1 and 17.5 gCO_{2e}/MJ fuel for Case 2, corresponding to emission reductions of 55.9 percent and 79.7 percent, respectively. The impact associated with the conversion and combustion of conventionally sourced components of MSW (i.e., plastics) was the single largest contributor to $CO_{2,eq}$ emissions in both scenarios. However, this impact was largely offset by the avoided impact of disposing of MSW in a landfill.

Incentives and MSW tipping fee: The minimum fuel credits required to meet the $2.50/gge target were estimated to be $3.07/gge and $5.38/gge for Case 1 and Case 2, respectively. Case 1 would qualify for lower-value renewable identification numbers (RINs) and LCFS credits, with 55.9 percent $CO_{2,eq}$ emission reduction. Case 2 could be eligible for higher-value credits, with 79.7 percent $CO_{2,eq}$ emission reduction. RINs and LCFS credits were adjusted to reflect the biogenic portion of the biofuel for both cases. Although Case 2 would qualify for higher-value credits, without consideration of MSW tipping fee credits, the required incentives to meet the target MFSP would exceed the available biofuel credits in both cases. When additional incentives from MSW tipping fees are included, both cases could achieve the target MFSP with upper quartile fuel credits by introducing a tipping fee of $47.3/ton MSW (for Case 1) or $54.1/ton MSW (for Case 2). These fees are slightly lower than the current state average of $58.5 per ton and significantly below the $120 per ton fee charged by the largest landfill in the potential site selected in this study.

Sensitivity and uncertainties: A sensitivity analysis based on key modeling assumptions revealed that plant scale, gasifier cost, and total capital investment were the most significant factors affecting MFSP. Capturing the combined impacts from, model accuracy in mass and energy balances, market prices of hydrogen and utilities, and the accuracy of the estimated capital cost of each process area, the uncertainty quantification suggested deviations in the estimated MFSP of approximately +10/−13 percent and +11/−15 percent for Case 1 and Case 2, respectively, without consideration of incentives or tipping fee credits.

Economics of scale: The impact of plant scale on the economic feasibility of the MSW-to-SAF pathway was evaluated for the selected site. During the scale-up, additional trains were considered for unit operations that had reached their size limitations. With a targeted SAF selling price of $2.50/gge, the minimum plant size required for a positive NPV was 2,100 TPD for Case 1 and 1,400 for Case 2, when RFS and MSW tipping fee credits were considered. These required minimums dropped significantly to 1,100 TPD for Case 1 and 900 TPD for Case 2 when RFS, LCFS, and MSW tipping fee credits were considered. A sensitivity analysis of incentive pricing

further confirmed that even in the worst-case scenario, the required minimum plant size was smaller than the total available MSW in the region, suggesting economic viability.

Table ES-1. Key performance, economic, and environmental measures of MSW-to-SAF design cases.

	Case 1 SAF-max	Case 2 Self-powered
Performance measures		
Fuel yield (w/w dry MSW)	0.19	0.12
Thermal efficiency (%, lower heating value, dry MSW)	36.4%	31.3%
Carbon efficiency (% of C in MSW)	39.3%	24.4%
Economic measures of base cases		
Plant scale (TPD RDF)[a]	1,000	1,000
Total capital investment (MM$)	482.5	479.5
MFSP w/o incentives & MSW tipping fee credits ($/gge)	$5.49	$7.75
Uncertainties in MFSP (%)	+11%/-10%	+15%/-13%
Environmental measures		
Life cycle $CO_{2,eq}$ emission (g CO_2/MJ)	37.9	17.5
$CO_{2,eq}$ emission reduction (%)	55.9%	79.7%
Impact of incentive programs		
Targeted SAF price with incentives ($/gge)	$2.5	$2.5
Potentially applicable RFS Code	D5 RINs	D3 RINs
RFS incentive ($/gge)	$0.52–$1.57	$1.75–$3.05
LCFS incentive ($/gge)	$0.45–$0.78	$0.65–$1.11
Potential MSW tipping fee ($/ton)	$58.5	$58.5
Incentive required for positive NPV w/o MSW tipping fee ($/gge)	$3.07	$5.38
MSW tipping fee required for positive NPV w/ 2018–2023 six-year averaged incentives ($/dry ton)	$47.3	$54.1
Impact of plant scale		
Targeted SAF price with incentives ($/gge)	$2.50	$2.50
Minimum plant scale w/ 2018–2023 six-year averaged RFS incentives & MSW tipping fee (TPD)	2,100	1,400

	Case 1 SAF-max	Case 2 Self-powered
Minimum plant scale w/ 2018–2023 six-year averaged LCFS and RFS incentives and MSW tipping fee (TPD)	1,100	900

[a] The plant scale for the design cases is based on 1,000 TPD of RDF. Detailed information on the required MSW quantities, sorting, and preprocessing steps for the MSW-to-RDF conversion can be found in Section 6.1.

Acknowledgments

This work was funded by the Alternative Fuels and Feedstocks Office in the Critical Minerals and Energy Innovation Office of the U.S. Department of Energy under Agreement 2.1.0.301 at Pacific Northwest National Laboratory, which is operated by Battelle for the U.S. Department of Energy under contract DE-AC05-76RL01830. The views and opinions of the authors expressed herein do not necessarily state or reflect those of the United States Government or any agency thereof. Neither the United States Government nor any agency thereof, nor any of their employees, makes any warranty, expressed or implied, or assumes any legal liability or responsibility for the accuracy, completeness, or usefulness of any information, apparatus, product, or process disclosed, or represents that its use would not infringe privately owned rights.

Acronyms and Abbreviations

AGR	acid gas removal
ATJ	alcohol to jet
CAPEX	capital expenditure
CARB	California Air Resources Board
$CO_{2,eq}$	carbon dioxide equivalent
CTE	critical technology element
DOE	Department of Energy
EIA	U.S. Energy Information Administration
EPA	U.S. Environmental Protection Agency
FT	Fischer–Tropsch
gge	gasoline gallon equivalent
HEFA	hydroprocessed esters and fatty acids
HP	high pressure
ICAO	International Civil Aviation Organization
IRR	internal rate of return
LCA	life cycle assessment
LCFS	Low Carbon Fuel Standard
MFSP	minimum fuel selling price
MSW	municipal solid waste
MTJ	methanol to jet
MTO	methanol to olefins
NPV	net present value
PNNL	Pacific Northwest National Laboratory
RDF	refuse-derived fuel
RIN	renewable identification number
RFS	Renewable Fuel Standard
SAF	sustainable aviation fuel
SWIS	Solid Waste Information System
TEA	techno-economic analysis
TPD	short tons per day
TRL	technology readiness level
WGS	water-gas shift

Contents

Executive Summary ii
Acknowledgments vii
Acronyms and Abbreviations viii
1.0 Introduction 1
2.0 Fuel Market and Drivers for Waste-to-Fuel Conversion 4
3.0 Incentive Programs 7
3.1 Incentive Programs Supporting SAF Production 7
3.2 Other Incentives for MSW Management 9
4.0 Technology Options 10
4.1 MSW Gasification 10
4.2 Oxygenated Intermediate Upgrading 15
5.0 Regional Resource Assessment 16
5.1 Region Selection 16
5.2 Feedstock Composition and Characteristics 17
5.3 Plant Capacity, Siting, and Transportation Logistics 18
6.0 Process Design 21
6.1 Area 100: MSW Sorting and Preprocessing 22
6.2 Area 200: Gasification 24
6.3 Area 300: Syngas Cleanup and Conditioning 26
6.4 Area 400: Methanol Synthesis 28
6.5 Area 500: Methanol to Sustainable Aviation Fuel 29
6.6 Area 600: Steam and Power Generation 31
6.7 Area 700: Waste Treatment and Balance of Plant 31
7.0 Base Case Economic Assessment 33
7.1 Total Capital Investment 33
7.2 Process Variable and Fixed Operating Costs 34
7.3 Minimum Fuel Selling Price 35
8.0 Base Case Environmental Assessment 37
8.1 Life Cycle Assessment Data Sources 38
8.2 $CO_{2,eq}$ Emission Results 38
9.0 Sensitivity and Uncertainty Analysis 41
9.1 Sensitivity Study of Key Performance and Economic Assumptions 41
9.2 Impact of Slag Utilization on TEA and LCA 42
9.3 Impact of Incentives on NPV and IRR 42
9.4 Combined Impact of MSW Tipping Fee and Fuel Incentives on MFSP 44
9.5 Uncertainties in the Techno-economic Analysis 46
9.6 Impact of Plant Scale on Economic Feasibility 48

10.0 Current State of Development/Commercialization 50
11.0 Conclusions and Next Steps 52
12.0 References 54
Appendix A – Conversion Life Cycle Inventory and Energy and Carbon Efficiencies A.1
Appendix B – Cost Factors and Financial Assumptions B.1
Appendix C – Key Sources of Uncertainties C.1
Appendix D – Detailed Process Flow Diagrams and Stream Tables D.1
Appendix E – Equipment List and Costing E.1

Figures

Figure 1. Disposition of municipal solid waste (MSW) in 2018. 2
Figure 2. Simplified block flow diagram of the process for converting municipal solid waste (MSW) into aviation fuels. RDF = refuse-derived fuel. 3
Figure 3. Analysis of renewable identification numbers (RINs) generated in 2024. Source: EPA. 5
Figure 4. Pathways and technology options to produce SAF from biomass and organic waste via oxygenated intermediate upgrading. 15
Figure 5. Annual landfill MSW acceptance rate (in million metric tons per year [MMT/yr]) by state (EPA, 2024a). 16
Figure 6. Selected sustainable aviation fuel plant location (circled in blue), featuring the largest landfill and multiple waste transfer/processing facilities in Los Angeles County, California (County of Los Angeles, 2013). 19
Figure 7. Block flow diagram of the process of converting municipal solid waste (MSW) into sustainable aviation fuel. 22
Figure 8. Block flow diagram of a facility's process of converting municipal solid waste (MSW) into refuse-derived fuel (RDF) (Jones et al., 2009). 23
Figure 9. Simplified process configuration of plasma gasification in Area 200: Gasification. 25
Figure 10. Simplified process configuration of Area 300: Syngas Cleanup and Conditioning. 27
Figure 11. Simplified process configuration of Area 400: Methanol Synthesis. 28
Figure 12. Simplified process configuration of Area 500: Methanol to SAF. 29
Figure 13. Baseline MFSP and cost allocation without incentives for Base Case 1 (SAF-max) and Base Case 2 (Self-powered). 36
Figure 14. Life cycle assessment system boundary. 37
Figure 15. $CO_{2,eq}$ emission results for Base Case 1 (SAF-max) and Base Case 2 (Self-powered) compared with a conventional jet-fuel baseline. 39
Figure 16. Breakdown of $CO_{2,eq}$ emissions of biofuel blendstocks from the MSW-to-SAF process for Base Case 1 (SAF-max) and Base Case 2 (Self-powered). 39
Figure 17. Sensitivity analysis for Case 1 (SAF-max). 41

Figure 18. Effect of potential sustainable fuel credits on the net present value (NPV) and internal rate of return (IRR) for two scenarios: a) Case 1 (SAF-max) and b) Case 2 (Self-powered) processes. 44
Figure 19. Minimum fuel selling price (MFSP) with municipal solid waste (MSW) tipping fee and combined fuel incentives (biogenic) for Case 1 (SAF-max) process. 45
Figure 20. Minimum fuel selling price (MFSP) with municipal solid waste (MSW) tipping fee and combined fuel incentives (biogenic) for Case 2 (Self-powered). 46
Figure 21. Uncertainties in the minimum fuel selling price (MFSP) without incentives for Case 1 (SAF-max). 47
Figure 22. Uncertainties in the minimum fuel selling price (MFSP) without incentives for Case 2 (Self-powered). 48
Figure 23. Impact of plant scale on the estimated minimum fuel selling price (MFSP) and internal rate of return (IRR) of Case 1 (SAF-max). 48
Figure 24. Impact of plant scale on the estimated minimum fuel selling price (MFSP) and internal rate of return (IRR) of Case 2 (Self-powered). 49
Figure 25. Technology readiness levels of critical technology elements in the municipal solid waste (MSW) to sustainable aviation fuel (SAF) plant. 50

Tables

Table 1. Summary of federal and state-level incentives for sustainable aviation fuel production (2018–2023 data). 8
Table 2. Operation conditions and parameters for different gasifier types (Arena, 2012; Chandolias et al., 2018; Cortazar et al., 2023; Pang, 2016; Shahabuddin and Alam, 2022). 11
Table 3. Pros and cons of different gasifier types. 12
Table 4. Examples of existing MSW and solid waste gasification plants (Arena, 2012; Ebara, 2024; GSTC, 2024a; Klean Industries, 2024; Leckner, 2015; Mitsubishi Power, 2021; NETL, 2024e; NRG Focus, 2013; Wang et al., 2023; Waste Today, 2017). 14
Table 5. MSW by waste category in California landfills (CalRecycle, 2022). 17
Table 6. Combustible refuse-derived fuel feedstock characteristics used in this study. 18
Table 7. Feedstock transportation logistics and economics (plant scale: 1,000 short tons per day [TPD] of refuse-derived fuel [RDF]) (Seiple et al., 2023). 19
Table 8. Key process specifications for refuse-derived fuel (RDF) facility. 23
Table 9. Mass and energy balances for Area 200: Gasification. 25
Table 10. Mass and energy balance of Area 300: Syngas Cleanup and Conditioning. 27
Table 11. Mass and energy balance of Area 400: Methanol Synthesis. 28
Table 12. Summary of experimental results for single-path oligomerization. 30
Table 13. Mass and energy balance for Area 500: Methanol to SAF. 30
Table 14. Operating parameters of the steam generator and steam turbine. 31
Table 15. Detailed project cost summary for 1,000 TPD MSW-to-SAF plants. 33

Table 16. Variable operating costs for the MSW-to-SAF plant.....34
Table 17. Fixed operating costs for the MSW-to-SAF plant for Base Case 1 (SAF-max).....34
Table 18. Fixed operating costs for the MSW-to-SAF plant for Base Case 2 (Self-powered).....35
Table 19. Key performance measures of the MSW-to-SAF process.....36
Table 20. Life cycle assessment data sources. 38
Table 21. Impact of slag utilization in the techno-economic analysis and life cycle assessment.....42
Table 22. Federal and state incentives applicable to Case 1 and Case 2 for SAF production. 43

1.0 Introduction

The Department of Energy (DOE) Bioenergy Technologies Office collaborates with industry, academia, and national laboratory partners to unlock new economic opportunities for rural and agricultural communities by advancing technology development and innovation across the entire biomass-to-bioenergy supply chain. Bioenergy is an abundant and renewable resource that can contribute to a more secure and economically sound future. Bioenergy Technologies Office collaborations are working to achieve the following aims:

- Transform domestic biomass and waste carbon resources into productive and affordable bioenergy and bioproducts; and
- Provide options for global energy competitiveness.[1]

One option for advancing technology development, increasing global energy competitiveness, and expanding U.S. supply chains is conversion of municipal solid waste (MSW) into aviation fuels. MSW comprises household waste, commercial or institutional waste, product packaging, yard trimmings, textiles, food waste, paper, etc. Using MSW as a feedstock for aviation fuels is also a means of diverting waste from landfills. The use of non-biogenic waste sources (e.g., plastic waste) to produce biofuel is controversial because of the environmental implications of producing the waste. However, plastic waste in the non-recyclable portion of MSW (including plastic films, packaging, and food-soiled multi-materials) represents an emerging environmental issue due to the lack of an efficient and technically sound strategy for its management (Shah et al., 2023). With limited options for recycling because of contamination and highly variable mixed plastic stream composition, the most common end-of-life practices are currently incineration or disposal in landfills. Current incinerators, however, still suffer from low efficiency and the release of toxic and persistent organic air pollutants, posing a threat to human health. Landfilling plastic waste also leads to long-term pollution because plastics can take hundreds to thousands of years to decompose, and, in the process, fragment into microplastics, which can spread through the environment.

The purpose of a design case study is to provide data-grounded analyses with emphasis on supporting the needs of stakeholders to help accelerate technology adoption. Design case studies target specific sites/regions and provide critical business-case-related outputs in collaboration with industrial stakeholder partners, such as technology providers. This design case study explores the economics of an MSW-to-aviation-fuels enterprise, including the following aspects:

- Technology options and maturity
- Market drivers and incentive programs
- Region selection and MSW resource assessment
- Plant siting analysis and logistics
- Life cycle emissions for two design cases
- Sensitivities and uncertainty considerations
- Economies of scale

[1] https://www.energy.gov/eere/bioenergy/bioenergy-technologies-office.

MSW is an abundant resource that can be used for the production of aviation fuels. According to U.S. Environmental Protection Agency (EPA) data, the total generation of MSW in 2018 was 292.4 million short tons, or 4.9 lb per person per day. The disposition of MSW is illustrated in Figure 1.

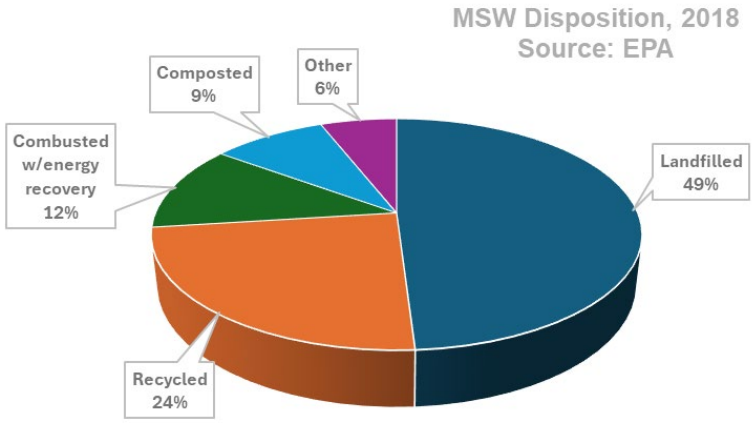


Figure 1. Disposition of municipal solid waste (MSW) in 2018.

Waste-to-energy projects currently face several obstacles, including delays in receiving operational permits, local opposition due to negative public perception, and technical challenges in handling MSW due to its highly variable composition. Primary concerns regarding the efficacy of waste-based fuels are due to the potential emission of hazardous chemicals in gaseous streams from thermochemical processes. In January 2022, the EPA announced a new effort to standardize the review of a growing number of applications for new transportation fuels made through the mixing of bio-based and petroleum-based feedstocks (EPA, 2023a). Consequently, today's proposed rules require notification and review by EPA before the manufacturing or processing of chemicals using waste-derived feedstocks that contain hazardous chemicals.

Preprocessing of MSW into refuse-derived fuel (RDF), followed by high-temperature gasification, is one alternative for handling the variability of MSW and treating inorganic and hazardous elements of the feedstock. Rationale for the gasifier configuration presented here is provided in Section 4.1. The objective of gasification is the production of synthesis gas—H_2 and CO. The decision on what H_2/CO ratio to use must be based on what catalyst is used downstream. This study assumes a process of syngas-to-methanol conversion followed by methanol to olefins (MTO), olefins oligomerization, and olefins hydrogenation. Fractionation to fuels. Modeling of mixed olefins oligomerization was based on a new Pacific Northwest National Laboratory (PNNL) catalyst system, described in Section 4.2. The simplified block flow diagram for converting MSW into aviation fuels is shown in Figure 2.

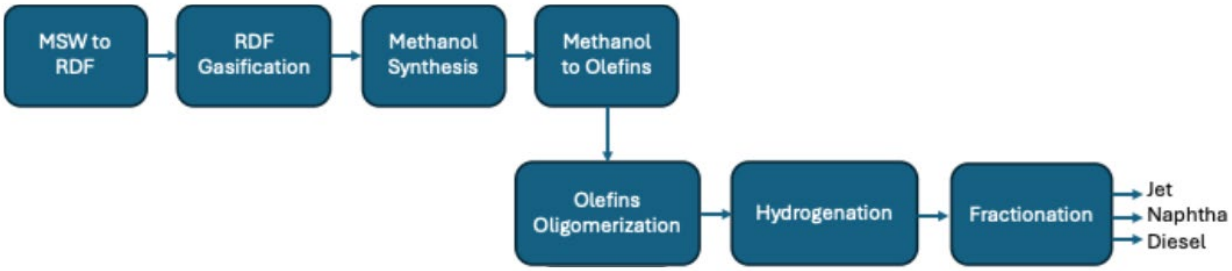


Figure 2. Simplified block flow diagram of the process for converting municipal solid waste (MSW) into aviation fuels. RDF = refuse-derived fuel.

The economic analyses presented here assumed an *n*th plant. The *n*th plant is hypothetical—it represents that the technology is mature, reliable, and well understood. For stakeholders applying this analysis to their own enterprises (or investments), additional assumptions and costs for redundant equipment require consideration. Fuel markets and drivers for waste-to-fuel conversion are described in Section 2.0. Incentive programs are presented in Section 3.0.

This site-specific design case study focused on the conversion of MSW to aviation fuel at a specific site in Southern California. Factors considered in the site selection are described in Section 5.0 and include the presence of two major airports with significant jet fuel demand (San Francisco International Airport [SFO] and Los Angeles International Airport [LAX]), the existing jet fuel pipeline and terminals, incentive schemes such as the Low Carbon Fuel Standard (LCFS), and the availability of regional data for MSW. This study considered incentive programs from both federal-level policies, such as the renewable identification number (RIN) from the EPA's Renewable Fuel Standard (RFS) program, and state-level policies.

The process design and economics for two operational cases are described in Sections 6.0 and 7.0, respectively. Base Case 1 (SAF-max) maximizes the yield of jet fuel. Base Case 2 (Self-powered) is characterized by its dedicated on-site syngas-to-power generation, which fully supplies the energy needed to meet all electrical requirements and eliminates reliance on grid electricity. They are called "base" cases because they are the foundation from which sensitivity analyses were performed. The economics presented include mass and energy balances, equipment sizing, capital expenditure (CAPEX) and operating cost, minimum fuel selling price (MFSP), net present value (NPV), and internal rate of return (IRR). Experimental data from PNNL's mixed olefin oligomerization research and development program were leveraged to inform the equipment design of the olefins to aviation process area. Life cycle inventories were used to quantify life cycle carbon dioxide equivalent ($CO_{2,eq}$) emissions, which allowed for determination of potentially applicable incentive programs, all presented in Section 8.0. Economics of scale were carefully evaluated to determine the minimum required plant scale to sell aviation fuel at a targeted price of $2.50/gge. Sensitivities and uncertainties are presented in Section 9.0. The current state of technological development and of commercialization of the pathway described herein—along with similar technology pathways—is described in Section 10.0, followed by conclusions and next steps in Section 11.0. The appendixes provide detailed inventories, assumptions, stream tables, and an equipment list and costing.

2.0 Fuel Market and Drivers for Waste-to-Fuel Conversion

Overall U.S. energy consumption continues to demonstrate a strong demand for petroleum products, and within that, jet fuel fuels are a key component. In 2023, petroleum accounted for 89 percent of energy use in the U.S. transportation sector. Petroleum-derived jet fuel comprised 12 percent of that total (EIA, 2024a). The U.S. Energy Information Administration (EIA) forecasts that jet fuel will face tight supply and demand conditions and a low inventory with only 21 days of supply, the lowest since 1963. This is mainly because of the combined impacts from (i) increased jet fuel consumption driven by rising air travel and freight and (ii) reduced refinery production driven by pending refinery closures (EIA, 2025). These inventory withdrawals may increase wholesale and retail fuel prices. Therefore, production of sustainable aviation fuel (SAF) from biomass and waste is important for expanding and securing energy supply, especially in the aviation sub-sector.

In 2022, the aviation industry contributed roughly 12 percent of transportation-related emissions, totaling nearly 800 million metric tons of $CO_{2,eq}$ worldwide (EIA, 2023a). As demand for air and freight travel continue to surge, global $CO_{2,eq}$ emissions could quadruple by 2050, falling short of the goals of the International Civil Aviation Organization (ICAO). Achieving these goals necessitates advanced aircraft, efficient operational practices, and significantly upscaled SAF production (ICAO, 2022). While some small aircraft can be powered by batteries and fuel cells (Gross, 2020), larger and transcontinental aircraft have demands that can only be met in the near term by SAF, thanks to its high energy density and compatibility with existing infrastructure (Goldner et al., 2023).

Biofuels accounted for about 53 percent of total biomass consumption in 2023. However, most of it contributed to ethanol and biodiesel. SAF production in the United States is still in its early stages, with a capacity of only 30 million gal at the beginning of 2024 (EIA, 2024b). An analysis of RINs revealed that 20 million gal of renewable jet fuels were generated in 2024 (Figure 3). Data for this analysis was obtained from the EPA.

U.S. Renewable Fuel Production by RIN million gallons		%
D6 Renewable fuel (–20% GHG)		70%
Ethanol	9,887	
Renewable diesel and gasoline	3	
D4 Biomass-based diesel (–50% GHG)		
Biodiesel	1,073	
Renewable diesel	1,926	
Renewable heating oil	0.1	
Renewable jet	20	
D5 Advanced Biofuels (–50% GHG)		1%
Ethanol	19	
Naphtha	31	
Other	3	
D3/D7 Cellulosic (–60% GHG)		4%
Ethanol	15	
Natural gas (compressed)	481	
Natural gas (liquified)	22	

RIN = Renewable identification number, note: another 0.7 billion gal of renewable fuels were imported, totaling 13.5 billion gal of RIN fuels

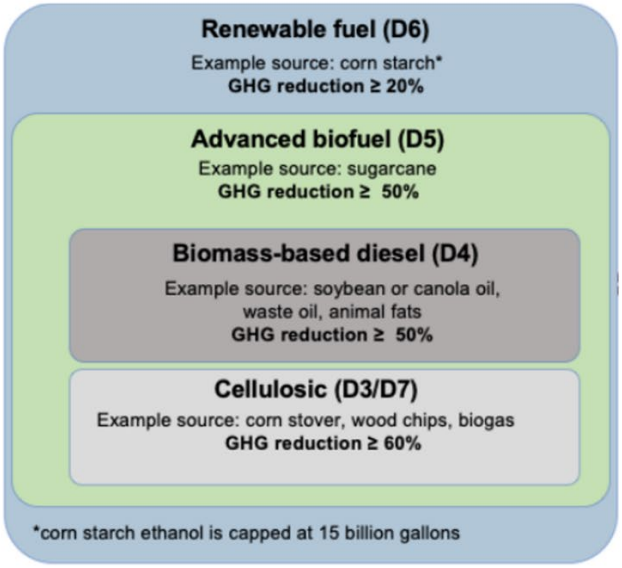


Figure 3. Analysis of renewable identification numbers (RINs) generated in 2024. Source: EPA[1].

Beyond the growing demands, SAF must adhere to strict criteria for performance, operability, and compatibility with existing infrastructure. This ensures safety and readiness in commercial and military missions (DOE, 2020). As of October 2021, ASTM International had approved nine distinct SAF production pathways, with blending limits ranging from 5 to 50 percent, depending on the feedstock and conversion method. These pathways include the following:

- Fischer–Tropsch (FT)
- Hydroprocessed esters and fatty acids (HEFA)
- Synthesized iso-paraffins (SIP),
- FT synthetic kerosene with aromatics (FT-SKA)
- Alcohol to jet (ATJ)
- Catalytic hydrothermolysis jet fuel (CHJ),
- Hydrocarbon-hydroprocessed esters and fatty acids (HC-HEFA)
- Co-hydroprocessing of esters and fatty acids (co-processed HEFA)
- Co-hydroprocessing of FT hydrocarbons (co-processed FT).

Currently, the HEFA process is the most widely used method for producing SAF and relies on a stable market of fats, oils, and grease (Delnegro, 2023). The approved ATJ process for converting alcohols to jet fuel offers potential, particularly through pathways using iso-butanol and ethanol derived from sources like corn grain (Wang and Tao, 2016). However, the limited supply of these feedstocks necessitates the expansion of production pathways and identification of alternative feedstocks for new conversion methods (IATA, 2023).

[1] https://www.epa.gov/renewable-fuel-standard/renewable-fuel-annual-standards

Waste-to-fuel conversion can contribute to energy dominance and provide a domestically sourced fuel supply. In addition, it can diversify energy sources by using cost-advantaged feedstocks. MSW as a domestic resource is abundant but not well utilized. The combination of rapidly filling landfills and consistently rising volume of MSW in the United States creates pressure to find alternative waste disposal or utilization methods (DOE, 2024). In particular, waste-to-fuel conversion can reduce methane leakage and flaring from waste decomposition in landfills and life cycle $CO_{2,eq}$ emissions. Additionally, improper waste disposal can lead to soil and water contamination. Waste-to-fuel technologies offer a controlled way to manage waste. While waste-to-fuel facilities can require a high initial investment, they can lead to long-term cost savings in waste management and create new revenue streams from the sale of produced fuels. The waste-to-fuel sector can also create opportunities for new business enterprises and jobs in technology development, plant operation, technical services, and fuel production. This study analyzed a methanol-based ATJ pathway from MSW.

3.0 Incentive Programs

3.1 Incentive Programs Supporting SAF Production

The RFS is a U.S. federal program intended to expand the volumes of renewable fuels. This program was created under the Energy Policy Act of 2005 and expanded under the Energy Independence and Security Act of 2007. Obligated parties under the RFS program are refiners or importers of gasoline or diesel fuel, and they achieve compliance by obtaining and retiring credits representing renewable fuel (i.e., RINs) to meet their renewable volume obligation for each renewable fuel category. The four renewable fuel categories under the RFS program are (i) cellulosic biofuel (D3 RIN); (ii) biomass-based diesel (D4 RIN); (iii) advanced biofuel (D5 RIN); and (iv) total renewable fuel (D6 RIN) (EPA, 2015).

Eligibility of a fuel pathway for different RIN types is determined on the basis of the feedstock, production process, and fuel type (see Figure 3 and Table 1). Cellulosic biofuel (D3) and advanced biofuel (D5) RINs were evaluated for the MSW-to-SAF pathway in this study. The value of each of the RINs considered in this study was determined with reference to historical RIN trade and price information, as obtained from the EPA Moderated Transaction System (EPA, 2018). RINs are based on ethanol production; therefore, credits were adjusted on the basis of the energy density of the biofuel. The historical data for D3 and D5 RINs exhibits significant fluctuations, ranging from $0.28 to $3.50 per RIN. In this study, the 25th percentile (lower quartile), 50th percentile (median), and 75th percentile (upper quartile) of the six-year (2018–2023) RIN credit data were considered, corresponding to a range of $1.69–$2.95 for D3 RINs and a range of $0.46–$1.53 for D5 RINs per ethanol-equivalent gallon of fuel.

The Clean Fuel Production Credit under 45Z is a newly established U.S. tax credit for both SAF and nonaviation fuels (ICAO, 2023). Effective January 1, 2025, it provides a per-gallon credit that scales with the fuel's reduction in life cycle CO_{2eq} emissions compared with the emissions of conventional fuels, as determined with tools adopted by the U.S. Department of the Treasury and Internal Revenue Service (i.e., 45Z-CF-GREET). To qualify for the credit, SAF production must meet the specifications of 45Z(d)(5)(A) and either ASTM D7566 annexes or ASTM D1655 Annex A1. As of the time that this report was written, the methanol to jet (MTJ) pathway, central to the MSW-to-SAF process investigated in this study, is still under evaluation and has not yet been incorporated into these approved ASTM International standards (Buffie, 2025).

In addition to federal incentives, there are state-level incentives for SAF production. Many states have implemented programs to encourage the production and use of sustainable fuels to meet their emissions reduction goals. California's LCFS is an emission trading rule designed to reduce the life cycle $CO_{2,eq}$ emissions of transportation fuels compared with those of conventional fuels. Emissions from fuels produced and consumed in 2005 are often used as a benchmark. In the present work, the $CO_{2,eq}$ emissions for each fuel were compared with a declining $CO_{2,eq}$ emissions benchmark for each year. Carbon fuels with emissions below the benchmark generate credits, while those with emissions above the $CO_{2,eq}$ emission benchmark generate deficits. Credits and deficits are expressed in terms of metric tons of $CO_{2,eq}$ emissions and can be traded under the LCFS scheme (Air Resource Board, 2024). Like RINs, LCFS credits in this study ranged from $70 to $213 per metric ton of $CO_{2,eq}$ reduction. Given the 25th, 50th, and 75th percentile of the six-year (2018–2023) historical credit data, carbon credits have a value in the range of $113–$194 per metric ton of CO_2. Under the assumption of an average credit of $169 per metric ton (50th percentile), the potential average carbon credits from LCFS amount to approximately $0.95/gal

of biofuel for a 50 percent $CO_{2,eq}$ emissions reduction and \$1.13/gal of biofuel for a 60 percent $CO_{2,eq}$ emissions reduction for SAF production.

Table 1 summarizes the RIN and LCFS credits considered for cellulosic and advanced biofuels in this study. To demonstrate the potential incentives, hypothetical scenarios are presented for processes achieving 50 percent and 60 percent $CO_{2,eq}$ emissions reductions, which serve as a basis to estimate the LCFS credit values. The combined incentive package from RINs and LCFS amounts to approximately \$2.41/gal of biofuel for a process achieving 50 percent $CO_{2,eq}$ emission reduction, thus qualifying for D5+LCFS50 credits. Similarly, the average total incentive package that a process achieving 60 percent $CO_{2,eq}$ emission reduction can be eligible for amounts to \$4.75/gal of fuel, considering stacked D3+LCFS60 incentives. However, when the historical minimum and maximum values for RINs and LCFS credits are taken into consideration, the total incentive range widens significantly, ranging between \$0.79 to \$6.61 per gallon of biofuel. Notably, the credit values provided represent the potential incentives for total renewable fuels. For MSW-derived fuels containing both biogenic and non-biogenic components, adjustments to these credits are necessary to account for the fraction of non-biogenic materials.

Table 1. Summary of federal and state-level incentives for sustainable aviation fuel production (2018–2023 data).

	Unit	Min	QL	Median	QU	Max
D3 RINs[a]	\$/gal of biofuel	0.76	2.56	3.62	4.47	5.30
D5 RINs[a]	\$/gal of biofuel	0.42	0.76	1.47	2.30	3.09
LCFS	\$/$MTCO_2$ reduction	70	113	179	194	206
LCFS50[b]	\$/gal of biofuel	0.37	0.60	0.95	1.02	1.09
LCFS60[b]	\$/gal of biofuel	0.44	0.72	1.13	1.23	1.31
D3+LCFS60[c]	\$/gal of biofuel	1.20	3.28	4.75	5.70	6.61
D5+LCFS50[c]	\$/gal of biofuel	0.79	1.35	2.41	3.33	4.18

[a] 1 RIN credit represents an ethanol-equivalent gallon of fuel. The credits were adjusted according to the energy density of the biofuel, with an equivalence value of 1.5 used for this study.
[b] LCFS50 and LCFS60 correspond to credits for 50 and 60 percent $CO_{2,eq}$ emission reduction, respectively.
[c] Cellulosic biofuel credits (D3 RINs) require a minimum of 60 percent $CO_{2,eq}$ emission reduction compared with the petroleum baseline; therefore, they are stacked with LCFS60. Advanced biofuel credits (D5 RINs) require a minimum of 50 percent $CO_{2,eq}$ emission reduction compared with the petroleum baseline; therefore, they are stacked with LCFS50.
$MTCO_2$ = metric ton of CO_2 emissions; QL = lower quartile; QU = upper quartile.

Eligibility of MSW under the RFS and LCFS: MSW represents an abundant and readily available feedstock for renewable fuel production under the RFS. However, its eligibility is subject to feedstock requirements aimed at ensuring compliance with the program's objectives of reducing $CO_{2,eq}$ emissions and promoting the use of renewable biomass. In this context, the biogenic components of the separated MSW would be considered eligible for RIN credit generation, provided that recyclables and non-biogenic components are separated from the feedstock stream to the extent reasonably practicable, as defined in EPA regulations (EPA, 2025). For an MSW feedstock containing non-biogenic components after separation, the volume of RIN generated is adjusted as follows:

$$V_{RIN} = EqV * V_S * R \quad (1)$$

where e V_{RIN} is the RIN volume in gallons that will be generated, EqV is the equivalence value for the batch of renewable fuel in terms of ethanol (based on its energy content), V_S is the standardized volume of the batch of renewable fuel at 60 °F in gallons, and R is the biogenic fraction of the fuel (measured in practice via the carbon-14 dating method, as required by the EPA) (EPA, 2025). Similarly, recent amendments to LCFS introduced specified source feedstock and sustainability requirements for incentive eligibility. Effective July 2025, the regulation mandates that only the organic fraction of the separated MSW is eligible for LCFS incentive generation (CARB, 2025, 2024). In this analysis, it is assumed that the methodology for estimating LCFS credits remains consistent with RFS guidelines, where credits are adjusted on the basis of the biogenic fraction of the MSW feedstock.

3.2 Other Incentives for MSW Management

MSW tipping fees are a critical component of current waste management economics. A tipping fee is a service fee that is charged for disposing material at a waste processing facility (e.g., landfill, transfer station, recycling center, or waste-to-energy facility). Landfilling is the predominant method of waste disposal; according to the EPA, 50 percent of MSW was directed to landfills in 2018, corresponding to 146.1 million short tons of MSW (EPA, 2020). The landfill tipping fees charged in 2023 in the United States range from $25.64 to $112.62 per short ton of MSW, with a national average of $56.80 per short ton (Aber, 2024).

In this context, diverting MSW from landfills creates an opportunity to reduce national waste disposal costs by over $8 billion annually. In the baseline scenarios presented in Section 7.3, no feedstock credit is received for diverting MSW from landfills. Additionally, MSW transportation and handling fees are covered by the SAF producer. However, certain incentive scenarios can be considered for MSW processing in which the SAF plant imposes a tipping fee on waste producers, effectively resulting in a negative feedstock cost for a plant that is functioning as a waste management facility.

For the single-point sensitivity analysis (Section 9.1), this study considered waste credits up to $120 per short ton of MSW, corresponding to the tipping fee charged by the landfill where the SAF plant is co-located. Additionally, the “MSW incentive scenario” in Section 9.4 considers waste credits up to $58.48 per short ton, representing the average landfill tipping fee in California, to evaluate the combined impact of sustainable fuel credits and MSW incentives (Aber, 2024). This scenario ensures that a certain portion of the MSW tipping fee revenue from landfills is diverted while the overall waste disposal costs continue to decrease.

4.0 Technology Options

4.1 MSW Gasification

Gasification is a high-temperature process that can convert any carbonaceous (carbon-based) raw material into gas, known as synthesis gas (syngas) after gas cleanup, primarily comprising CO and H_2 (NETL, 2024a). Gasification is a partial oxidation process, meaning that it uses less oxygen than is required for combustion (i.e., complete oxidation). Typically, gasification uses only 25–40 percent of the theoretical oxygen needed for combustion (either pure oxygen or air) to generate heat for gasifying the feedstock (NETL, 2024a).

Compared with conventional combustion methods, gasification presents numerous benefits. Operating in a low-oxygen (or reducing) environment lessens dioxin formation and lowers SO_x and NO_x emissions. The reducing requirement also results in a smaller volume of process gas as well as cost-effective gas cleaning equipment (Zafar, 2009). This is because partial oxidation consumes a fraction of the feedstock and results in higher temperatures than indirect gasification—where sand (or a catalyst) is used to transfer heat to the feedstock. Therefore, the syngas cleanup is more of a "polishing" than tar reforming. The resulting synthesis gas can be burned to produce power or further processed to produce transportation fuels or chemicals.

Gasification originated in the 1800s. For the next 100 years, gasification of coal and biomass was used to produce "town gas"[1] —primarily for cooking and lighting. In the 1930s, gasification was used to power farming equipment via produced gas and even liquids. As a direct response to the oil crisis (Wang et al., 2023), the primary objective of gasification in the 1970s was to find alternative sources of energy, such as coal and other carbonaceous materials that can be converted into syngas. By the 1990s, gasification technology entered a new generation. This generation saw the development of mature technologies, particularly in the power generation sector, where integrated gasification combined cycle plants demonstrated the potential for electricity production from various solid feedstocks.

Gasifier configurations vary with respect to the specific requirements of the process. Generally, gasifiers can be classified into four common types: (i) fixed-bed/moving-bed gasifiers, (ii) fluidized-bed gasifiers, (iii) entrained flow gasifiers, and (iv) plasma (or plasma-enhanced) gasifiers. Table 2 summarizes some of the design parameters of each type of gasifier. The first three types are more conventional, with mature technologies and a long history of utilization. Table 3 summarizes the features, advantages, and disadvantages of each type of gasifier. Plasma and plasma-enhanced gasification technologies are more advanced, offer greater feedstock flexibility, and achieve very high temperatures/high-temperature zones, making them uniquely suitable for MSW.

Table 2 to Table 4 include examples of existing MSW gasification plants and their main characteristics. Among those projects, MSW gasification predominantly employs conventional gasifiers such as fixed-bed/moving-bed and fluidized-bed technologies. Plasma technology is poised to be an important asset in the waste management ecosystem, demonstrating remarkable flexibility in handling diverse waste streams, including unsorted MSW. While this technology is currently in its growth phase, its advantages and ongoing advancements are driving it toward increased scalability and affordability. MSW gasification is promising for waste management,

[1] Town gas primarily comprises methane, hydrogen, carbon monoxide, and some contaminants. Town gas is often referred to as the predecessor to natural gas.

offering solutions to reduce MSW volume and generate renewable energy or chemicals like methanol and transportation fuels.

Table 2. Operation conditions and parameters for different gasifier types (Arena, 2012; Chandolias et al., 2018; Cortazar et al., 2023; Pang, 2016; Shahabuddin and Alam, 2022).

	Fixed-Bed/Moving-Bed Gasifiers	Fluidized-Bed Gasifiers	Entrained Flow Gasifiers	Plasma Gasifiers
Feeding condition	Dry	Dry	Dry/slurry	Dry/slurry
Feed particle size for waste (mm)	<100	<150 for bubbling fluidized bed, <100 for circulating fluidized bed	<1	No limitation
Feed morphology	Uniform	Uniform	Uniform	No limitation
Feed moisture	<20% for downdraft, <50% for updraft	<55%	15% for dry, <40% for slurry	No limitation
Feed ash content	<5%db for downdraft, <15%db for updraft	<25%db	<20%db	No limitation, but high ash content affects performance
Bulk density (kg/m^3)	>500	>100	>400	>100
Residence time (s)	~900–3,600	~10–100	~1.5–4	No data
Yield	99%	96%	99%	Near 100%
Tar content (g/Nm^3)	~1–30 downdraft, >100 for updraft	~1–10 for circulating, ~1–40 for bubbling	~0–5	Near 0
Scale at current state	Small/medium scale	Small to large scale	Large scale	Small/demonstration scale
Costs	Relatively low	Moderate to high	High	Very high

Table 3. Pros and cons of different gasifier types.

Gasifier Type	Operating Conditions	Characteristics	Pros	Cons
Fixed-bed/moving-bed gasifiers (Khan and Al-attab, 2022; NETL, 2024b; Sánchez and Martín, 2022; Shahabuddin and Alam, 2022)	Moderately high pressure (368–440 psi) Dry-ash mode: moderate temperature (~1,000–1,800 °F) Slagging mode: High temperature (2,000–3,600 °F)	Updraft, downdraft, and cross-draft configuration. Feedstocks are loaded into the top of the vessel and move downward through the bed by gravity. Gasifying agents are injected at the bottom/side of the vessel and flow in countercurrent contact (updraft)/concurrent contact (downdraft)/ cross contact (cross-draft) and react with the feedstock.	• Simple design and operation • High equipment efficiency • Can handle feedstock with high reactivity and moisture • No need for temperature heat recovery units • Low cost • Low oxidant requirement • Able to handle heterogeneous feedstock like MSW	• Long residence time • Requires careful control of feed size distribution • Tars formed need gas cleaning process • Explosion hazard • Small scale, challenging to scale-up • High methane content in syngas
Fluidized-bed gasifiers (Huber et al., 2006; Khan and Al-attab, 2022; Molaeimanesh and Torabi, 2022; NETL, 2024c; Shahabuddin and Alam, 2022)	Moderately high temperature (~15,00–2,000 °F) Pressure varies depending on syngas end use (~44–435 psi)[30]	Bubbling fluidized-bed design/circulating fluidized-bed design. Feedstock particles are suspended in an oxygen- or steam-rich gas, and the resulting bed acts like a fluid. Particles are usually small in size (<6 mm) for feedstock (coal). Oxygen agents enter near the bottom with high velocity to suspend or fluidize the bed.	• High load flexibility • High heat transfer rates • High fuel and feed flexibility, supporting a wide range of feedstocks • Moderate oxidant and steam requirements • Uniform temperature • Lower tar formation than fixed-bed gasifiers • Large-scale applications	• Feedstocks must have a small particle size • Extensive char recycling is required • Defluidization is caused by bed agglomeration • High energy demand
Entrained flow gasifiers (Higman, 2011; Khan and Al-attab, 2022; NETL, 2024d; Shahabuddin and Alam, 2022)	High temperature (>2,282 °F)[31] High pressure (~290–1,160 psi)[31] Extremely turbulent flow	Feed and oxygen agents are fed cocurrently to the gasifier, resulting in the oxidant and steam surrounding or entraining the feed particles as they are in the form of dense clouds inside. Widely utilized in coal gasification.	• High fuel flexibility • Large capacity • Generate clean, nearly tar-free syngas • Environmentally friendly • Short residence time • High carbon conversion rate • High-temperature slagging operation	• Low gasifier thermal efficiency • High oxygen demand • Complex operation, high operating cost • Heat recovery process is required • Extensive pretreatment process for feedstock

Gasifier Type	Operating Conditions	Characteristics	Pros	Cons
				• Creating slurries from soft or fibrous materials can be challenging and expensive
Plasma, plasma-enhanced gasifiers (NETL, 2024e)	Extremely high temperature [32] Ambient pressure	To create the plasma, electrical discharge is initiated through the gas, then the electric arc breaks down the gas into electrons and ions, causing extremely high temperatures. It can operate in the absence or near-absence of O_2[33]. Generally, the plasma gasifier is a conventional vertical shaft used in foundry industry for re-melting the scrap iron and steel, plasma torches or chambers can be installed near the bottom of the reactor[33].	• High feed flexibility, including suitability for MSW • Ambient pressure operation • High yield (>99%) for converting organics to syngas • No tar in syngas • No char, ash, or residual carbon; produces glassy slag • Can achieve near-zero waste accumulation • Avoid NO_x and SO_2 formation • Low CO_2 emissions • Low environmental impacts	• New technology with limited process understanding • Moderate community readiness level • Limited commercialization success • Energy intensive and high cost • High level of process control required • Currently operated at a smaller scale than traditional gasifiers

Table 4. Examples of existing MSW and solid waste gasification plants (Arena, 2012; Ebara, 2024; GSTC, 2024a; Klean Industries, 2024; Leckner, 2015; Mitsubishi Power, 2021; NETL, 2024e; NRG Focus, 2013; Wang et al., 2023; Waste Today, 2017).

Company/Process	Country	Gasifier Type	Feedstock	Capacity	Product
Enerkem[a]	Canada	Bubbling fluidized bed	MSW	~100,000–400,000 tons/yr	Methanol, ethanol
Hitachi Metals	Japan	Plasma gasifier	MSW	170 tons/day	Power, CHP
Air Products	UK	Plasma gasifier	MSW	1,000 tons/day	Power
Alter NRG	Canada	Plasma gasifier	MSW	~8–90 kt/yr	Syngas
Sunshine Kaidi (Wuhan Kaidi)	China	Plasma gasifier	Biomass waste	100 tons/day	Transportation fuel
Mitsubishi Heavy Industries Environmental & Chemical Engineering Co	Japan	Fluidized-bed gasifier and ash melting system	MSW	240 MT/day	Power
Mitsubishi Power	Japan	Entrained bed gasifier	Woody biomass		SAF
Westinghouse Plasma Corp	USA	Plasma gasifier	Biomass waste, MSW, etc.		Syngas
OMNI Conversion Technologies	Canada	Fixed-bed updraft Gasification & Plasma Refining System (GPRS™)	MSW	200 MT/day (135 MT/day MSW)	Syngas
Asahi Clean Centre	Japan	Conventional gasification and ash melting system	MSW	420 MT/day	Power
Cogent Energy Solutions	USA	Plasma gasifier	MSW, biomass	~1–4 tons/day for each unit	Power, H_2, liquid fuels
Plasco Conversion Technologies	Canada	Moving-bed Plasma gasification	MSW	multiple 73,000 tons/yr	Power
Sierra Energy	USA	Blast furnace (FastOX)	MSW	36,500 tons/yr	Hydrogen, Power
Energos	Norway/UK	Chain furnace	MSW	~80–100 kt/yr	Power, CHP
Wildfire Energy	Australia	Mobile jet horizontal gasification	MSW	60 kW_{th}(pilot unit)	Power, H_2
Advanced Biofuel Solutions	UK	Fluidized-bed gasifier (RadGas)	MSW	8,030 tons/yr	Bio-methane, CO_2, vitrified ash
SUNY Cobleskill/ Caribou Biofuels	USA	Inclined rotary gasification	MSW	730 tons/yr	Power

Company/Process	Country	Gasifier Type	Feedstock	Capacity	Product
Ebara Corporation/ UBE Corporation	Japan	Fluidized-bed gasification	Waste plastics	71,200 tons/yr	Ammonia, methanol, olefin
Taylor Biomass Energy	USA	Dual bed fluidized-bed gasifier	MSW	400 /day	-

[a] Closed; construction is planned for a new commercial plant (Enerkem, 2025).

4.2 Oxygenated Intermediate Upgrading

As shown in Figure 4, various oxygenated intermediates, such as methanol, ethanol, butanol or C_2-C_5 mixed alcohols, can be produced from biomass or organic waste, which can be used as building blocks and further upgraded to SAF and/or bioproducts. Regardless of which oxygenated intermediate is selected, all conversion pathways include four major steps: production of light olefins, olefin oligomerization, hydrogenation, and product separation. Technology and conversion pathway selection for this design case (Figure 2) is based on the relatively high technology readiness level (TRL) of most of the conventional steps involved in MSW-to-methanol and MTJ (as detailed in Section 10.0). As shown in Figure 2, the process includes RDF production, gasification, methanol synthesis, production of light olefins, olefin oligomerization, hydrogenation, and product separation. In the MTJ pathway, methanol is converted into C_2–C_5 light olefins via the UOP/HYDRO MTO process (UOP, 2004; Vora et al., 1998), followed by oligomerization to C_{8+} olefins.

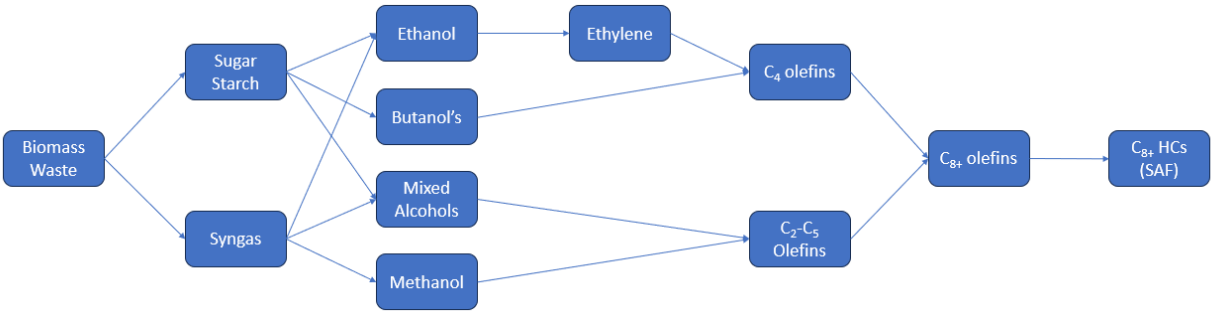


Figure 4. Pathways and technology options to produce SAF from biomass and organic waste via oxygenated intermediate upgrading.

Integrating the MTJ pathway into existing infrastructure offers promising economics for SAF development and diversifies feedstocks for SAF production. While both MSW gasification and MTJ have garnered significant attention, detailed design case studies of the integrated system are still relatively scarce in the literature. Recent research has focused on developing heterogeneous catalysts with nickel active sites for oligomerizing light olefins into jet fuel. While these catalysts have shown promise, they often suffer from limited product selectivity, primarily yielding dimers or trimers. To meet the carbon chain length requirements of jet fuel (C_8–C_{16}), new catalysts are needed that can effectively oligomerize C_2–C_5 olefins. The differing reactivity of these olefins presents a challenge, as current industrial processes use different catalysts for ethylene and higher olefins. Developing catalysts that combine both metal and acid active sites is a key area of research to produce jet-range compounds.

5.0 Regional Resource Assessment

5.1 Region Selection

Several factors should be considered for region selection to ensure favorable conditions for biofuel supply chains. This includes feedstock availability, which directly affects the process capacity for continuous production. Market demand, specifically in sectors that have limited alternative fuel options, such as aviation and transportation, ensures a stable and substantial market for biofuels. Additionally, the existence of incentive schemes at state and local levels can be critical for building resilient supply chains.

MSW is particularly advantageous as a biomass feedstock because of its large-scale availability and existing collection infrastructure. Unlike other biomass types, MSW is already collected at waste processing facilities nationwide, with the majority of it ultimately being disposed of in landfills. The EPA's Landfill Methane Outreach Program database provides technical data on U.S. landfills, including their locations, operational status (active/closed), total waste capacity, annual waste acceptance rate, and closure date (EPA, 2024a). Aggregation of the waste acceptance rates of active landfills indicates that an estimated 334.47 million metric tons of solid waste is disposed of annually across the United States. Figure 5 illustrates the spatial distribution of MSW by state. California alone contributes 11.7 percent of this total, with a significant feedstock availability of 39.06 million metric tons per year (MMT/yr), making it an ideal location for implementing a SAF production plant.

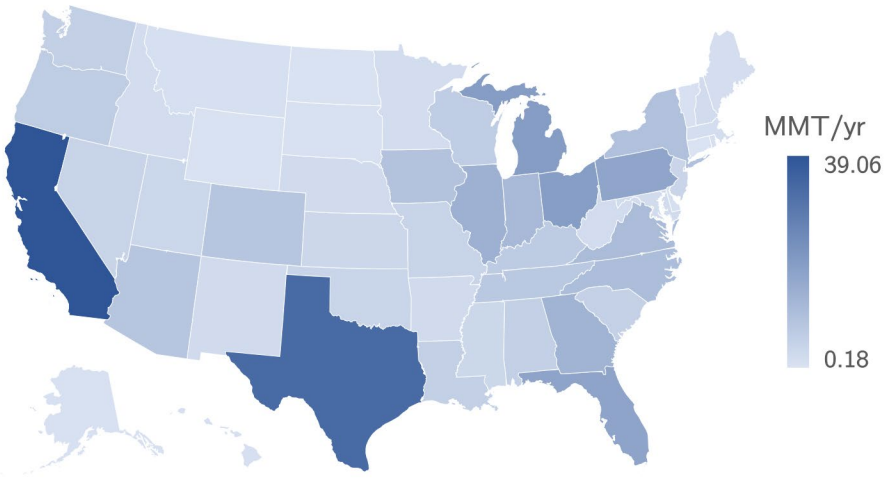


Figure 5. Annual landfill MSW acceptance rate (in million metric tons per year [MMT/yr]) by state (EPA, 2024a).

Moreover, according to the EIA, California uses 82.9 million barrels/yr and has the highest jet fuel consumption in the United States, accounting for 14.6 percent of nationwide demand (EIA, 2023b). Having an SAF plant in proximity to major airports would allow SAF fuels to be transported easily using trucks or existing pipeline systems at a lower cost.

Finally, the existence of low-carbon fuel standards, which are regulations designed to incentivize the production of renewable fuels used in transportation, creates a market opportunity for renewable fuels by generating an additional revenue stream through financial incentives. These

policy components can make California a more economically attractive candidate for in-state SAF production. Permitting is an entirely different matter and is not covered in this design case study.

5.2 Feedstock Composition and Characteristics

The feedstock considered in this study was mixed waste and trash destined for final disposal in landfills with no planned separation or diversion processes, such as sorting or material recovery (CalRecycle, 2022). Consequently, certain recyclable materials, such as plastics and paper, were mixed in with and contaminated in the waste stream, making them impractical to sort or recycle. The feedstock characterization in this work was based on a regional waste characterization study conducted by CalRecycle, which periodically performs waste characterization analyses. Data was sampled from the largest 45 landfills in California, representing approximately 90 percent of the total waste landfilled in the state and providing comprehensive and representative coverage of the MSW composition in the region (CalRecycle, 2022). Table 5 details the composition of the MSW assumed in this study.

For the MSW-to-SAF conversion process, the gasifier feed is assumed to be composed of waste types such as paper, plastics, organics, and miscellaneous waste (rock, soil, fines, textiles, carpet, tires, household miscellaneous waste, etc.). It is assumed that metals in the MSW stream are separated prior to gasification to recover their economic value through recycling and to increase the process efficiency by increasing the combustible feedstock yield. Recovered metals are either baled for sale, where they can be processed in recycling facilities, or directed to landfill if they are not suitable for recycling. Construction and demolition waste (concrete, asphalt, gypsum, and composites) and bulky items are assumed not to be mixed with conventional MSW processing facilities; thus, they are not included in the separation and preprocessing of MSW. After separation and size reduction (see Section 6.1), the remaining combustible portion of MSW is conversion-ready feedstock, referred to as RDF.

Table 5. MSW by waste category in California landfills (CalRecycle, 2022).

Waste Category	Amount (short tons)	Composition, wt%
Glass	926,882	3.22
Metal	1,960,400	6.80
Paper	6,193,825	21.49
Plastics and rubber	5,445,299	18.89
Organics – food	4,362,949	15.14
Organics – wood	4,251,969	14.75
Organics – yard trimmings, grass, and other	2,690,792	9.34
Rock, soil, and fines	201,767	0.70
Miscellaneous waste	2,789,982	9.68
Total	28,823,805	100.00

RDF, which would be fed to the gasification unit, was used for feedstock characterization. In line with previous proximate and ultimate analysis studies, the composition of RDF was characterized on the basis of the weighted averages of compositions (C, H, O, N, S for ultimate analysis and fixed carbon, volatile matter, moisture content, and ash for proximate analysis) and the corresponding waste category types listed in Table 5. Table 6 presents the ultimate analysis (Boumanchar et al., 2019; Shen et al., 2015) and proximate analysis (Ibikunle et al., 2018; Mazzoni et al., 2017; Shen et al., 2015; Shi et al., 2016; Zhao et al., 2022) results for the RDF

feed used in this study. Notably, composition and characterization of MSW can vary widely depending on the geographic region, waste management practices, and seasonal variations. For the purposes of this analysis, specific assumptions were made to standardize feedstock characteristics. However, further screening and characterization of RDF on the basis of primary data collection is vital to refine these assumptions, validate their applicability, and improve the accuracy of predictions regarding feedstock behavior and process performance.

Table 6. Combustible refuse-derived fuel feedstock characteristics used in this study.

Ultimate Analysis	Main Compositions, wt%
Carbon	52.53
Hydrogen	6.97
Oxygen	39.02
Nitrogen	1.23
Sulfur	0.25
HHV (MJ/kg)	20.19
Proximate analysis	
Fixed carbon	16.83
Volatile matter	65.41
Moisture content	7.86
Ash	9.91

5.3 Plant Capacity, Siting, and Transportation Logistics

The processing capacity of existing commercial plasma/plasma-enhanced gasification plants ranges from 100 to 1,000 tons per day (Table 4). In accordance with the literature and existing plasma-enhanced gasification plant data, the assumed design capacity for this study was 1,000 short tons per day (TPD) of RDF. Under the assumption of a 90 percent on-stream factor (7,884 operating hours per year), the annual MSW feedstock requirement is approximately 345,650 dry tons per year.

Conducting the local siting analysis for the SAF plant involved (i) identifying the locations of landfills, waste collection points (transfer stations), and their waste acceptance capacities, (ii) estimating the transportation distances between transfer stations and landfills, and (iii) selecting large-scale landfills and transfer stations with adequate MSW feedstock supply within proximity to each other to ensure cost-effective transportation of MSW. The EPA's Landfill Methane Outreach Program database provides technical data on U.S. landfills, including their locations and annual waste acceptance rate. Similarly, the Solid Waste Information System (SWIS) database contains information on solid waste facilities throughout California (CalRecycle, 2019). The EPA's Landfill Methane Outreach Program database and California's SWIS database were used to identify major landfills in the area and their corresponding waste transfer stations, respectively.



Figure 6. Selected sustainable aviation fuel plant location (circled in blue), featuring the largest landfill and multiple waste transfer/processing facilities in Los Angeles County, California (County of Los Angeles, 2013).

From resource screening and siting analysis, the SAF plant was assumed to be located near a large-scale landfill in the Southern California region (Figure 6). Several waste transfer stations in the SWIS inventory were identified near the candidate location, and their proximity to the SAF plant was calculated. The waste transfer stations are estimated to be able to supply MSW feedstock to the selected SAF plant location at a rate up to 7,100 TPD, with an average transportation distance of 14.7 miles (29.4 miles round-trip). The transportation cost of MSW feedstock for an SAF plant processing 1,143 TPD of MSW (1,000 TPD of RDF) is estimated to be $6.35 per ton of RDF ($5.56 per ton of unsorted MSW), according to the trucking and transportation cost factors detailed in Table 7.

Table 7. Feedstock transportation logistics and economics (plant scale: 1,000 short tons per day [TPD] of refuse-derived fuel [RDF]) (Seiple et al., 2023).

	Unit	Value
Conversion-ready feedstock (RDF)	TPD	1,000
Imported municipal solid waste	TPD	1,142.97
Gasification feedstock (w/ ash)	%	82.26
Non-combustibles	%	9.88
Waste moisture	%	7.86
Transportation cost factors		

	Unit	Value
Truck capacity	dry short ton	15.96
Operation cost	$/mile	3
Number of trucks	# trucks	70
Transportation distance (round-trip)	miles	29.4
MSW source to transfer station	miles	9.8
Transfer station to plant	miles	19.6
Delivery cost	$/dry short ton of RDF	6.35

6.0 Process Design

As shown in Figure 7, the proposed MSW-to-SAF process includes seven main process areas:

- Area 100: MSW Sorting and Preprocessing
- Area 200: Gasification
- Area 300: Syngas Cleanup and Conditioning
- Area 400: Methanol Synthesis
- Area 500: Jet-Fuel Production and Separation
- Area 600: Steam Plant and Power Generation
- Area 700: Waste Treatment and Balance of Plant

A chemical process simulation was performed in Aspen Plus V14 to generate rigorous material and energy balances for each unit operation and the integrated process. Techno-economic analysis (TEA) was performed to estimate CAPEX and operating expense (OPEX) for the biorefinery. A discounted cash flow economic model was used to calculate MFSP. A life cycle assessment (LCA) was performed to evaluate the life cycle $CO_{2,eq}$ emission from producing SAF from MSW, which was then compared against a conventional jet fuel baseline. In Area 100, MSW is converted into RDF via sorting, glass and metal removal, shredding, and screening. RDF, basically the ground organic portion of MSW, is then gasified to produce raw syngas (containing H_2, CO, CO_2, and various impurities) in Area 200. In Area 300, raw syngas is cleaned through syngas conditioning, while the H_2/CO_2 is adjusted to the desired value for downstream conversion. In Area 400, the clean syngas is converted into methanol. In Area 500, methanol is converted into SAF via the four-step approach (MTO, olefin oligomerization, hydrogenation, and fractionation). In addition to SAF, small amounts of renewable naphtha and diesel by-products are produced. Steam and power are produced in Area 600, and Area 700 primarily consists of the cooling water system and waste treatments. The process areas are described in more detail in the following sections.

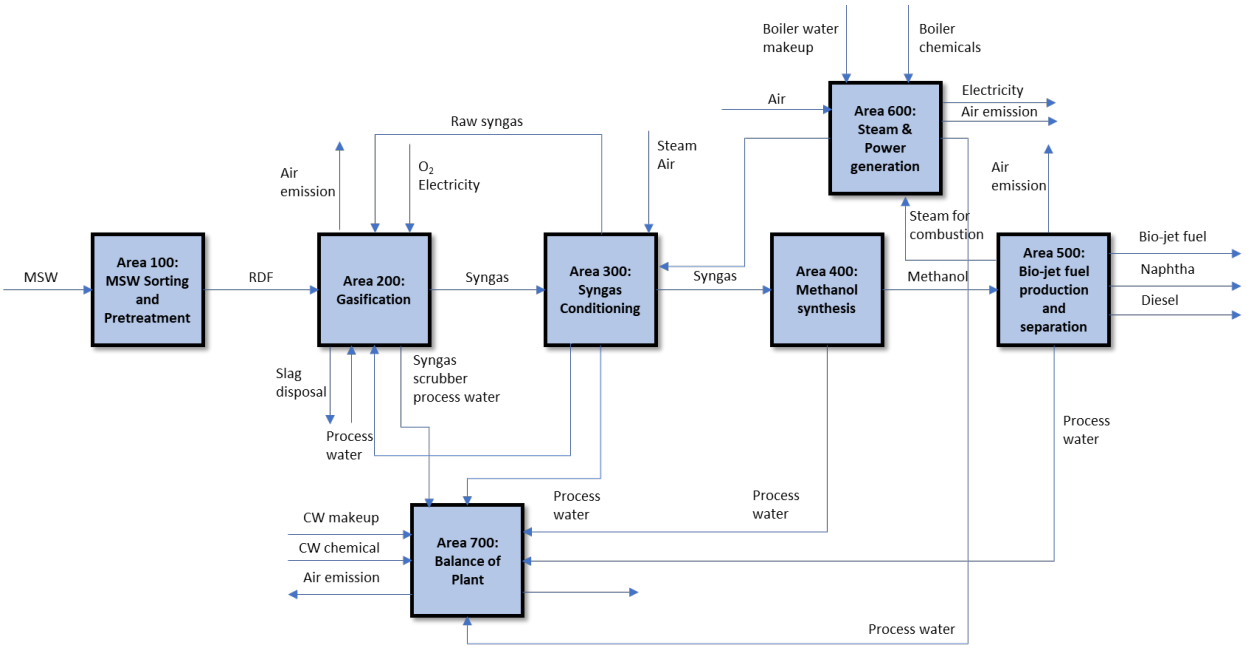


Figure 7. Block flow diagram of the process of converting municipal solid waste (MSW) into sustainable aviation fuel.

Because significant amounts of electricity and steam are consumed during the conversion process, two design cases were investigated in the design case study:

- **Case 1 (SAF-max):** All syngas produced from Area 300 is sent to Area 400 for methanol production, while Area 600 only leverages waste heat and light gases generated during conversion for steam and power production. In this case, the on-site steam and power generation unit cannot support the utility demands of the entire plant, with the balance satisfied through the purchase of electricity from the grid. Although this case maximizes SAF production, relying on grid electricity may limit its overall $CO_{2,eq}$ emission reduction benefits.
- **Case 2 (Self-powered):** In addition to waste heat and light gases, a portion of syngas from Area 300 is sent to Area 600 to generate power and steam on-site, creating a self-sufficient energy system. This case can maximize the $CO_{2,eq}$ emission reduction benefits because no grid electricity is required. However, its SAF production rate is lower than that of Case 1 because a portion of the syngas produced from MSW is not sent to the methanol synthesis unit, potentially resulting in higher production costs.

6.1 Area 100: MSW Sorting and Preprocessing

Separating non-combustible materials from raw MSW ensures higher-quality feedstock with more homogenous composition and higher heating value, which is desirable for efficient conversion. Although plasma-enhanced gasification technology can handle a wide variety of feedstocks, metals present in MSW are assumed to be separated for increased syngas yields as a result of improved conversion efficiency. Although metals are assumed to be recovered, the separation of plastics and paper was not considered in this study because of several practical and economic limitations. The waste stream considered in this study primarily consists of mixed waste and trash intended for landfill disposal that has not undergone sorting at the collection point or represents the residues generated by material recovery facilities that were deemed unrecyclable (rejects) and directed to landfill (CalRecycle, 2022). The lack of upstream trash separation and the quality

issues for MRF rejects indicate that potentially recyclable materials in the mixed waste stream, such as plastics and paper, are often degraded and heavily contaminated by organic waste, dirt, moisture, or other residues. This contamination significantly diminishes their quality, complicating the feasibility and economics of including separation and recycling in the scope of this study (Brown et al., 2022; Pivnenko et al., 2016; Qureshi et al., 2020).

As shown in Figure 8, the separation and preprocessing area is assumed to be analogous to an RDF production line, including (i) shredding, (ii) ferrous material recovery using magnetic separators, (iii) aluminum recovery using eddy current separators, (iv) categorization by size and weight using disc screens and an air classifier, and (v) further grinding. The recovered metal portion of the RDF is baled and sold as scrap metal, whereas reject materials that mainly contain heavy material with high water content and low-quality recovered materials with no end use are directed to a landfill.

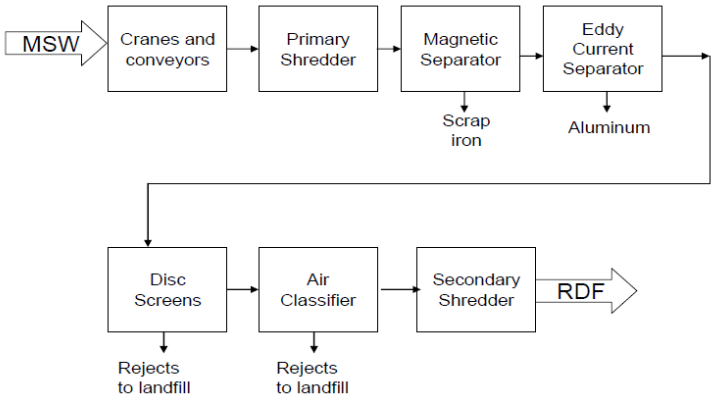


Figure 8. Block flow diagram of a facility's process of converting municipal solid waste (MSW) into refuse-derived fuel (RDF) (Jones et al., 2009).

In this design case study, the RDF plant is assumed to be co-located with the SAF plant. The facility is expected to operate on a similar schedule with material recovery facilities. In this study, the RDF facility is assumed to operate for 16 h/day (2 shifts, 8 h per shift) with a total MSW processing capacity of 71.4 short tons per hour and two separate process lines (35.7 short tons per hour per line), ensuring operations within material recovery facility capacity limits (Thompson, 2020). This rate is necessary to provide a 1,000 TPD feedstock to the gasifier, which operates continuously. Table 8 summarizes the key parameters for the RDF facility.

Table 8. Key process specifications for refuse-derived fuel (RDF) facility.

Variables	Specifications
SAF Plant Scale	1,000 TPD RDF
Recovered metal composition by wt%:	
Metal | Al (recyclable)	1.53%
Metal | Al – CRV (recyclable)	4.60%
Metal | ferrous (recyclable)	24.49%
Metal | other[a] (non-recyclable)	69.38%

Variables	Specifications
RDF composition by wt%:	
Combustibles, dry ash free basis (wet with ash)	78.23% (95.12%)
Metal[b]	0.70%
Glass[c]	3.43%
Rock, soil, and fines[c]	0.75%
Operating hours per day (8 h/shift, 2 shifts)	16 h
Number of MSW-to-RDF process lines	2
MSW throughput for preprocessing	1,143 TPD or 35.7 TPH/line

[a] Other category is the remaining lower-quality portion that is recovered and disposed at landfill along with other rejects.
[b] Remaining metal (20 percent aluminum and 80 percent ferrous metals) in MSW stream after magnetic and eddy current separation steps. Average metal recovery efficiency of the RDF line is assumed as 90.5 percent.
[c] Small particles such as glass, soil, rocks and fines are not completely separated to minimize the loss of combustible materials in the sorting process. These materials cannot be recycled as metals, making up only a small fraction of the feedstock.
MSW = municipal solid waste; TPD = short tons per day; TPH = short tons per hour; CRV = California redemption value.

6.2 Area 200: Gasification

To better understand current challenges and opportunities, industry outreach and technology reviews were conducted, as detailed in Section 4.1. The directly heated fluidized-bed and plasma gasifiers were selected for further analysis because of their commercial viability and technological advantages. Both configurations operate at very high temperatures, resulting in low tar and methane yields, which can eliminate the need for costly and pragmatical tar reforming. Compared with other gasifier types, these configurations can handle a wider range of feedstocks, including hazardous waste, with minimal preprocessing, making them ideal for MSW gasification. This choice was also made to provide a different perspective from the direct-heated gasification and tar reforming technologies that have been more extensively studied.

Plasma gasifiers use plasma torches to break down the waste solid into syngas. Plasma-enhanced gasifiers often employ a plasma melter at the bottom of a downdraft gasifier. Plasma, often referred to as the fourth state of matter (alongside solid, liquid, and gas), is a very hot, highly ionized (charged) gas that can conduct electrical current, just like lightning, a kind of natural plasma. Human-made plasma is formed by passing an electrical discharge through a gas such as air or O_2. The electric arc dissociates the gas into electrons and ions and causes the temperature to increase significantly, often exceeding 10,832 °F (NETL, 2024e). Such high temperatures easily and rapidly break down heterogeneous feedstocks, including hard-to-gasify wastes. In a typical plasma gasifier (e.g. WPC plasma gasifier or Alter NRG gasifier), the feedstock enters from the top of the vessel, slowly moving downward, and the air or oxygen feed enters at the bottom of the vessel; in the gasifier configuration used in this study, the syngas product is concurrently extracted from the side at the top of the vessel.

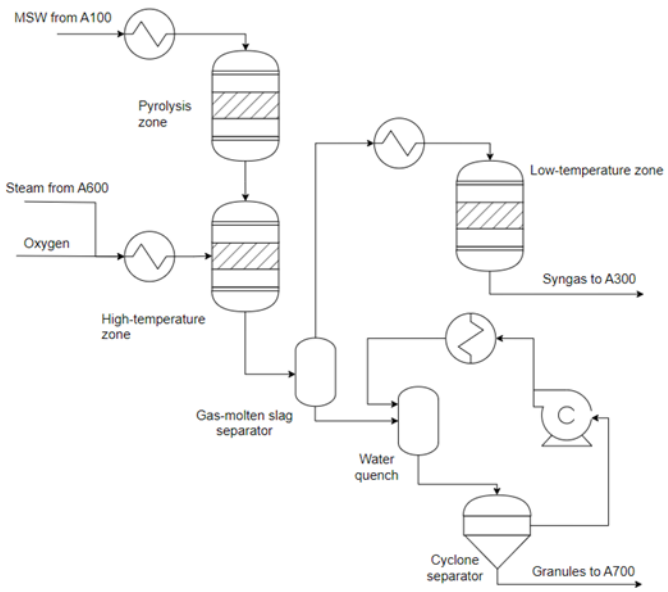


Figure 9. Simplified process configuration of plasma gasification in Area 200: Gasification.

In this work, the plasma-enhanced gasification unit was modeled in Aspen Plus following the method used by Janajreh et al. (2013), where the gasification is divided into three different zones: pyrolysis, high-temperature, and low-temperature zones (Janajreh et al., 2013). In this study, for the proximate and ultimate analyses, RDF was modeled as a nonconventional solid with the characteristics detailed in Table 6. RDF first enters the pyrolysis zone, where thermal decomposition occurs. This pyrolysis zone is modeled as a yield reactor converting solid fuel into C, H_2, O_2, N_2, S, ash, and H_2O, whose yields were estimated on the basis of the proximate and ultimate analyses. A mixture of pure O_2 (77 °F, 14.7 psia) from the air separation unit and low-pressure steam (287 °F, 52.9 psia) from Area 600 is used as the plasma gas. This mixture is first heated to 4,496 °F by a cross-heat exchanger and then heated further to 7,232 °F by an electric heater to produce plasma gas. The plasma gas and the decomposed MSW stream are fed into the high-temperature zone, where a Gibbs reactor is used to estimate the conversion rate and product selectivity at chemical equilibrium. The exothermic energy from the high-temperature zone is transferred to the pyrolysis zone for solids decomposition. Molten slag is separated from the gas product, mixed with quench water to lower its temperature 194 °F, and discharged as solid granules. The syngas stream is then sent to the low-temperature zone operating at 2,282 to 2,399 °F (Mazzoni and Janajreh, 2017). The low-temperature zone is modeled as an adiabatic Gibbs reactor. The O_2 flow rate is controlled to ensure a temperature of 4,532 °F at the high-temperature zone outlet, while the steam flow rate is specified to maintain a hydrogen-to-carbon monoxide (H_2/CO) molar ratio of 0.9 to 1 in the raw syngas leaving the gasifier. The gasification process is modeled as a set of seven reactors running in parallel with a processing capacity of 150 TPD/reactor and one spare reactor serving as a backup to allow maintenance for the main reactors. The mass balance and energy balance of Area 200 are summarized in Table 9; the values are the same for both base cases.

Table 9. Mass and energy balances for Area 200: Gasification.

	Base Cases 1 & 2	Units
Raw material inputs		
RDF from Area 100	0.630	lb/lb raw syngas

	Base Cases 1 & 2	Units
O_2 from air separation unit	0.265	lb/lb raw syngas
LP steam from Area 600	0.195	lb/lb raw syngas
Fresh water	0.010	lb/lb raw syngas
Utility consumptions		
Cooling water	58.23	Btu/lb raw syngas
Electricity	0.239	hp/lb raw syngas
Product outputs		
Raw syngas to Area 300	1	lb/lb raw syngas
Granules	0.1	lb/lb raw syngas

LP = low pressure; RDF = refuse-derived fuel.

6.3 Area 300: Syngas Cleanup and Conditioning

In the syngas cleanup and condition unit, impurities (e.g., HCl, CO_2, and H_2S) are removed from raw syngas and the H_2/CO molar ratio is adjusted to 2, as required in the downstream methanol synthesis unit. A simplified process configuration of Area 300 is illustrated in Figure 10, and a detailed process flow diagram is presented in Appendix D. The hot raw syngas from Area 200 is first cooled to 307 °F via heat recovery and steam generation. It is further cooled to 140 °F in a water-cooled heat exchanger and then to 124 °F via water quenching, where about 66 percent of water in the raw syngas is condensed and sent to the wastewater treatment unit. As reported by Pullao et al. (2024), chlorine originating from polyvinyl chloride in MSW feedstocks reacts with metals such as cesium (Cs) and copper (Cu) within a plasma gasifier, primarily ending up in the slag phase (Pullao et al., 2024). However, trace amounts of HCl may remain in the syngas stream and must be removed to prevent catalyst poisoning and equipment corrosion in downstream processes. The European Investment Bank (2024) also highlights that chlorine thresholds for biofuel applications should remain below 0.8–2 percent, depending on the end-use sector (European Investment Bank, 2024). To meet these specifications, an HCl removal unit is critical to control residual chlorine levels before the dry syngas enters subsequent conditioning and conversion steps. The selection of HCl removal technology depends on process conditions and the chlorine concentration in the freestream. In general, caustic wet scrubbing is the most commonly applied method for HCl removal for syngas derived from biomass or coal gasification (NETL, 2025). This approach can reduce HCl concentrations to below 1 ppm (Hrbek et al., 2025). Another viable approach is solid bed adsorption, in which sorbents such as Na_2CO_3, K_2CO_3, or $NaAlO_2$ are employed, with operating temperatures exceeding 400 °C. This method has also demonstrated effectiveness in removing HCl from syngas (Marcantonio et al., 2021). Given that the expected HCl concentration is low and the process design is in the conceptual stage, the specific HCl removal technology for plasma gasifier syngas has not yet been finalized. The process simulation and associated TEA do not explicitly model HCl removal because of its minor impact. However, it must be noted that an HCl removal unit remains essential and must be implemented if residual chlorine is detected in the syngas. After HCl removal, the dry syngas is preheated to 376 °F and sent to the COS hydrolysis reactor to convert COS into H_2S, allowing sulfur impurities to be easily removed in the acid gas removal (AGR) unit. The H_2/CO ratio is adjusted in the water-gas shift (WGS) reactor, where CO and H_2O are converted into H_2 and CO_2, as shown in Equation (2), in a fixed-bed catalytic reactor. Notably, the WGS reaction is equilibrium-limited, favoring elevated operating temperature and pressure. Recycling a portion of the WGS reactor product after CO_2 removal and feeding the extra amount of steam to the reactor can favor the forward reaction.

$$CO + H_2O \leftrightarrow H_2 + CO_2 \quad (2)$$

In Case 1 (SAF-max), all syngas from the COS hydrolysis reactor is cooled and compressed to 420 psia and then fed into the AGR unit, along with the cooled WGS reactor outlet. In Case 2 (Self-powered), a portion of syngas from the COS hydrolysis reactor bypasses the compressor and is sent to Area 600 for steam and power generation to avoid purchasing electricity from grid. In the AGR unit, amine-based solvent is used to remove CO_2 and H_2S from syngas. A portion of the clean syngas from the AGR unit is sent to the WGS reactor, operated at 430 psia and 907 °F, along with superheated HP steam to achieve the targeted H_2/CO ratio, while the remaining clean syngas is sent to Area 400 for methanol production. The shifted syngas from the WGS reactor is then cooled via heat integration and the use of cooling water before being sent back to the AGR unit. Table 10 summarizes the mass and energy balance for Area 300.

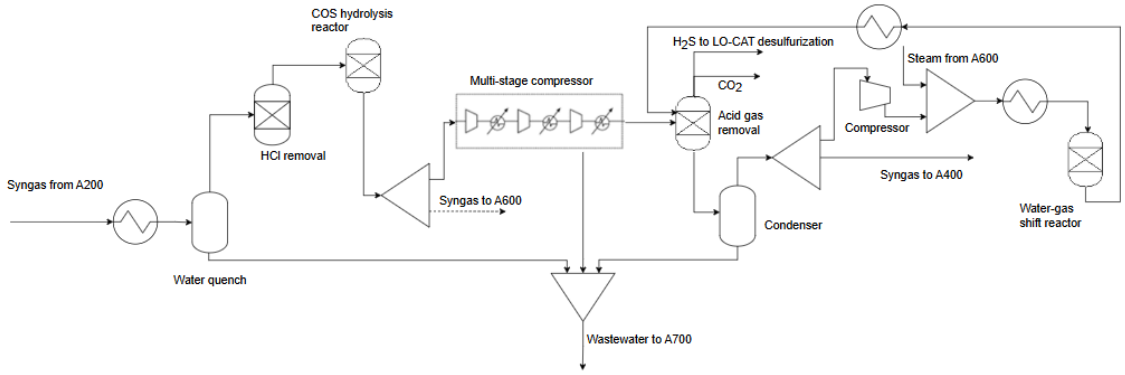


Figure 10. Simplified process configuration of Area 300: Syngas Cleanup and Conditioning.

Table 10. Mass and energy balance of Area 300: Syngas Cleanup and Conditioning.

	Base Case 1 (SAF-max)	Base Case 2 (Self-powered)	Units
Raw material inputs			
Raw syngas from Area 200	2.464	3.974	lb/lb clean syngas
High-pressure steam from Area 600	0.741	0.742	lb/lb clean syngas
Utility consumptions			
Cooling water	2,075	2,310	Btu/lb clean syngas
Heater	41.6	41.53	Btu/lb clean syngas
Electricity	0.22	0.22	hp/lb clean syngas
Product outputs			
Clean syngas to Area 400	1	1	lb/lb clean syngas
Raw syngas to Area 600		1.249	lb/lb clean syngas
Sulfur to Area 700	0.003	0.003	lb/lb clean syngas
CO_2	1.344	1.344	lb/lb clean syngas
Wastewater to Area 700	0.862	1.123	lb/lb clean syngas

6.4 Area 400: Methanol Synthesis

In the process configuration for Area 400: Methanol Synthesis (Figure 11), the clean syngas from Area 300 is sent to knockout drum to remove entrained water and compressed to 925 psia before being sent to the methanol synthesis reactor, operating at 500 °F. The methanol synthesis reactions, as shown in Equations (3) and (4), are exothermic, meaning that the reaction heat needs to be continuously removed to maintain the reaction temperature. Therefore, a shell-and-tube type reactor is used, where clean syngas is fed to the tube side packed with copper/zinc oxide/alumina catalyst, and cooling water is fed to the shell side to remove the reaction heat.

$$CO + 2H_2 \leftrightarrow CH_3OH \quad (3)$$

$$CO_2 + 3H_2 \leftrightarrow CH_3OH + H_2O \quad (4)$$

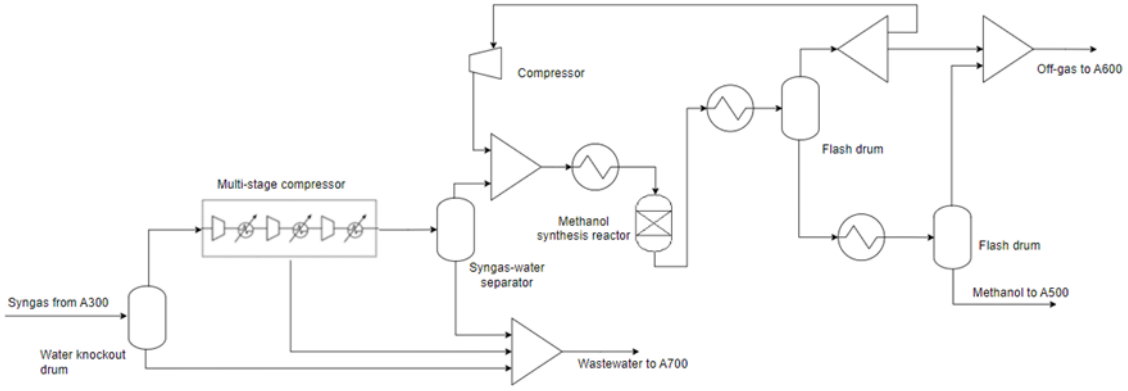


Figure 11. Simplified process configuration of Area 400: Methanol Synthesis.

The single-pass conversion of CO is 16.5 percent, and the overall conversion of CO to methanol is 99.8 percent. Methanol synthesis is highly exothermic, and heat from the reactor is removed via steam generation on the shell side of the reactor. The heat from the reactor effluent stream is recovered via preheating of the reactor inlet stream. The product stream is sent to a flash drum to separate unreacted syngas and other inert gases from liquid raw methanol. Approximately 97 wt% of the vapor phase is recycled back to the methanol synthesis reactor, and the remaining 3 wt% is purged to the furnace for heat generation. The liquid methanol is recovered by first reducing the liquid stream pressure to 65 psia and directing it to a second flash drum where methanol with 93.14 wt.% purity is obtained. The mass balance and energy consumption for Area 400: Methanol synthesis is summarized in Table 11.

Table 11. Mass and energy balance of Area 400: Methanol Synthesis.

	Base Case 1 (SAF-max)	Base Case 2 (Self-powered)	Units
Raw material inputs			
Clean syngas from Area 300	1.178	1.178	lb/lb methanol
Utility consumptions			
Cooling water	1,844.27	1,844.22	Btu/lb methanol
Electricity	0.06	0.06	hp/lb methanol

	Base Case 1 (SAF-max)	Base Case 2 (Self-powered)	Units
Product outputs			
Methanol to Area 500	1	1	lb/lb methanol
Off-gas to Area 600	0.176	0.176	lb/lb methanol
Wastewater to Area 700	0.002	0.002	lb/lb methanol

6.5 Area 500: Methanol to Sustainable Aviation Fuel

The production of SAF via methanol involves MTO, olefin oligomerization, hydrogenation, and fuel separation, as shown in Figure 12. The MTO process, modeled on the basis of the UOP/Hydro Process (UOP2004; Vora1998; US6166282), starts with preheating the methanol stream to 241 °F at 65 psia. The preheated methanol is then sent to a fluidized-bed reactor filled with SAPO-34 catalyst. Methanol is converted into light olefins (ethylene, propylene, 1-butene, and 1-pentene) with a 99.9 percent methanol conversion rate and high selectivity toward olefins (93.26 percent carbon efficiency).

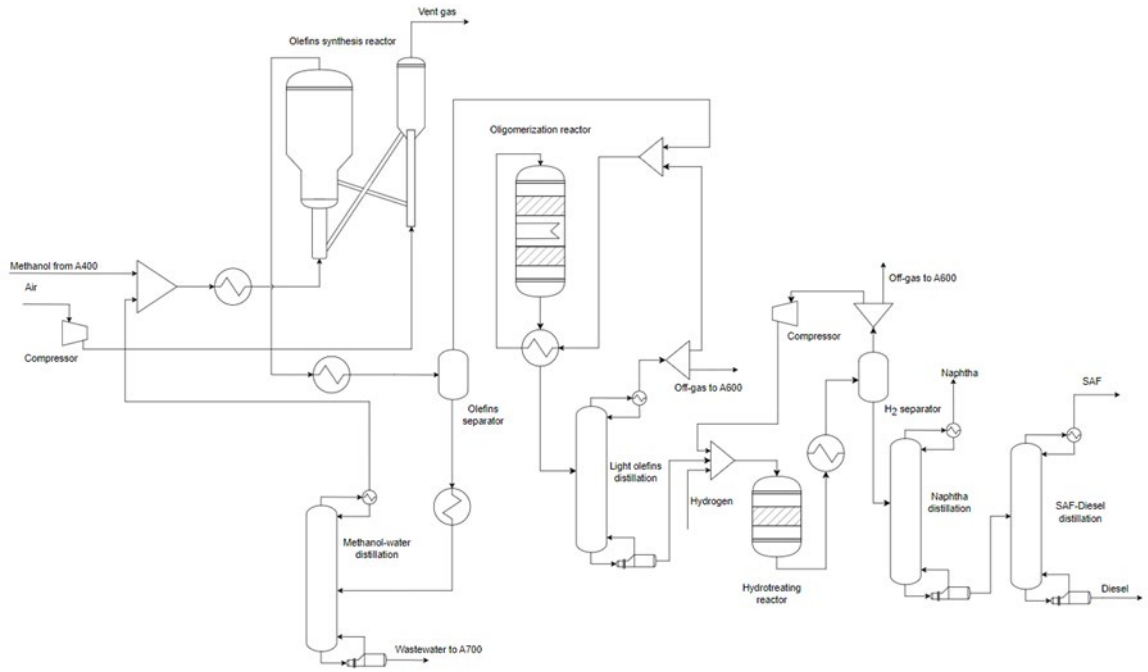


Figure 12. Simplified process configuration of Area 500: Methanol to SAF.

The reactor inlet stream is preheated to recover heat from the reactor effluent stream (831 °F, 65 psia). Coke formed during the reaction is burned periodically to prevent rapid deactivation of SAPO-34 catalyst. The MTO reactor effluent—which contains 57.4 wt% water, 40.4 wt% olefins, 1.7 wt% paraffins, 0.4 wt% H_2, CO, and CO_2 mixture, and 0.1 wt% methanol—is then directed to a series of flash drums to separate olefins from the methanol/water mixture. The olefin-rich gas mixture is recovered from the top of the tower, whereas the methanol/water mixture is collected from the bottom and sent to a stripper. In the steam stripper, methanol is removed from water and recycled back to the MTO reactor, and the remaining water is sent to a wastewater treatment plant. The olefin-rich mixture recovered from the flash drum is further separated from acid gases by a scrubber using 50 wt% aqueous caustic solution.

The experimental results collected from PNNL's continuous flow system with an on-stream time of 24 h were used to model the oligomerization process. In the experiment, a bifunctional Ni/SiO_2-Al_2O_3 (metal)/Zeolites (acid) catalyst was placed in a single reactor operated at 482 °F, 300 psi with a weight hourly space velocity of 0.5055 h^{-1} for single-step co-oligomerization of C_2 to C_5 mixed olefins. The oligomerization process was modeled in Aspen Plus as a series of six stoichiometric reactors with intermediate coolers. The oligomerization reaction is exothermic; therefore, heat needs to be removed to keep the temperature constant at 482 °F. A complete mass balance and atom balance for C and H was conducted. The stoichiometric coefficients were first calculated under the assumption of no recycling of the unconverted reagents. A second set of stoichiometric coefficients were then calculated after the addition of the recycled stream. The oligomerization process also included the formation of aromatics, produced at a rate of 2 percent of the feedstock. Because it releases hydrogen in the system, aromatics formation is thought to be responsible for the hydrogenation of alkenes into alkanes and carbon loss.

The experimental results indicated a 100 percent mass balance closure (Table 12). This meant that no data reconciliation was necessary before the chemical process simulation, thereby improving the accuracy of the results. The jet-range olefin selectivity in liquid products was over 74 wt%, while the carbon loss to C_2–C_5 alkanes and heavy alkanes (C_{19+}) was 1.5 wt% and 0.5 wt%, respectively. Light hydrocarbons (C_2-C_5) are separated via distillation and recycled to the oligomerization reactor, whereas heavy olefins (C_{6+}) from the distillation bottoms are routed to the hydrotreating step.

The hydrotreater was modeled as an adiabatic RStoic reactor operating at 572 °F and 136 psi, with a controlled hydrogen flowrate to maintain an inlet H_2-to-olefins molar ratio of 3.5. The reactions assume complete conversion of olefins to paraffins. The hydrotreated product stream is subsequently separated into H_2-rich gas, naphtha (C_5-C_7), SAF (C_8-C_{18}), and diesel (C_{19+}) through flash drum followed by two distillation columns. The mass balance and energy consumption for Area 500: methanol to SAF are summarized in Table 13.

Table 12. Summary of experimental results for single-path oligomerization.

Total Input	**46.9 g**	**Total Output**	**46.9 g**				
Conversion	%	Liquid products	g	wt%	Gas products	g	wt%
$C_{2=}$	93	Jet range (C_8–C_{18})	34.8	74.1	Recycle (C_2–C_5)	2.3	4.9
$C_{3=}$	97	Recycle (C_5–C_7)	8.2	17.4	Purge (C_2–C_5)	1.5	3.1
$C_{4=}$	98	C loss (C_{19+} alkanes)	0.2	0.5			
$C_{5=}$	98	Total liquid	43.1	91.9	Total gas	3.8	8.1

Table 13. Mass and energy balance for Area 500: Methanol to SAF.

	Base Case 1 (SAF-max)	**Base Case 2 (Self-powered)**	**Units**
Raw material inputs			
Methanol from Area 400	2.915	2.915	lb/lb SAF
Hydrogen	0.016	0.016	lb/lb SAF
Air	2.807	2.807	
Utility consumptions			
Cooling water	2,459.33	2,458.96	Btu/lb SAF

	Base Case 1 (SAF-max)	Base Case 2 (Self-powered)	Units
Heater	382.69	382.90	Btu/lb SAF
Electricity	0.18	0.18	hp/lb SAF
Product outputs			
Sustainable Aviation Fuel (SAF)	1	1	lb/lb SAF
Naphtha	0.082	0.082	lb/lb SAF
Diesel	0.007	0.007	lb/lb SAF
Off-gas to Area 600	0.31	0.31	lb/lb SAF
Flue gas	2.830	2.830	
Wastewater to Area 700	1.509	1.509	lb/lb SAF

6.6 Area 600: Steam and Power Generation

Area 600 is designed to burn off-gases from Area 400 and Area 500 and/or split raw syngas stream from Area 300 to produce steam and electricity that can be used in the main conversion area. As mentioned at the beginning of Section 6.0, because of the high electricity consumption in Area 200 (Table 9), two cases were considered for the baseline design. Case 1 maximizes SAF production by utilizing all raw syngas produced from Area 200 for methanol synthesis. In this case, the combustion of off-gas, without the need for external natural gas, is sufficient to supply the low-pressure steam required by Area 200, the HP steam required by Area 300, and other required process heat, which can also produce 10.2 MW of electricity. However, the use of an electric heater to produce plasma gas, which requires 23.6 MW of electricity, necessitates external electricity to be purchased from grid. In Case 2, a portion of raw syngas is sent to Area 600 to produce sufficient electricity on-site and avoid the purchase of electricity from the grid. This case can potentially maximize $CO_{2,eq}$ emission reduction, at the expense of lower SAF yield. Table 14 lists the steam turbine operating parameters and the generated steam conditions.

Table 14. Operating parameters of the steam generator and steam turbine.

	Base Case 1 (SAF-max)	Base Case 2 (Self-powered)
HP steam (°F, psi)	831, 682	842, 1305
IP steam (°F, psi)	655, 315	655, 315
LP steam (°F, psi)	287, 53	287, 53
Steam turbine, in/out pressure (psi)	682/1	1,305/14.5
Power output (MW)	10.2	31.8
Power efficiency (LHV), %	35.3	60.7

HP = high pressure; IP = Intermediate pressure; LHV = lower heating value; LP = low pressure.

6.7 Area 700: Waste Treatment and Balance of Plant

This area is used to track the utilities required by the SAF production facility, including cooling water, process water, and plant air. This area also tracks the electricity usage throughout the plant. The primary wastes generated in this process are solid granules from plasma-enhanced gasification and wastewater from Areas 300, 400, and 500. Solid granules are disposed of via landfill. The wastewater contains contaminants such as ammonia, sulfur, and methanol. Therefore, a wastewater treatment system is implemented to remove these contaminants,

allowing the cleaned water to be returned to the water cycle or reused. Additionally, acid gases like H_2S and CO_2 from the syngas cleanup process must be controlled to minimize environmental impact and ensure safety. In this study, the LO-CAT sulfur removal process is used to convert H_2S into elemental sulfur, which is then disposed of via landfill. The waste CO_2 is directly emitted into the atmosphere.

A cooling tower is utilized to generate cooling water for the process. In the cooling tower, water collected from all the water coolers is cooled from 68 °F down to 60 °F and then recycled back into the system. Ambient air at 59 °F flows through the cooling tower, removing heat from the cooling water, and exits into the atmosphere at 65 °F.

7.0 Base Case Economic Assessment

To evaluate the economic feasibility of the process, a TEA model was developed using material and energy balance information from Aspen Plus. A discounted cash flow analysis was performed to determine the MFSP required to obtain an NPV with a certain IRR. Equipment costs were estimated using literature cost-correlations (Dutta et al., 2015, 2011; Phillips et al., 2007). CAPEX values were converted into 2020 dollars using the Chemical Engineering Plant Cost Index (CEI, 2008). Equation (5) was used to calculate the purchase cost for equipment given a baseline equipment size:

$$New\ cost = (Base\ cost)\left(\frac{New\ size}{Base\ size}\right)^{n} \quad (5)$$

where *n* is a characteristic scaling exponent (typically in the range of 0.6 to 0.7) based on the equipment characteristics (Humbird et al., 2011). Once the total installed equipment cost was evaluated for the year of interest, indirect costs were added (including for engineering, site development, contractors, and project contingency) to calculate the fixed capital investment. The total capital investment was calculated as the sum of the fixed capital investment and the land and working capital costs.

7.1 Total Capital Investment

Table 15. Detailed project cost summary for 1,000 TPD MSW-to-SAF plants.

	Base Case 1 (SAF-max)		Base Case 2 (Self-powered)	
	Capital Costs, MM$		Capital Costs, MM$	
Process Area	**Purchased**	**Installed**	**Purchased**	**Installed**
Area 100: MSW Sorting and Preprocessing	6.1	8.8	6.1	8.8
Area 200: Gasification	76.8	189.7	76.8	189.7
Area 300: Syngas Cleanup and Conditioning	13.8	28.8	9.8	20.4
Area 400: Methanol Synthesis	10.9	24.8	10.0	23.2
Area 500: Methanol to SAF	11.7	28.1	8.5	20.4
Area 600: Steam and Power Generation	10.6	17.7	21.8	36.7
Area 700: Waste Treatment and Balance of Plant	2.2	6.1	2.2	6.1
Total	132.2	303.8	135.2	305.3
Site development		10.8		10.1
Total Direct Cost		**314.7**		**315.4**
Engineering, site development, piping, other		157.3		157.7
Project contingency		31.5		31.5
Total Indirect Cost		188.8		189.2
Fixed Capital Investment (FCI)		503.5		504.6
Land		1.7		1.7
Working capital		25.1		25.1
Total Capital Investment		**530.3**		**531.5**
Lang factor (FCI/purchased equip cost)		**4.01**		**3.93**

MSW = municipal solid waste; SAF = sustainable aviation fuel; TPD = Short tons per day.

Table 15 shows the contributions of process areas to the total CAPEX. Combined, Area 200: Gasification and Area 300: Syngas Cleanup and Conditioning contributed to 71 percent and 69 percent of the total direct cost in Base Case 1 and Base Case 2, respectively. Area 200: Gasification was the single largest contributor (62 percent of the total direct cost). Notably, in addition to the required set of gasifiers running in parallel, one spare gasifier was considered to ensure on-stream time. Area 500: Methanol contributed to 9 percent and 7 percent, and Area 400: Methanol Synthesis contributed to 8 percent and 7 percent of the total direct costs in Base Case 1 and Base Case 2, respectively. Combined, the remaining areas (Area 100: MSW Sorting and Preprocessing, Area 600: Steam Plant and Power Generation, and Area 700: Waste Treatment and Balance of Plant) contributed to 11 percent and 17 percent of the total direct costs in Base Case 1 and Base Case 2, respectively. The cost for Area 600 is higher in Base Case 2 than in Base Case 1 because of the production of electricity on-site. However, given the lower mass flow of syngas that is converted, the capital costs of Areas 300, 400, and 500 are lower in Base Case 2 than in Base Case 1. Overall, the two effects offset each other, and the total capital investment is only marginally lower in Base Case 1.

7.2 Process Variable and Fixed Operating Costs

Table 16 shows the contributions of variable operating costs in Base Cases 1 and 2. In Base Case 1, electricity consumption is the main contribution, corresponding to 53 percent of variable operating costs. By contrast, in Base Case 2, the main contribution is the feedstock (39 percent), and the contribution of electricity consumption is only 8 percent. Overall, the conversion cost per gasoline-gallon equivalent is 37 percent lower in Base Case 2 than in Base Case 1.

Table 17 and Table 18 show the fixed operating costs in Base Case 1 and 2, which include labor costs and overheads. Because of its lower mass flows of products, Base Case 2 has much higher labor costs and total fixed operating costs (including overheads) per gasoline-gallon equivalent (more than 60 percent) compared with Base Case 1.

Table 16. Variable operating costs for the MSW-to-SAF plant.

$/gge product (MM$/yr)	Base Case 1 (SAF-max)	Base Case 2 (Self-powered)
Municipal solid waste	0.22 (4.9)	0.36 (4.9)
Hydrogen	0.08 (1.8)	0.08 (1.1)
Catalysts & Chemicals	0.14 (3.1)	0.17 (2.3)
Waste Disposal	0.15 (3.2)	0.24 (3.2)
Electricity and other utilities	0.67 (14.8)	0.07 (1.0)
Conversion cost, $/gal product	1.27	0.92
Conversion cost, $/gge product	1.26	0.92

MSW = municipal solid waste; SAF = sustainable aviation fuel.

Table 17. Fixed operating costs for the MSW-to-SAF plant for Base Case 1 (SAF-max).

Fixed Operating Costs	2020 Salary	# Required	Cost	MM$/yr	Cents/gge
Plant Manager	195,725	1	195,725		
Plant Engineer	93,202	1	93,202		

Fixed Operating Costs	2020 Salary	# Required	Cost	MM$/yr	Cents/gge
Maintenance Supervisor	75,893	1	75,893		
Lab Manager	74,562	1	74,562		
Shift Supervisor	63,911	6	383,463		
Lab Technician	53,258	3	159,775		
Maintenance Tech	53,258	16	852,134		
Shift Operators	53,258	27	1,437,977		
Yard Employees	37,281	12	447,376		
Clerks & Secretaries	47,932	3	143,797		
Total Salaries				**3.86**	**17.53**
Other Overhead					
Overhead				3.48	15.77
Maintenance				15.11	68.52
Insurance & Taxes				3.52	15.99
Total fixed operating costs				**25.97**	**117.81**

MSW = municipal solid waste; SAF = sustainable aviation fuel.

Table 18. Fixed operating costs for the MSW-to-SAF plant for Base Case 2 (Self-powered).

Fixed Operating Costs	2020 Salary	# Required	Cost	MM$/yr	Cents/gge
Plant Manager	195,725	1	195,725		
Plant Engineer	93,202	1	93,202		
Maintenance Supervisor	75,893	1	75,893		
Lab Manager	74,562	1	74,562		
Shift Supervisor	63,911	6	383,463		
Lab Technician	53,258	3	159,775		
Maintenance Tech	53,258	16	852,134		
Shift Operators	53,258	27	1,437,977		
Yard Employees	37,281	12	447,376		
Clerks & Secretaries	47,932	3	143,797		
Total Salaries				**3.86**	**28.97**
Other Overhead					
Overhead				3.48	25.41
Maintenance				15.14	110.61
Insurance & Taxes				3.53	25.81
Total fixed operating costs				**26.01**	**190.06**

MSW = municipal solid waste; SAF = sustainable aviation fuel.

7.3 Minimum Fuel Selling Price

A discounted cash flow economic model was used to estimate the MFSP. In this section, the MFSP represents the combined MFSP of jet fuel, naphtha, and diesel blendstocks produced from the process. The MFSP results and cost allocation are shown in Figure 13. The MFSPs for Base Case 1 and Base Case 2 are $5.49/gge and $7.75/gge, respectively. The contributions of

electricity to MFSP are 12.2 and 1.0 percent in Base Case 1 and in Base Case 2, respectively. The higher MFSP in Base Case 2 is mainly due to the lower product yields in this scenario, given that 38 percent of the syngas produced by gasification is used for electricity production instead of for conversion, resulting in significantly lower fuel production compared with Base Case 1.

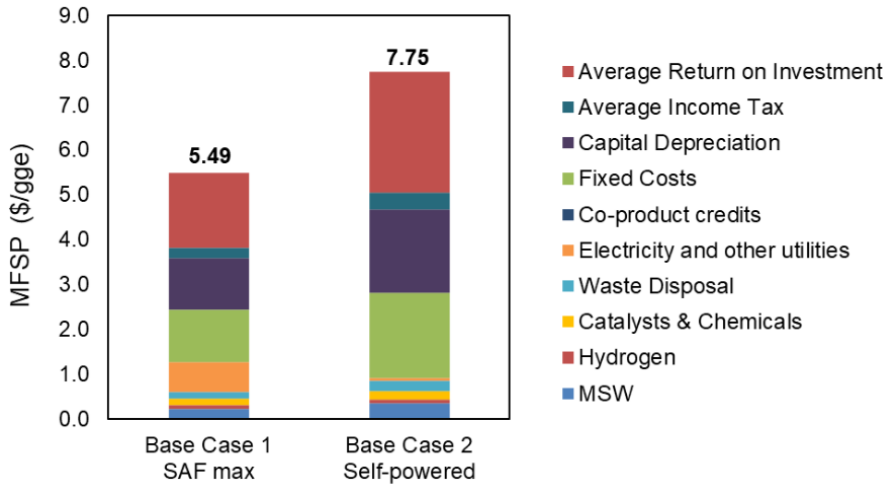


Figure 13. Baseline MFSP and cost allocation without incentives for Base Case 1 (SAF-max) and Base Case 2 (Self-powered).

Table 19 summarizes the main key performance measures of the MSW-to-SAF process. The fuel yield, calculated as the ratio of the mass of the products divided by the mass of MSW on a dry basis, is 0.19 and 0.12 for Base Case 1 and Base Case 2, respectively. The carbon efficiency is considerably lower in Base Case 2 (24.4) than in Base Case 1 (39.3) because of the loss of carbon for electricity production. The thermal efficiency, calculated from the lower heating value of RDF on a dry basis, is 36.4 and 31.3 percent in Base Case 1 and Base Case 2, respectively. The electricity consumption per gasoline-gallon equivalent is reduced from 9.55 kWh/gge in Base Case 1 to only 0.24 kWh/gge in Base Case 2.

Table 19. Key performance measures of the MSW-to-SAF process.

Performance Measures	Base Case 1 (SAF-max)	Base Case 2 (Self-powered)
Fuel yield (w/w dry MSW)	0.19	0.12
Carbon efficiency (% of C in MSW)	39.3%	24.4%
Thermal efficiency (%, LHV, dry MSW)	36.4%	31.3%
Electricity consumption (kWh/gge)	9.97	0.91

LHV = lower heating value; MSW = municipal solid waste; SAF = sustainable aviation fuel.

8.0 Base Case Environmental Assessment

An LCA was performed to evaluate the $CO_{2,eq}$ emissions of the biofuel and compare them against the $CO_{2,eq}$ emissions of conventional fuels. The system boundary of the LCA is "cradle-to-grave" and includes all the impacts from the acquisition of the raw material (i.e., MSW collection and preprocessing) to SAF production and use (i.e., combustion in an aircraft engine). The results were evaluated through comparison with conventional jet fuel (Figure 14). The functional unit is 1 MJ of energy produced from burning jet fuel in an aircraft engine.

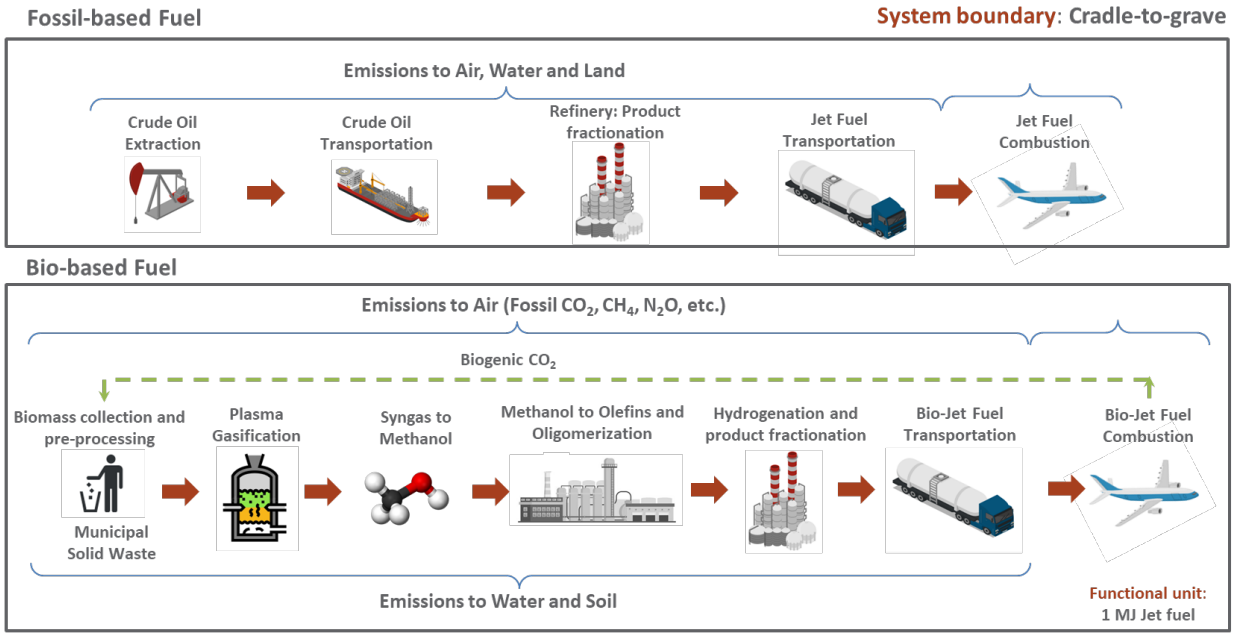


Figure 14. Life cycle assessment system boundary.

MSW consists of biogenic materials such as organics and paper and other materials such as plastics, synthetic fibers, and rubber. The emissions associated with the biogenic carbon in MSW are considered carbon-neutral (i.e., the CO_2 emissions from fuel production or combustion are offset by the CO_2 absorbed by biomass during the growth phase, thus serving as part of the fast carbon cycle). By contrast, emissions from remaining materials are considered long-term carbon emissions originating from conventional sources. RDF has an estimated 31.5 percent conventional carbon and 68.5 percent biogenic carbon, according to the resource assessment results in Section 5.2. The emissions related to the plastic portion of the feedstock are estimates based on the process mass balance and CO_2 emissions tracked from three primary sources: (i) biofuel production process, (ii) RDF combustion for process heat, and (iii) biofuel combustion.

Landfilling is the most common end-of-life solution for MSW. Organic waste decomposing in landfills generates methane, a greenhouse gas with a global warming potential 30 times greater than that of CO_2 over a 100-year period (Myhre et al., 2013). The decomposition of the organic portion of MSW makes landfills the third-largest source of human-related methane emissions in the United States (EPA, 2024b). Utilizing MSW for biofuel production diverts organic waste from landfills; for this reason, the impact of avoided landfill gas emissions was also quantified. The emissions from organic materials were estimated using the California Air Resources Board (CARB) Landfill Gas Tool (CARB, 2021). The tool considers the organic carbon degradation rates for each waste category as well as methane emissions as a result of decaying carbon under

anaerobic conditions. Additionally, the tool assumes collection efficiencies up to 95 percent and flaring efficiency of 99.77 percent, representing the gas collection and control systems installed in California landfills (EPA, 2016). The net landfill emissions for organic waste were quantified using the weighted average of CO_2 emissions for each category and their corresponding weight percentages (see Section 5.2). The details of estimated landfill emission factors are presented in Appendix A.

8.1 Life Cycle Assessment Data Sources

Mass and energy balances from the Aspen Plus model were used in conjunction with data from GREET, Ecoinvent, the CARB Landfill Gas tool, and the EPA Waste Reduction Model (WARM) tool (Argonne, 2022; CARB, 2021; Ecoinvent, 2013; EPA, 2023b). The main sources used for the LCA are summarized in Table 20. The life cycle inventories for Base Case 1 and Base Case 2 are reported in Appendix A.

Table 20. Life cycle assessment data sources.

Input/Output	Source
Electricity	GREET model, WECC grid
Hydrogen	GREET model
Slag and waste disposal	Ecoinvent database
Wastewater	Ecoinvent database
CO_2 emissions - fossil	Aspen Plus model
Landfill emissions (avoided)	CARB, 2021
Metal recycling credits	EPA WARM v16

8.2 $CO_{2,eq}$ Emission Results

The $CO_{2,eq}$ emissions results are presented in Figure 15. The overall $CO_{2,eq}$ emissions of the biofuel blendstocks are 37.9 and 17.5 gCO_{2e}/MJ for Base Case 1 and Base Case 2, respectively, corresponding to $CO_{2,eq}$ emission reductions of 55.9 and 79.7 percent compared with the emissions of conventional fuels.

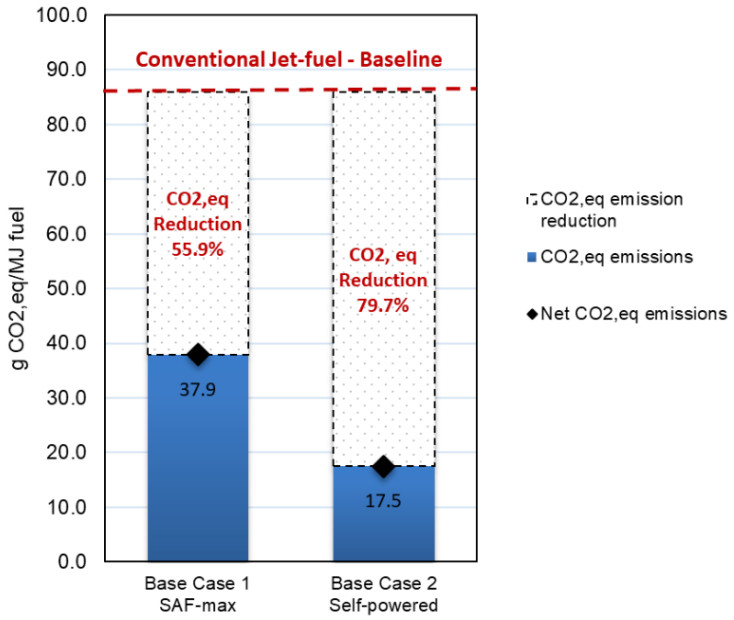


Figure 15. $CO_{2,eq}$ emission results for Base Case 1 (SAF-max) and Base Case 2 (Self-powered) compared with a conventional jet-fuel baseline.

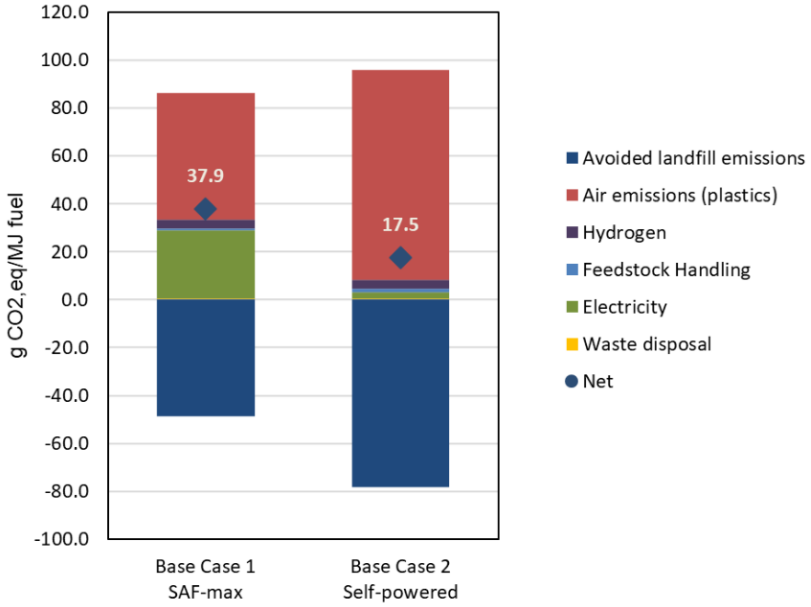


Figure 16. Breakdown of $CO_{2,eq}$ emissions of biofuel blendstocks from the MSW-to-SAF process for Base Case 1 (SAF-max) and Base Case 2 (Self-powered).

The results of the contribution analysis are presented in Figure 16. The $CO_{2,eq}$ emissions include impacts from fossil-based $CO_{2,eq}$ emissions from hydrogen production, feedstock handling, electricity, waste disposal, and conversion and combustion of fossil-based components of MSW (i.e., plastics), including combustion in an aircraft engine. Regarding feedstock handling, the net impact includes the transportation of MSW, MSW-to-RDF conversion, and disposal of reject materials to the landfill, which are impacts that are partially offset by metal recycling credits. The analysis also included the avoided impact of disposing MSW in landfill as a negative contribution.

The results indicate that the impact associated with conversion and combustion of conventionally sourced components of MSW is the single largest contributor to the $CO_{2,eq}$ emissions in both scenarios. However, this impact is largely offset by the avoided impact of disposing of MSW in a landfill. This contribution is higher in Base Case 2 than in Base Case 1 because of the lower product yield.

These results suggest that separating plastic components from the MSW stream before gasification would result in much lower direct emissions during the conversion and combustion stages. However, given the high heating value of plastics, separating plastics before gasification would likely result in lower syngas production and a lower subsequent product yield. On the other hand, the avoided impact from decomposition of MSW in landfill is mainly due to methane emissions from the organic portion of MSW (e.g., food, wood, yard trimmings, etc.), which are characterized by higher decomposition rates compared to non-organic portions of MSW. Future work may analyze the feasibility and trade-offs of separating plastics from MSW in the MSW-to-SAF conversion process.

Additionally, the results highlight that despite the lower product yield, the production of electricity on-site (Base Case 2) contributes to achieving a 60 percent $CO_{2,eq}$ emission reduction. This, in turn, would potentially allow SAF producers to access RIN D3 credits, which have a greater economic value than the alternative RIN D5 credits (which require a 50 percent $CO_{2,eq}$ emission reduction), thus contributing to reducing the overall MFSP. TEA results that account for incentive schemes are discussed in detail in Section 9.0.

9.0 Sensitivity and Uncertainty Analysis

9.1 Sensitivity Study of Key Performance and Economic Assumptions

Figure 17 presents the MFSP results of the sensitivity analysis around the key technical and financial assumptions. Several model variables were selected because of associated uncertainties: SAF plant scale, plasma-enhanced gasifier capital cost, total capital investment, process jet fuel yield, plant on-stream factor, debt interest, and investment equity. Each category on the tornado chart (Figure 17) varies one parameter value at a time to represent single-point sensitivity of the related parameter on the overall MFSP. For this analysis, since key technical and economic assumptions were the same for the selected parameters in both cases, the results follow a similar trend; therefore, only the results for Case 1 are presented.

As shown in Figure 21, increasing the plant scale to 2,000 TPD lowers the MFSP by $1.09/gge; conversely, lowering the scale to 500 TPD results in an increase of $1.66/gge. This variation in MFSP with respect to scale is expected, given that the economic feasibility of a process is directly related to its scale of operation (i.e., economies of scale). Furthermore, with the inclusion of an MSW tipping fee of $120.0/ton (negative cost), a value decided on the basis of the charging rate of the largest landfill considered in the study area where the SAF plant is co-located, the MFSP decreases by $1.65/gge (Sunshine Canyon Landfill, 2024). The plasma gasifier is a major expense in capital investment, and these cost estimates vary significantly in the literature. Considering a ±25 percent variation for the gasifier cost results in ±$0.48/gge fluctuation in MFSPs. Similarly, a ±40 percent change in total capital investment leads to a ±$1.14/gge price variation. Varying IRR by 50 percent affects the MFSP by about −$1.02/gge for 5 percent IRR and +$1.05/gge for 15 percent IRR, relative to the baseline assumption of 10 percent IRR for the *n*th plant. Jet fuel yield was ranged from 24 to 28 percent on the basis of variation around experimental fuel yield results, which affects the MFSP by +$0.35/gge to −$0.30/gge. Finally, lowering the on-stream factor from 90 to 80 percent results in an increase of $0.54/gge in MFSP, and varying the interest rate on debt financing ±4 percent incurs a roughly +$0.40/gge to −$0.37/gge impact on MFSP, whereas variations around investment equity are found to be nonsignificant compared with the rest of the categories in the tornado chart (Figure 17).

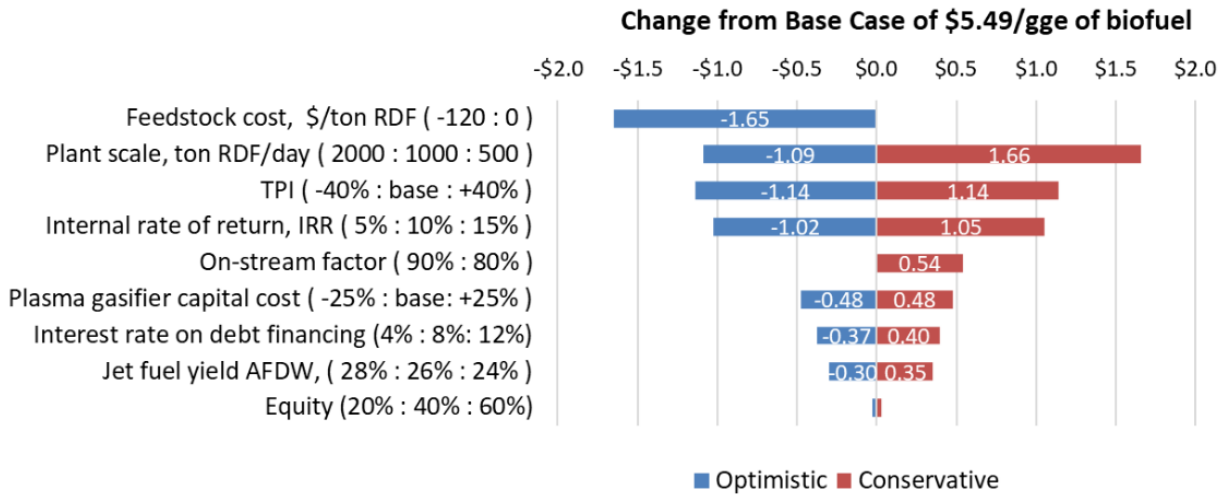


Figure 17. Sensitivity analysis for Case 1 (SAF-max).

9.2 Impact of Slag Utilization on TEA and LCA

In this study, the slag produced from the plasma gasifier is sent for disposal. However, as reported by Clark and Rogoff (2010) and Zhao et al. (2010), instead of being disposed of in landfills, the slag can be utilized as construction material, such as road paving material, rock wool, and bricks (Clark and Rogoff, 2010; Zhao et al., 2010). A detailed composition analysis conducted by Zhao et al. (2010) showed that water-cooled slag from a plasma gasifier contained 35.5 percent SiO_2 and 61.6 percent metal oxides. A typical composition of slag from coal gasification plants can be considered 35.8–59.2 percent SiO_2 and 40.8–64.2 percent metal oxides (Arroyo Torralvo et al., 2017). Steel slag typically contains 10–19 percent SiO_2 (U.S. Department of Transportation, 2016). Given the compositional similarities, the potential utilization of plasma gasifier slag could be distinct from steel slag but similar to slag from coal gasifiers. Shah et al. (2014) suggested that slag from the coal gasification process could be reused after waste treatment, resulting in zero disposal fees (Shah et al., 2014). Choudhry et al. (2001) conducted a comprehensive technical and economic viability study on using coal gasification slag for producing lightweight aggregates, which can be further used for making lightweight blocks, structural concrete, and concrete panels (Choudhry et al., 2001). To evaluate the impact of slag utilization on the TEA and LCA results, a sensitivity analysis with different scenarios, including zero disposal fees and lightweight aggregate production, was conducted. Table 21 shows the variation of MFSP and $CO_{2,eq}$ emissions across different scenarios. The variation in slag production rate and its associated utilization methods have a minor impact on the final fuel selling price and $CO_{2,eq}$ emission levels. This indicates that from both TEA and LCA perspectives, slag utilization brings economic and environmental benefits to the overall process, but its impact is relatively small (less than 2–5 percent).

Table 21. Impact of slag utilization in the techno-economic analysis and life cycle assessment.

Scenarios	Case 1 (SAF-max)		Case 2 (Self-powered)	
	MFSP $/gge	$CO_{2,eq}$ Emission gCO_2/MJ fuel	MFSP $/gge	$CO_{2,eq}$ Emission gCO_2/MJ fuel
Slag for disposal with disposal cost (baseline)	5.49	37.9	7.75	17.5
Slag for disposal with zero disposal fee	5.45	37.6	7.67	16.9
Slag for materials production	5.35	37.3	7.51	16.5

9.3 Impact of Incentives on NPV and IRR

The potential credits applicable to Case 1 and Case 2 are summarized in Table 22. The reduction in $CO_{2,eq}$ emissions achieved by both design cases (see Section 8.2) were used to estimate cumulative incentives from the current federal and state policies (see Section 3.1). Design Case 1 results in a 55.9 percent $CO_{2,eq}$ emission reduction; therefore, it would only qualify for D5 RINs. Design Case 2 achieves a 79.7 percent $CO_{2,eq}$ emission reduction, qualifying for D3 RINs, which hold a significantly higher value compared with D5 RINs. In both design cases, RINs and LCFS credit values were adjusted to reflect the biogenic portion of the biofuel. This adjustment accounts for the requirement that only the biogenic portion of the feedstock qualifies for the incentives. The non-biogenic $CO_{2,eq}$ emissions occurring in the process are still accounted for in the overall $CO_{2,eq}$ emissions for both design cases, as discussed in Section 8.0. The combined LCFS and RIN credits considered are $0.97–$2.35/gge for Case 1 and $2.40–$4.16/gge for Case 2.

Table 22. Federal and state incentives applicable to Case 1 and Case 2 for SAF production.

	Unit	Min	QL[a]	Median	QU[a]	Max
Case 1 (SAF-max[b])						
D5 RINs (biogenic)	$/gge of biofuel	0.29	0.52	1.00	1.57	2.11
LCFS56[b] (biogenic)	$/gge of biofuel	0.28	0.45	0.72	0.78	0.83
D5+LCFS (biogenic)	$/gge of biofuel	0.57	0.97	1.72	2.35	2.94
Case 2 (Self-powered[b])						
D3 RINs (biogenic)	$/gge of biofuel	0.52	1.75	2.47	3.05	3.61
LCFS80[c] (biogenic)	$/gge of biofuel	0.40	0.65	1.03	1.11	1.18
D3+LCFS (biogenic)	$/gge of biofuel	0.92	2.40	3.50	4.16	4.80

[a] QL = lower quartile (25th percentile) and QU = upper quartile (75th percentile) of the credit range, estimated using historical data of RIN and LCFS credits considered from 2018 to 2023.
[b] Both RFS and LCFS credits were adjusted to account only for biogenic portion of the fuel using a conversion factor of 0.685 (see Section 8.0).
[c] LCFS56 and LCFS80 correspond to credits for 56 percent and 80 percent $CO_{2,eq}$ emission reduction, representing Case 1 and Case 2, respectively.
LCFS = Low-carbon Fuel Standard; RIN = renewable identification number; SAF = sustainable aviation fuel.

Figure 18 shows the impact of potential fuel credits on the NPV and IRR after tax. NPV represents the total profit discounted to its present value using an IRR of 10 percent over a 30-year project lifetime. IRR, on the other hand, indicates the maximum interest rate at which the NPV achieves zero by the end of the plant's lifetime; a higher IRR indicates a greater return on an investment. For this analysis, the fuel selling price was fixed at $2.50/gge, potential MSW tipping fee credits were excluded, and NPV and IRR were calculated with respect to a range of potential credit values.

Figure 18(a) shows that a minimum sustainable fuel credit of $3.07/gge is required to make Case 1 economically feasible, indicating that existing incentives would be insufficient to meet the $2.50/gge target. Moreover, for credits of less than $2.00/gge, the IRR (NPV = 0) will drop below 5 percent in Case 1. Similarly, total fuel credits of $5.38/gge are required to make Case 2 economically feasible at 10 percent IRR (Figure 18.b). The required credits exceed the applicable credits for Case 2, where the median credit value is $3.50/gge and the upper quartile value is $4.16/gge. In light of the results of this analysis, the SAF plant's eligibility for only a fraction of sustainable fuel incentives restricts its economic viability under existing incentive frameworks.

To enhance the economic viability of MSW-to-SAF production, it is worth exploring opportunities to improve the eligibility of MSW feedstock for incentives, strategically leverage MSW tipping fee credits to mitigate operating costs, and increase the plant scale. The latter two options are further discussed in Sections 9.4 and 9.6. Furthermore, current waste separation, recycling, and collection practices face economic and practical limitations due to existing sorting/recycling technologies, market conditions, and waste management infrastructure. Advancements in waste management practices could improve the efficiency and economics of feedstock preparation, potentially increasing the fraction of feedstock eligible for incentives. These advancements could improve MSW's utilization as a feedstock and its economic feasibility, potentially enabling the MSW-to-SAF process to achieve the $2.50/gge MFSP target.

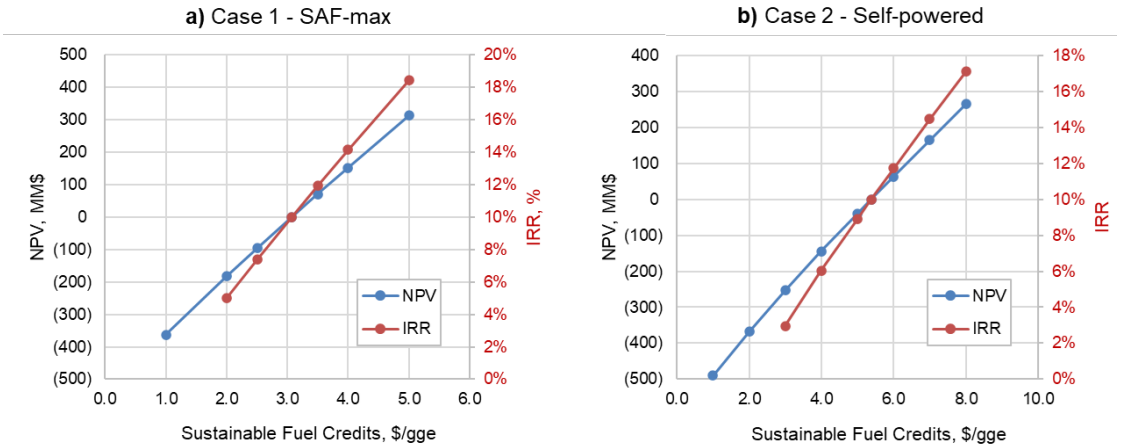


Figure 18. Effect of potential sustainable fuel credits on the net present value (NPV) and internal rate of return (IRR) for two scenarios: a) Case 1 (SAF-max) and b) Case 2 (Self-powered) processes.

9.4 Combined Impact of MSW Tipping Fee and Fuel Incentives on MFSP

The base cases presented in Section 7.0 do not account for waste processing credits, such as MSW tipping fees, as the value of the tipping fee varies depending on local policy and the business model. Nevertheless, the base case scenarios include the costs associated with transportation and preprocessing of MSW and its conversion to RDF. In this section, an additional incentive for MSW is considered (see Section 3.2), in which tipping fees ranging from $0/ton to $58.5/ton unsorted MSW ($2020) are credited to the SAF plant as feedstock credits.

Specifically, three tipping fee scenarios were considered for this analysis: (i) $0 per ton of MSW, representing the baseline, (ii) $16.2 per ton of MSW, representing a credit that covers the feedstock transportation and handling costs, and (iii) $58.5 per ton of MSW, representing the average landfill tipping fee charged in California (Aber, 2024).

Figure 19 illustrates the MFSP results with the combined sustainable fuel incentives (adjusted with respect to the biogenic fraction of the fuel) and MSW tipping fee incentive for Case 1. The sustainable fuel credits for this case result in MFSP values ranging from $3.20/gge to 4.55/gge. When the median fuel credit value is considered, the MFSP is estimated as $3.82/gge, which is considerably higher than the target of $2.50/gge. However, this target MFSP value can be achieved if the SAF plant charges a tipping fee of $47.3/ton of MSW, when combined with the upper quartile sustainable fuel credits (see the purple line in Figure 19), suggesting that a tipping fee exceeding the current state average would be necessary to meet the target in the case of a drop in fuel incentive values.

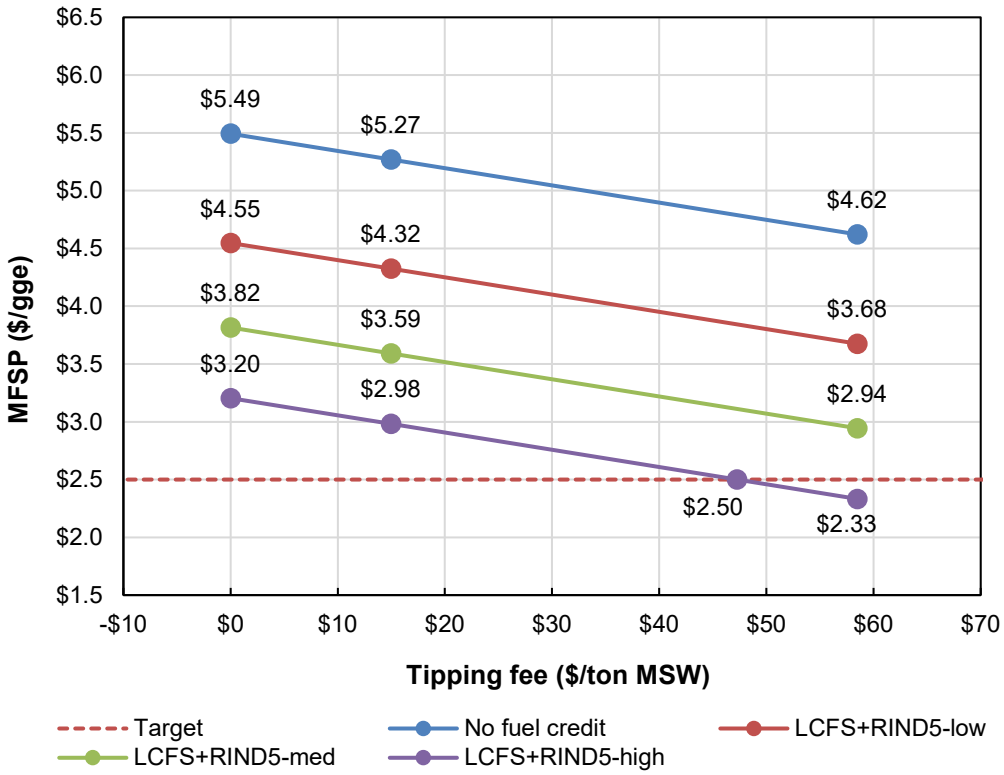


Figure 19. Minimum fuel selling price (MFSP) with municipal solid waste (MSW) tipping fee and combined fuel incentives (biogenic) for Case 1 (SAF-max) process.

Figure 20 shows the MFSP results with the combined biofuel (adjusted on the basis of the biogenic fraction of the fuel) and MSW tipping fee incentives for Case 2. The sustainable fuel credits for this case result in MFSP values ranging from $3.70/gge to 5.42/gge which is considerably lower than the baseline MFSP of $7.75/gge (representing no incentives). This is because Case 2 is eligible for RIN D3, which has a significantly higher monetary value than RIN D5, and the increased LCFS credits because of its lower $CO_{2,eq}$ emissions of fuel blendstocks. When the median fuel credit value is considered, the MFSP is estimated to be $4.34/gge (not considering MSW tipping fee credit), which is considerably higher than the target $2.50/gge. Similar to Case 1, Case 2 can achieve the target MFSP value of $2.50/gge if the SAF plant charges a tipping fee of $54.1/ton MSW, when combined with the upper quartile sustainable fuel credits (see the purple line in Figure 19), suggesting that a tipping fee exceeding the current state average would be necessary to meet the target in the event that fewer fuel incentives are received.

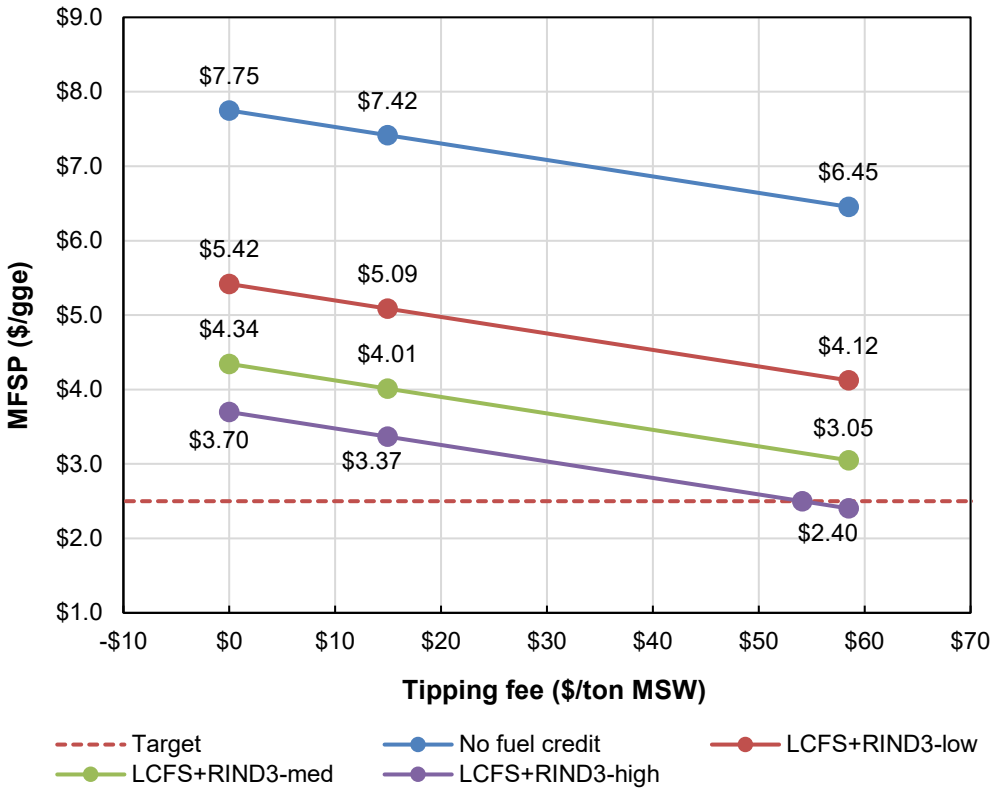


Figure 20. Minimum fuel selling price (MFSP) with municipal solid waste (MSW) tipping fee and combined fuel incentives (biogenic) for Case 2 (Self-powered).

Notably, these results represent an ideal-case scenario based on *n*th plant assumptions with mature technology and established feedstock supply chains. Additionally, the analysis assumed that the feedstock and its processing comply with RFS and LCFS requirements for receiving fuel incentives. However, even under these ideal conditions with incentives, the economic assessment of the MSW-to-SAF process suggests that further research and development are necessary to improve process efficiency and economics for commercialization. Nevertheless, the analysis results provide valuable insights for evaluating the feasibility of deploying plasma gasification technology under existing incentive programs and its potential for valorizing feedstocks that would otherwise be directed to landfills.

9.5 Uncertainties in the Techno-economic Analysis

The sensitivity analysis presented in Sections 9.1 to 9.3 isolated the impact of individual factors. To assess the combined effect of multiple variables, uncertainty quantification was conducted. The results provide a deeper understanding of the technology's economic viability. Here, Oracle Crystal Ball, a spreadsheet-based tool for risk measurement, was used to generate 10,000 sets of Monte Carlo samples. For each sample, model inputs were assigned semi-random values subject to predetermined probability distribution, while the key model results were collected for statistical analysis. For the MSW-to-SAF process, key uncertainty sources include MSW tipping fee, electricity price, hydrogen price, SAF yield, utility consumption, and capital cost estimation for each area. MFSP without incentives was selected as the key economic measure for uncertainty quantification, the results of which are presented in Figure 21 for Case 1 and Figure

22 for Case 2. Detailed descriptions and predetermined probability distributions of each identified input variables can be found in Appendix C. Details on the Monte Carlo simulation can be found in our previous publications (Jiang et al., 2023b, 2023a; Li et al., 2021). As shown in Figure 21 and Figure 22, this design case study was subject to roughly ±13 percent uncertainty in the estimated MFSP without incentives. The median estimated MFSP without incentives is $5.31/gge for Case 1 and $7.54/gge for Case 2. The uncertainties in the estimated MFSP of Case 2 (+15/−13 percent) are slightly larger than those for Case 1 (+11/−10 percent), as Case 2 has a lower SAF yield per ton of MSW consumed and more on-site electricity generation using syngas from MSW gasification. The median MFSP values of both cases are slightly lower than that of the base case value, as the base case does not consider any MSW tipping fee. In addition, the probability distributions of input variables are not necessarily symmetrical, as shown in Appendix C.

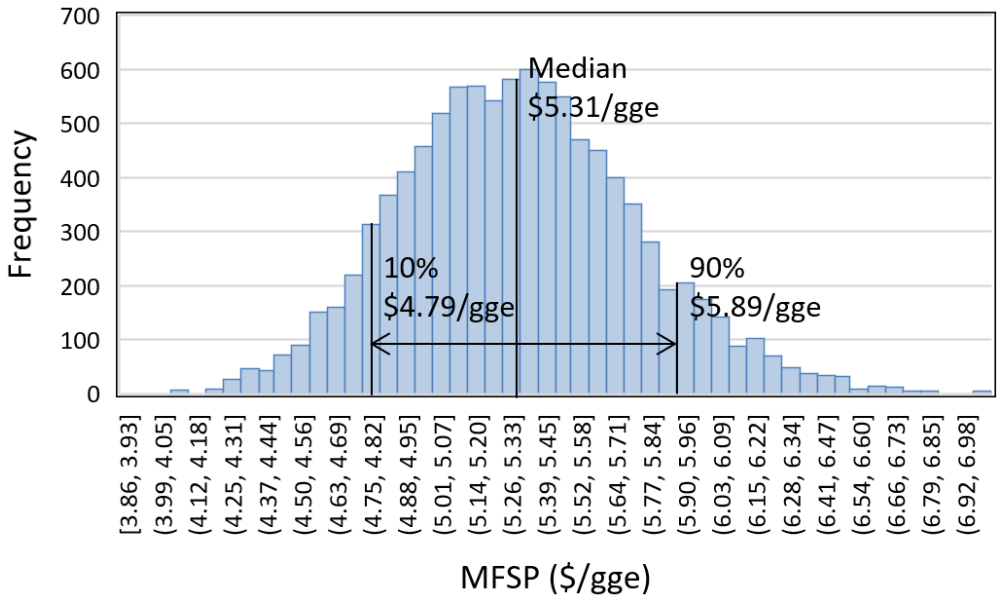


Figure 21. Uncertainties in the minimum fuel selling price (MFSP) without incentives for Case 1 (SAF-max).

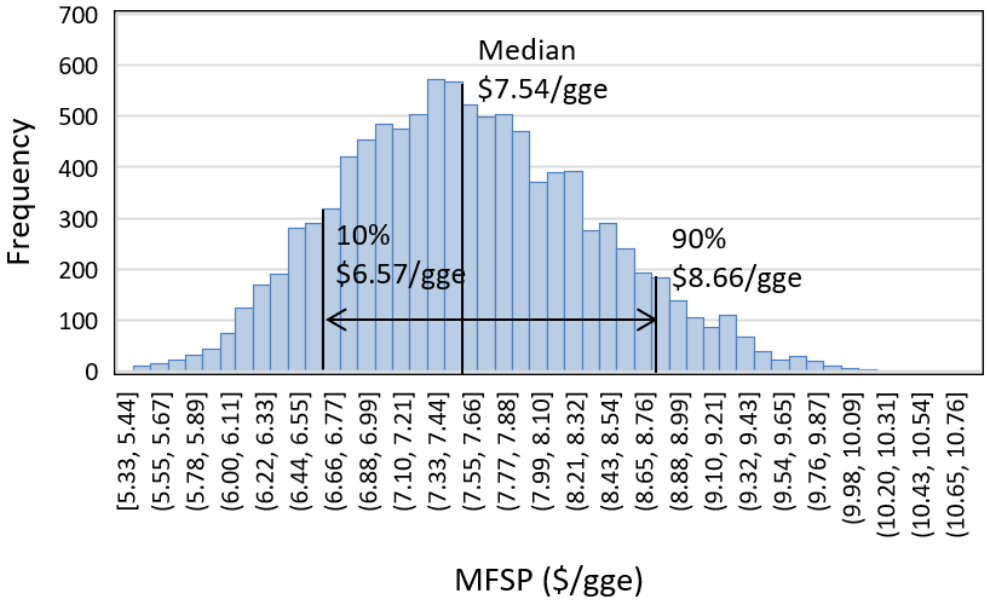


Figure 22. Uncertainties in the minimum fuel selling price (MFSP) without incentives for Case 2 (Self-powered).

9.6 Impact of Plant Scale on Economic Feasibility

Plant scale is a key economic driver for commercial processes. In this design case study, the plant scale was set to 1,000 TPD for the base cases, a decision based on the size of existing MSW gasification plants (Table 4). On the other hand, the results of the regional resource assessment (Section 4.0) suggest that up to 7,100 TPD MSW can be provided, with low transportation costs, to the selected site located near a large-scale landfill in the Southern California region. A sensitivity analysis was conducted to evaluate the impact of plant scale on the economic feasibility of MSW-to-SAF conversion. For both design cases, the plant scale varies from 250 to 7,100 TPD. As detailed in Section 7.3, the MFSP was estimated using an NPV of 0 and IRR of 10 percent. In addition, IRR was evaluated as an alternative economic metric using an SAF selling price of $2.50/gge. At different plant scales, additional trains were considered for unit operations that reached their size limitations (i.e., MSW sorting and plasma gasifier). The results are presented in Figure 23 for Case 1 and Figure 24 for Case 2.

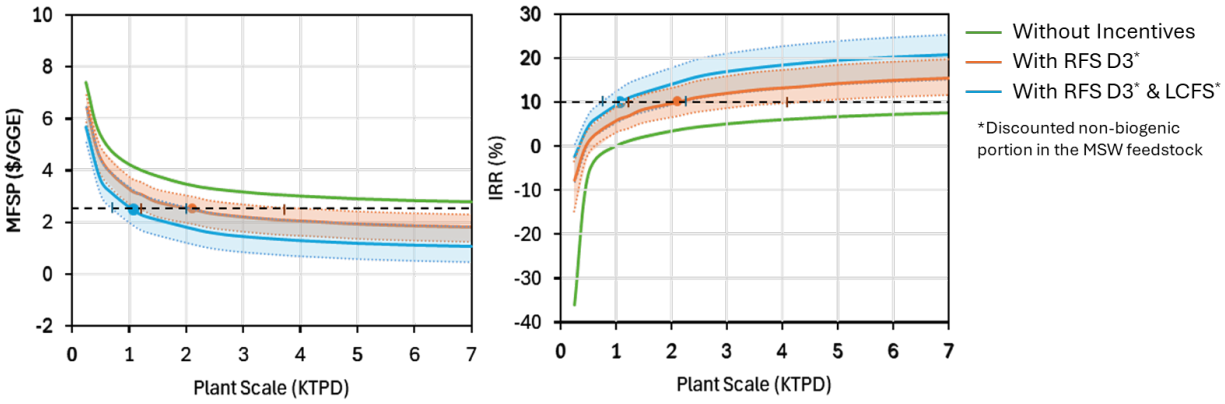


Figure 23. Impact of plant scale on the estimated minimum fuel selling price (MFSP) and internal rate of return (IRR) of Case 1 (SAF-max).

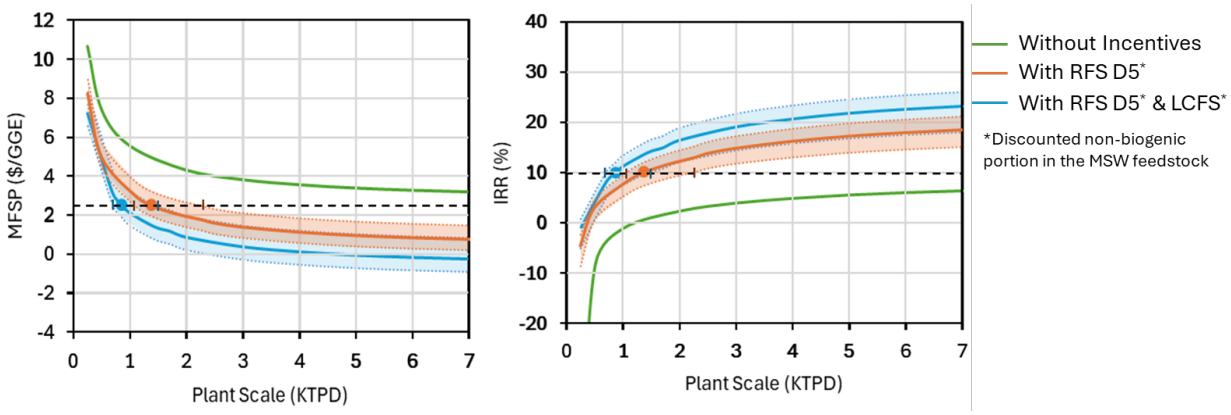


Figure 24. Impact of plant scale on the estimated minimum fuel selling price (MFSP) and internal rate of return (IRR) of Case 2 (Self-powered).

For both cases, an MSW tipping fee of $58.30/ton was included, and three incentive scenarios were evaluated. The green line in Figure 23 and Figure 24 shows a scenario without any fuel incentives. The orange line represents a scenario considering only RFS incentives. The blue line represents a scenario considering both LCFS and RFS incentives. The shaded areas around each line indicate the impact of fluctuating incentive prices (see Section 3.1). For all cases and scenarios, the plant scale has a significant impact on the MFSP and IRR when it is below 500 TPD. As the plant scale increases, the MFSP decreases and the IRR increases. However, the impact of plant scale lessens when it exceeds 4,000 TPD for Case 1 and 5,000 TPD for Case 2.

The horizontal dashed line in Figure 23 and Figure 24 reflects the economic feasibility targets: an MFSP of $2.50/gge and an IRR of 10 percent. These targets were used to determine the minimum plant scale required for economic viability in Case 1 and Case 2. As shown in both figures, the dashed and green lines do not intersect, which indicates that the MSW-to-SAF process requires fuel incentives to be economically viable, even at large scales. As indicated in Figure 23, a minimum plant scale of 1,100 TPD is required for Case 1 (SAF-max), if stacked six-year average LCFS and RFS incentives are included. This value can range from 700 to 2,200 TPD under fluctuating incentive prices. Similarly, a minimum plant scale of 2,100 TPD is required if only the six-year average RFS incentive is included. This value can range from 1,200 to 4,300 TPD. As indicated in Figure 24, a minimum plant scale of 900 TPD is required for Case 2 (Self-powered), if the stacked six-year average LCFS and RFS incentives are included. This value can range from 700 to 1,400 TPD under fluctuating incentive prices. If only RFS incentives are included, the minimum plant scale of Case 2 increases to 1,400 TPD and can range from 1,000 to 2,300 TPD. The results suggest that even in the worst-case scenario, the selected region can provide a sufficient amount of MSW to meet the minimum plant scale required to sell SAF at $2.50/gge.

10.0 Current State of Development/Commercialization

The MSW-to-SAF process is currently under active development, with TRLs ranging from 5 to 7. As illustrated in Figure 25, the TRL of each individual critical technology element (CTE) within the process varies. While some CTEs are well established (with a TRL of 9) in industries like chemicals and petrochemicals, the integration of these CTEs into a complete MSW-to-SAF system presents unique challenges and has not been demonstrated at a commercial scale.

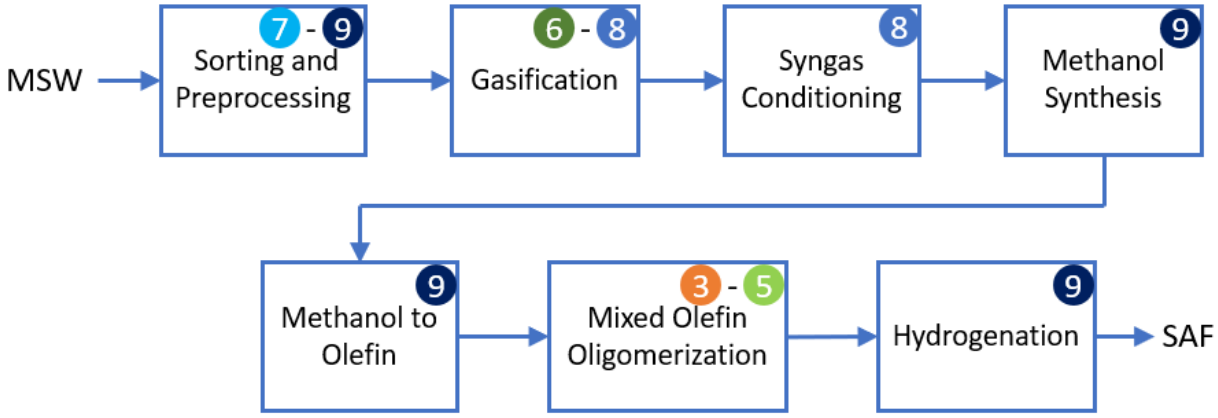


Figure 25. Technology readiness levels of critical technology elements in the municipal solid waste (MSW) to sustainable aviation fuel (SAF) plant.

As shown in Figure 25, methanol synthesis from syngas, MTO, and hydrogenation are the three most mature CTEs, with a TRL of 9.

- **Methanol Synthesis from Syngas**: This well-established technology is commercially deployed, with a high TRL of 9. Globally, most methanol production utilizes syngas as a feedstock, with 15 operational plants in the United States alone (Siram et al., 2014).
- **Methanol to Olefins**: MTO is a mature process (TRL 9) widely used in the petrochemical industry. It converts methanol into mixed light olefins, which are essential building blocks for various products, including plastics and synthetic rubber. As an example, UOP's first commercial advanced MTO plant started up in 2013 at Wison Clean Energy Company Ltd. in Nanjing, China, with a light olefin production rate of 295,000 tonnes per year (UOP, 2019).
- **Olefin Hydrogenation**: This established technology (TRL 9) is commonly used in refineries to upgrade and finalize fuel blendstocks.

While the above CTEs are well established, integrating them with other parts of the MSW-to-SAF conversion process presents additional challenges. For instance, even though syngas-to-methanol conversion itself is commercially viable, its integration with upstream processes like gasification necessitates further development.

- **Syngas Conditioning:** This CTE ensures the quality of syngas produced from waste is suitable for methanol synthesis, effectively linking the gasification and methanol synthesis stages. While commercially demonstrated in coal gasification plants and in MSW gasification for power generation, it requires modifications and re-optimization for different syngas sources and desired purity levels. A demonstration facility was built in Westbury, Canada, for converting MSW into methanol, although commercial-scale syngas conditioning has not yet been demonstrated for MSW-to-methanol specifically (Labrie, 2015). Ongoing research and

development efforts focus on improving energy efficiency, cost-effectiveness, and impurity removal efficiency for this specific application (GSTC, 2024b).

While demonstrations have been performed at relevant scales and under relevant operational conditions, the TRLs of MSW sorting and preprocessing, gasification, and olefin oligomerization vary depending on the feedstock composition and technology used.

- **Municipal Solid Waste Sorting and Preprocessing**: This CTE has been demonstrated in operational environments, but its specific TRL depends on the exact configuration and plant scale. In Europe, MSW-derived RDF is widely used in the cement kiln industry (with >60 percent substitution potential for fossil fuels), while the market has grown fast because of the imposition of landfill taxes (European Investment Bank, 2024). Wiscon Envirotech in China provides a commercial RDF solution with scales ranging from 500 to 10,000 kg/h. In the United States, the Arnold O. Chantland Resource Recovery Plant, built in 1975 in Iowa, is the first full-scale RDF facility, and RDF is sent from this facility to a local power plant as supplemental fuel (City of Ames, 2024).
- **Municipal Solid Waste Gasification:** Section 4.1 provides a detailed review of existing gasification technologies and commercial practice of the selected plasma gasification technology. Overall, MSW gasification has been successfully demonstrated via numerous pilot and demonstration projects, with some commercial-scale plants in operation. However, it still faces challenges from feedstock variability that affect gasification performance, liquid and solid by-product management for proper handling and disposal, and economic viability. Notably, certain species in MSW result in feeding difficulties that reduce the throughput of feedstock and therefore reduce production. As research and development continues, further advancements in TRL and wider adoption can be expected for MSW gasification.
- **Olefin Oligomerization**: This CTE was first commercialized in the 1960s, using ethylene or mixed olefins as the feedstock (Lavrenov et al., 2016; LiBretto et al., 2021). Commercialized technologies or catalysts include DuPont Versipol, SABIC/Linde alpha-SABLIN, UOP Linear-1, and Shell Higher Olefin Process (Keim, 2013). Recently, as SAF has gained increasing interest and demand, olefin oligomerization has been widely adopted in ASTM International–approved ATJ, especially ethanol-to-jet conversion processes, including Honeywell UOP's ethanol-to-jet conversion, LanzaJet ATJ, and Axens's Jetanol (Axens, 2023; LanzaJet, 2023; UOP, 2023). Despite its proven maturity, olefin oligomerization faces challenges in process optimization toward higher SAF range olefin yield, economic feasibility, and flexibility to accommodate varying feedstock quality. Additionally, factors like reactor design, heat management, and capability for handling large flow rates need to be addressed to ensure efficient operation at a commercial scale.

11.0 Conclusions and Next Steps

This study examined the technical, economic, and environmental feasibility of converting MSW into SAF through plasma-enhanced gasification, MTO, and olefin oligomerization. The Southern California region was selected as the potential plant site because of its feedstock availability, market demand, and availability of incentive schemes. Several waste transfer stations were identified near the selected location, capable of supplying MSW feedstock up to a rate of 7,100 TPD within an approximate distance of 14.7 miles. Two different design cases were analyzed: Case 1 (SAF-max), for maximizing SAF production, and Case 2 (Self-powered), for minimizing $CO_{2,eq}$ emissions through partial use of syngas for on-site electricity production.

In the base cases, the plant scale was set to 1,000 TPD, with no incentives or MSW tipping fee credits considered. The TEA results for Base Case 1 indicated an MFSP of $5.49/gge. The plasma gasifier was the single largest contributor to the CAPEX (>50 percent), while the electricity consumption was the largest contributor to variable operating costs. The LCA results showed a $CO_{2,eq}$ emission reduction of 55.9 percent, with electricity consumption and conversion/combustion of conventionally sourced components of MSW (e.g., plastics) being the largest contributors. In Case 2, the 100 percent on-site electricity production achieves a 79.7 percent $CO_{2,eq}$ emission reduction compared with conventional jet fuel but has a 38 percent lower SAF product yield. Therefore, the TEA results indicate that without any incentives, Base Case 2 achieves an MFSP of $7.75/gge, higher than that of Base Case 1.

When federal and state incentives are taken into account, the benefits are greater for Case 2 than for Case 1. This can be explained by the lower $CO_{2,eq}$ emissions in Case 2; this makes the fuel products eligible for RIN D3 credits, which have a relatively high economic value. In both cases, the RINs and LCFS credit values were adjusted to account for the biogenic portion of the biofuel. When LCFS, RINs, and MSW tipping fee incentives are all considered, both Base Cases achieve the target MFSP of $2.50/gge, but only under optimistic incentive assumptions. In Case 1, the target MFSP is achieved when the upper quartile fuel credits (LCFS+RIN D5) and a tipping fee of $47.3/ton unsorted MSW are included. For Case 2, the required tipping fee is higher, at around $54.1/ton unsorted MSW, combined with upper quartile fuel credits (LCFS+RIN D3).

If targeting a SAF selling price of $2.50/gge, Case 1 requires a minimum plant scale of 1,100 TPD with both LCFS and RFS incentives to be economically viable, or a minimum plant scale of 2,100 TPD with only RFS incentives. Case 2 requires a minimum plant scale of 900 TPD with both LCFS and RFS incentives, or 1,400 TPD with only RFS incentives. Notably, the fluctuating incentive prices can significantly affect the estimated minimum plant scale. However, even in the worst-case scenario, the selected region can provide a sufficient amount of MSW to meet the scale requirement.

Overall, the MSW-to-SAF conversion process through plasma-enhanced gasification, MTO, and olefin oligomerization holds significant promise for producing SAF at a competitive price and with substantial environmental benefits compared with conventional fossil-based jet fuel. If technological integration challenges are addressed and economic incentives are leveraged, this pathway could contribute to domestic supply chains for the aviation sector. The following next steps will be critical for advancing this technology toward commercial viability:

- Optimization of process design and operating conditions—especially for MSW sorting and preprocessing, gasification, and olefin oligomerization—to enhance overall system efficiency and simultaneously maximize economic and environmental benefits.

- Analysis of regional availability and variability of MSW to evaluate the effect of MSW composition on gasification and product yields, variations in logistic pathways, and avoided impact from MSW decomposition in landfill in different U.S. regions.
- Continuous improvement of process design, with the TEA and LCA incorporating updated experimental data and direct feedback from industrial partners and other stakeholders.
- Evaluation of the feasibility and trade-offs of separating plastics from MSW in the MSW-to-SAF conversion process.

12.0 References

Aber, S., 2024. Analyzing Municipal Solid Waste Landfill Tipping Fees. The Environmental Research & Education Foundation. https://erefdn.org. Environmental Research & Education Foundation.

Air Resource Board, 2024. Low Carbon Fuel Standard | California Air Resources Board. https://ww2.arb.ca.gov/our-work/programs/low-carbon-fuel-standard/about.

Arena, U., 2012. Process and technological aspects of municipal solid waste gasification. A review. Waste Management 32, 625–639. https://doi.org/10.1016/j.wasman.2011.09.025

Argonne, 2022. Argonne GREET Model [WWW Document]. URL https://greet.es.anl.gov/ (accessed 5.10.18).

Arroyo Torralvo, F., Fernández Pereira, C., Font Piqueras, O., 2017. By-products from the integrated gas combined cycle in IGCC systems, in: Integrated Gasification Combined Cycle (IGCC) Technologies. Elsevier, pp. 465–494. https://doi.org/10.1016/B978-0-08-100167-7.00014-7

Axens, 2023. Jetanol. https://www.axens.net/markets/renewable-fuels-bio-based-chemicals/saf-renewable-diesel#4323 [WWW Document]. URL https://www.axens.net/markets/renewable-fuels-bio-based-chemicals/saf-renewable-diesel#4323 (accessed 9.18.24).

Boumanchar, I., Chhiti, Y., M'hamdi Alaoui, F.E., Sahibed-dine, A., Bentiss, F., Jama, C., Bensitel, M., 2019. Municipal solid waste higher heating value prediction from ultimate analysis using multiple regression and genetic programming techniques. Waste Manag Res 37, 578–589. https://doi.org/10.1177/0734242X18816797

Brown, R.M., Hoover, A.N., Klinger, J.L., Wahlen, B.D., Hartley, D., Lee, H., Thompson, V.S., 2022. Decontamination of Mixed Paper and Plastic Municipal Solid Waste Increases Low and High Temperature Conversion Yields. Front. Energy Res. 10. https://doi.org/10.3389/fenrg.2022.834832

Buffie, N.E., 2025. The Section 45Z Clean Fuel Production Credit. https://www.congress.gov/crs-product/IF12502.

CalRecycle, 2022. 2021 Disposal Facility-based Characterization of Solid Waste in California. https://www2.calrecycle.ca.gov/Publications/Details/1738.

CalRecycle, 2019. Solid Waste Information System (SWIS) database. https://www2.calrecycle.ca.gov/SolidWaste/Site/Search.

CARB, 2025. 2025 LCFS Amendment Implementation FAQ | California Air Resources Board. https://ww2.arb.ca.gov/resources/fact-sheets/2025-lcfs-amendment-implementation-faq.

CARB, 2024. Low Carbon Fuel Standard | California Air Resources Board. https://ww2.arb.ca.gov/rulemaking/2024/lcfs2024.

CARB, 2021. CARB's Landfill Gas Tool | California Air Resources Board. https://ww2.arb.ca.gov/resources/documents/carbs-landfill-gas-tool.

CEI, 2008. Chemical Engineering Index. 2008. www.che.org.

Chandolias, K., Richards, T., Taherzadeh, M.J., 2018. Combined Gasification-Fermentation Process in Waste Biorefinery, in: Waste Biorefinery. Elsevier, pp. 157–200. https://doi.org/10.1016/B978-0-444-63992-9.00005-7

Choudhry, V., Kwan, S., Hadley, S.R., 2001. Utilization of Lightweight Materials Made from Coal Gasification Slags Cooperative Agreement No. DE-FC21-94MC30056.

City of Ames, 2024. Resource Recovery System (serving Story County). City of Ames, IA. https://www.cityofames.org/government/departments-divisions-i-z/resource-recovery-system [WWW Document]. URL (accessed 9.18.24).

Clark, B.J., Rogoff, M.J., 2010. Economic feasibility of a Plasma Arc Gasification Plant, City of Marion, Iowa. Proceedings of the 18th Annual North American Waste-to-Energy Conference, NAWTEC18, May 11-13, 2010, Orlando, FL, USA.

Cortazar, M., Santamaria, L., Lopez, G., Alvarez, J., Zhang, L., Wang, R., Bi, X., Olazar, M., 2023. A comprehensive review of primary strategies for tar removal in biomass gasification. Energy Conversion and Management 276, 116496. https://doi.org/10.1016/j.enconman.2022.116496

County of Los Angeles, 2013. Green Waste Management Resource Guide for Los Angeles County Residents and Businesses. https://dpw.lacounty.gov/epd/sbr/pdfs/Green-Waste-Management-Resource-Guide.pdf.

Delnegro, L., 2023. The Journey of SAF: The Production Methods & Documentation. Aviation International News. https://www.ainonline.com/aviation-news/business-aviation/2023-04-01/journey-saf-production-methods-documentation.

DOE, 2024. U.S. Department of Energy. Billion-Ton Report: An Assessment of U.S. Renewable Carbon Resources. M. H. Langholtz (Lead). Oak Ridge, TN: Oak Ridge National Laboratory. ORNL/SPR-2024/3103. doi: 10.23720/BT2023/2316165 (2024.

DOE, 2020. Sustainable Aviation Fuel. Review of Technical Pathways. https://www.energy.gov/sites/default/files/2020/09/f78/beto-sust-aviation-fuel-sep-2020.pdf.

Dutta, A., Sahir, A., Tan, E., 2015. Process Design and Economics for the Conversion of Lignocellulosic Biomass to Hydrocarbon Fuels: Thermochemical Research Pathways with In Situ and Ex Situ Upgrading of Fast Pyrolysis Vapors.

Dutta, A., Talmadge, M., Hensley, J., Worley, M., Dudgeon, D., Barton, D., Groendijk, P., Ferrari, D., Stears, B., Searcy, E.M., Wright, C.T., Hess, J.R., 2011. Process Design and Economics for Conversion of Lignocellulosic Biomass to Ethanol: Thermochemical Pathway by Indirect Gasification and Mixed Alcohol Synthesis (No. NREL/TP-5100-51400, 1015885). https://doi.org/10.2172/1015885

Ebara, 2024. Ebara Ube Process Pressurized twin internally circulating fluidized-bed gasification system. [WWW Document]. URL https://www.eep.ebara.com/en/business_technology/technology_3.html (accessed 8.16.24).

Ecoinvent, 2013. Ecoinvent database and methodology. Ecoinvent, the Centre for Life Cycle Inventories, Swiss Federal Institute of Technology. Zürich, Switzerland. url: http://www.ecoinvent.org/database/ecoinvent-version-2.

EIA, 2025. Refinery closures and rising consumption will reduce U.S. petroleum inventories in 2026 - U.S. Energy Information Administration (EIA). https://www.eia.gov/todayinenergy/detail.php?id=64644.

EIA, 2024a. U.S. Energy Information Administration. Monthly Energy Review - April 2024.

EIA, 2024b. EIA: US sustainable aviation fuel production capacity to grow exponentially this year. https://www.biobased-diesel.com/post/eia-us-sustainable-aviation-fuel-production-capacity-to-grow-exponentially-this-year.

EIA, 2023a. Annual Energy Outlook 2023 Electricity Generating Capacity. https://www.eia.gov/outlooks/aeo.

EIA, 2023b. U.S. Energy Information Administration Independent Statistics and Analysis. https://www.eia.gov/state/seds/data.php?incfile=/state/seds/sep_fuel/html/fuel_jf.html [WWW Document].

Enerkem, 2025. Ecoplanta Receives Approval: A Major Step Forward with Enerkem's Groundbreaking Waste-to-Methanol Technology. https://enerkem.com/newsroom/ecoplanta-receives-approval-a-major-step-forward-with-enerkems-groundbreaking-waste-to-methanol-technology.

EPA, 2025. 40 CFR 80.1426 -- How are RINs generated and assigned to batches of renewable fuel? https://www.ecfr.gov/current/title-40/part-80/section-80.1426.

EPA, 2024a. Landfill Technical Data. https://www.epa.gov/lmop/landfill-technical-data [WWW Document]. URL https://www.epa.gov/lmop/landfill-technical-data (accessed 8.16.24).

EPA, 2024b. Basic Information about Landfill Gas. https://www.epa.gov/lmop/basic-information-about-landfill-gas.

EPA, 2023a. EPA Proposes New Protections for Communities from Fuels Made Using Plastic Waste Based Feedstocks. https://www.epa.gov/chemicals-under-tsca/epa-proposes-new-protections-communities-fuels-made-using-plastic-waste-based.

EPA, 2023b. WARM version16 (2023). EPA Office of Resource Conservation and Recovery, Documentation for Greenhouse Gas Emission and Energy Factors Used in the Waste Reduction Model (WARM) https://www.epa.gov/warm.

EPA, 2020. Advancing Sustainable Materials Management: 2018 Fact Sheet. https://www.epa.gov/sites/default/files/2021-01/documents/2018_ff_fact_sheet_dec_2020_fnl_508.pdf.

EPA, 2016. Documentation for Greenhouse Gas Emission and Energy Factors Used in the Waste Reduction Model (WARM) - Background Chapters.

EPA, O., 2018. RIN Trades and Price Information. https://www.epa.gov/fuels-registration-reporting-and-compliance-help/rin-trades-and-price-information#regulatory-categories [WWW Document]. URL (accessed 9.19.24).

EPA, O., 2015. Renewable Fuel Standard Program. https://www.epa.gov/renewable-fuel-standard-program [WWW Document]. URL (accessed 8.20.24).

European Investment Bank, 2024. Managing refuse-derived and solid recovered fuels: best practice options for EU countries. https://www.eib.org/attachments/lucalli/20230376_managing_refuse_derived_and_solid_recovered_fuels_en.pdf. Publications Office, LU.

Goldner, W., Bredlau, J., Brown, N., Haq, Z., Brown, C., 2023. Grand Challenge Roadmap Flight Plan for Sustainable Aviation Fuel. U.S. Department of Energy, U.S. Department of Transportation, U.S. Department of Agriculture, U.S. Environmental Protection Agency.

Gross, S., 2020. The challenge of decarbonizing heavy transport. https://www.brookings.edu/wp-content/uploads/2020/09/FP_20201001_challenge_of_decarbonizing_heavy_transport.pdf.

GSTC, 2024a. Plasma Gasification. Global Syngas Technologies Council. URL https://globalsyngas.org/syngas-technology/syngas-production/waste-to-energy-gasification/plasma-gasification/ (accessed 8.16.24).

GSTC, 2024b. Global Syngas Technologies Council. https://globalsyngas.org/ [WWW Document]. URL https://globalsyngas.org/ (accessed 9.18.24).

Higman, C., 2011. 5 - Gasification process technology, in: Khan, M.R. (Ed.), Advances in Clean Hydrocarbon Fuel Processing, Woodhead Publishing Series in Energy. Woodhead Publishing, pp. 155–185. https://doi.org/10.1533/9780857093783.2.155

Hrbek, J., Pfeifer, C., Blanco-Sanchez, P., Baldwin, R., Swanson, M., Strege, J., 2025. Gas Cleaning from Gasification for Production of Biofuels and Biochemicals.

Huber, G.W., Iborra, S., Corma, A., 2006. Synthesis of Transportation Fuels from Biomass: Chemistry, Catalysts, and Engineering. Chem. Rev. 106, 4044–4098. https://doi.org/10.1021/cr068360d

Humbird, D., Davis, R., Tao, L., Kinchin, C., Hsu, D., Aden, A., Schoen, P., Lukas, J., Olthof, B., Worley, M., Sexton, D., Dudgeon, D., 2011. Process Design and Economics for Biochemical Conversion of Lignocellulosic Biomass to Ethanol. NREL Report.

IATA, 2023. SAF Volumes Growing but Still Missing Opportunities. International Air Transport Association. Press Release N: 69. https://www.iata.org/en/pressroom/2023-releases/2023-12-06-02.

Ibikunle, R.A., Titiladunayo, I.F., Akinnuli, B.O., Lukman, A.F., Ikubanni, P.P., Agboola, O.O., 2018. Modelling the energy content of municipal solid waste and determination of its physicochemical correlation, using multiple regression analysis. International Journal of Engineering and Technology.

ICAO, 2023. SAF Conversion processes. https://www.icao.int/SAF/saf-conversion-processes.

ICAO, 2022. States adopt net-zero 2050 global aspirational goal for international flight operations. https://www.icao.int/Newsroom/Pages/States-adopts-netzero-2050-aspirational-goal-for-international-flight-operations.aspx.

Janajreh, I., Raza, S.S., Valmundsson, A.S., 2013. Plasma gasification process: Modeling, simulation and comparison with conventional air gasification. Energy Conversion and Management 65, 801–809. https://doi.org/10.1016/j.enconman.2012.03.010

Jiang, Y., Mevawala, C., Li, S., Schmidt, A., Billing, J., Thorson, M., Snowden-Swan, L., 2023a. Uncertainty analysis for techno-economic and life-cycle assessment of wet waste hydrothermal liquefaction with centralized upgrading to produce fuel blendstocks. Journal of Environmental Chemical Engineering 11, 109706. https://doi.org/10.1016/j.jece.2023.109706

Jiang, Y., Zaimes, G.G., Li, S., Hawkins, T.R., Singh, A., Carlson, N., Talmadge, M., Gaspar, D.J., Ramirez-Corredores, M.M., Beck, A.W., Young, B., Sittler, L., Brooker, A., 2023b. Economic and environmental analysis to evaluate the potential value of co-optima diesel bioblendstocks to petroleum refiners. Fuel 333, 126233. https://doi.org/10.1016/j.fuel.2022.126233

Jones, S.B., Zhu, Y., Valkenburg, C., 2009. Municipal Solid Waste (MSW) to Liquid Fuels Synthesis, Volume 2: A Techno-economic Evaluation of the Production of Mixed Alcohols (No. PNNL-18482, 962845). https://doi.org/10.2172/962845

Keim, W., 2013. Oligomerization of Ethylene to α-Olefins: Discovery and Development of the Shell Higher Olefin Process (SHOP). Angewandte Chemie International Edition 52, 12492–12496. https://doi.org/10.1002/anie.201305308

Khan, M.J., Al-attab, K.A., 2022. Steam Gasification of Biomass for Hydrogen Production – A Review and Outlook. ARFMTS 98, 175–204. https://doi.org/10.37934/arfmts.98.2.175204

Klean Industries, 2024. Zero waste using gasification to convert municipal solid waste into clean energy & heating. https://kleanindustries.com/resource-recovery-projects/solid-waste-recycling/gasification-municipal-trash/ [WWW Document]. URL (accessed 8.16.24).

Labrie, M.-H., 2015. Waste-to-methanol: a commercial reality with Enerkem.

LanzaJet, 2023. Sustainable Fuels. https://www.lanzajet.com/sustainable-fuels [WWW Document]. URL https://www.lanzajet.com/sustainable-fuels (accessed 9.18.24).

Lavrenov, A.V., Karpova, T.R., Buluchevskii, E.A., Bogdanets, E.N., 2016. Heterogeneous oligomerization of light alkenes: 80 years in oil refining. Catal. Ind. 8, 316–327. https://doi.org/10.1134/S2070050416040061

Leckner, B., 2015. Process aspects in combustion and gasification Waste-to-Energy (WtE) units. Waste Management 37, 13–25. https://doi.org/10.1016/j.wasman.2014.04.019

Li, S., Jiang, Y., Snowden-Swan, L.J., Askander, J.A., Schmidt, A.J., Billing, J.M., 2021. Techno-economic uncertainty analysis of wet waste-to-biocrude via hydrothermal liquefaction. Applied Energy 283, 116340. https://doi.org/10.1016/j.apenergy.2020.116340

LiBretto, N.J., Xu, Y., Quigley, A., Edwards, E., Nargund, R., Vega-Vila, J.C., Caulkins, R., Saxena, A., Gounder, R., Greeley, J., Zhang, G., Miller, J.T., 2021. Olefin oligomerization by main group Ga3+ and Zn2+ single site catalysts on SiO2. Nat Commun 12, 2322. https://doi.org/10.1038/s41467-021-22512-6

Marcantonio, V., Müller, M., Bocci, E., 2021. A Review of Hot Gas Cleaning Techniques for Hydrogen Chloride Removal from Biomass-Derived Syngas. Energies 14, 6519. https://doi.org/10.3390/en14206519

Mazzoni, L., Almazrouei, M., Ghenai, C., Janajreh, I., 2017. A comparison of energy recovery from MSW through plasma gasification and entrained flow gasification. Energy Procedia 142, 3480–3485. https://doi.org/10.1016/j.egypro.2017.12.233

Mazzoni, L., Janajreh, I., 2017. Plasma gasification of municipal solid waste with variable content of plastic solid waste for enhanced energy recovery. International Journal of Hydrogen Energy 42, 19446–19457. https://doi.org/10.1016/j.ijhydene.2017.06.069

Mitsubishi Power, 2021. Mitsubishi Power | Mitsubishi Power's Gasification Technology Contributes to Supplying Sustainable Aviation Fuel from Woody Biomass for Regularly Scheduled Flight -- Entrained Bed Gasification Technology Contributing to Decarbonization in Aviation -- [WWW Document]. Mitsubishi Power. URL https://power.mhi.com/news/20210618.html (accessed 8.16.24).

Molaeimanesh, G.R., Torabi, F., 2022. Fuel Cell Modeling and Simulation. Elsevier.

Myhre, G., Shindell, D., Bréon, F.-M., Collins, W., Fuglestvedt, J., Huang, J., Koch, D., Lamarque, J.-F., Lee, D., Mendoza, B., Nakajima, T., Robock, A., Stephens, G., Zhang, H., Aamaas, B., Boucher, O., Dalsøren, S.B., Daniel, J.S., Forster, P., Granier, C., Haigh, J., Hodnebrog, Ø., Kaplan, J.O., Marston, G., Nielsen, C.J., O'Neill, B.C., Peters, G.P., Pongratz, J., Ramaswamy, V., Roth, R., Rotstayn, L., Smith, S.J., Stevenson, D., Vernier, J.-P., Wild, O., Young, P., Jacob, D., Ravishankara, A.R., Shine, K., 2013. Anthropogenic and Natural Radiative Forcing. In: Climate Change 2013: The Physical Science Basis. Contribution of Working Group I to the Fifth Assessment Report of the Intergovernmental Panel on Climate Change [Stocker, T.F., D. Qin, G.-K. Plattner, M. Tignor, S.K. Allen, J. Boschung, A. Nauels, Y. Xia, V. Bex and P.M. Midgley (eds.)]. Cambridge University Press, Cambridge, United Kingdom and New York, NY, USA.

NETL, 2025. Syngas Contaminant Removal and Conditioning. https://www.netl.doe.gov/research/coal/energy-systems/gasification/gasifipedia/cleanup.

NETL, 2024a. Gasification Introduction. https://netl.doe.gov/research/Coal/energy-systems/gasification/gasifipedia/intro-to-gasification [WWW Document]. URL (accessed 8.16.24).

NETL, 2024b. Fixed (Moving) Bed Gasifiers. https://netl.doe.gov/research/Coal/energy-systems/gasification/gasifipedia/fmb [WWW Document]. netl.doe.gov. URL https://netl.doe.gov/research/Coal/energy-systems/gasification/gasifipedia/fmb (accessed 8.16.24).

NETL, 2024c. Fluidized Bed Gasifiers. https://netl.doe.gov/research/coal/energy-systems/gasification/gasifipedia/fluidizedbed [WWW Document]. URL (accessed 8.16.24).

NETL, 2024d. Entrained Flow Gasifiers. https://netl.doe.gov/research/coal/energy-systems/gasification/gasifipedia/entrainedflow [WWW Document]. URL (accessed 8.16.24).

NETL, 2024e. Plasma Gasification. https://netl.doe.gov/research/Coal/energy-systems/gasification/gasifipedia/westinghouse [WWW Document]. URL (accessed 8.16.24).

NRG Focus, 2013. Delivering the World's Largest Plasma Gasifier.

Pang, S., 2016. Fuel flexible gas production, in: Fuel Flexible Energy Generation. Elsevier, pp. 241–269. https://doi.org/10.1016/B978-1-78242-378-2.00009-2

Phillips, S., Aden, A., Jechura, J., Dayton, D., 2007. Thermochemical Ethanol via Indirect Gasification and Mixed Alcohol Synthesis of Lignocellulosic Biomass. Technical Report NREL/TP-510-41168. https://www.nrel.gov/docs/fy07osti/41168.pdf.

Pivnenko, K., Olsson, M.E., Götze, R., Eriksson, E., Astrup, T.F., 2016. Quantification of chemical contaminants in the paper and board fractions of municipal solid waste. Waste Management 51, 43–54. https://doi.org/10.1016/j.wasman.2016.03.008

Pullao, J.A., Benedetto, F.E., Binetti Basterrechea, G.F., Neira Poblete, L.A., Lago, D.C., Prado, M.O., 2024. Plasma Gasification of a Simulated Low-Level Radioactive Waste: Co, Cs, Sr, and Ce Retention Efficiency. Processes 12, 1919. https://doi.org/10.3390/pr12091919

Qureshi, M.S., Oasmaa, A., Pihkola, H., Deviatkin, I., Tenhunen, A., Mannila, J., Minkkinen, H., Pohjakallio, M., Laine-Ylijoki, J., 2020. Pyrolysis of plastic waste: Opportunities and challenges. Journal of Analytical and Applied Pyrolysis 152, 104804. https://doi.org/10.1016/j.jaap.2020.104804

Sánchez, A., Martín, M., 2022. Thermochemical processes, in: Sustainable Design for Renewable Processes. Elsevier, pp. 133–192. https://doi.org/10.1016/B978-0-12-824324-4.00018-4

Seiple, T., Jiang, Y., Snowden-Swan, L.J., Betzsold, N., Ramasamy, K.K., Fuller, C., 2023. Cost-Effective Opportunities to Produce Sustainable Aviation Fuel from Low-Cost Wastes in the U.S. ACS Sustainable Chem. Eng. 11, 12326–12335. https://doi.org/10.1021/acssuschemeng.3c02147

Shah, H.H., Amin, M., Iqbal, A., Nadeem, I., Kalin, M., Soomar, A.M., Galal, A.M., 2023. A review on gasification and pyrolysis of waste plastics. Front. Chem. 10, 960894. https://doi.org/10.3389/fchem.2022.960894

Shah, V., Kuehn, N., Turner, M., 2014. Cost and Performance Baseline for Fossil Energy Plants - Volume 4: Coal-to-Liquids via Fischer-Tropsch Synthesis (No. DOE/NETL-2011/1477, 1513211). https://doi.org/10.2172/1513211

Shahabuddin, M., Alam, T., 2022. Gasification of Solid Fuels (Coal, Biomass and MSW): Overview, Challenges and Mitigation Strategies. Energies 15, 4444. https://doi.org/10.3390/en15124444

Shen, X., Huang, G., Yang, Z., Han, L., 2015. Compositional characteristics and energy potential of Chinese animal manure by type and as a whole. Applied Energy 160, 108–119. https://doi.org/10.1016/j.apenergy.2015.09.034

Shi, H., Mahinpey, N., Aqsha, A., Silbermann, R., 2016. Characterization, thermochemical conversion studies, and heating value modeling of municipal solid waste. Waste Management 48, 34–47. https://doi.org/10.1016/j.wasman.2015.09.036

Siram, P., Nash, M., Maronneaud, O., 2014. Chemical Economics Handbook Methanol (674.5000), IHS Chemical, May 2014.

Sunshine Canyon Landfill, 2024. Disposal & Material Costs. https://sunshinecanyonlandfill.com/drop-off-information/disposal-costs/.

Thompson, V., 2020. Q4 Milestone ReportBioenergy Technologies Office. Idaho National Laboratory. INL/EXT-20-60571-Revision-0.

UOP, 2023. Honeywell ethanol to jet. https://ess.honeywell.com/content/dam/ess/en/documents/document-lists/uop/events/afpm-annual-meeting/renewable-fuels/Ethanol-to-Jet-Datasheet.pdf.

UOP, 2019. UOP Advanced Methanol to Olefins (MTO) Process. https://uop.honeywell.com/content/dam/uop/en-us/documents/industry-solutions/petrochemicals/olefins/uop-advanced-methanol-to-olefins-process-datasheet.pdf.

UOP, 2004. UOP/HYDRO MTO Process - Methanol to Olefins Conversion.

U.S. Department of Transportation, 2016. User Guidelines for Waste and Byproduct Materials in Pavement Construction. FHWA-RD-97-148.

Vora, B.V., Marker, T.L., Nilsen, H.R., 1998. Process for producing light olefins from crude methanol. US 5714662A.

Wang, B., Gupta, R., Bei, L., Wan, Q., Sun, L., 2023. A review on gasification of municipal solid waste (MSW): Syngas production, tar formation, mineral transformation and industrial challenges. International Journal of Hydrogen Energy 48, 26676–26706. https://doi.org/10.1016/j.ijhydene.2023.03.086

Wang, W.-C., Tao, L., 2016. Bio-jet fuel conversion technologies. Renewable and Sustainable Energy Reviews 53, 801–822. https://doi.org/10.1016/j.rser.2015.09.016

Waste Today, 2017. Cogent Energy Systems selected for Department of Energy Small Business Vouchers Award [WWW Document]. URL https://www.wastetodaymagazine.com/news/cogent-energy-systems-selected-doe-small-business-voucher/ (accessed 8.16.24).

Zafar, S., 2009. Gasification of Municipal Solid Waste [WWW Document]. URL https://www.altenergymag.com/article/2009/06/gasification-of-municipal-solid-waste/545/ (accessed 8.16.24).

Zhao, J., Wang, Z., Li, J., Yan, B., Chen, G., 2022. Pyrolysis of food waste and food waste solid digestate: A comparative investigation. Bioresource Technology 354, 127191. https://doi.org/10.1016/j.biortech.2022.127191

Zhao, P., Ni, G., Jiang, Y., Chen, L., Chen, M., Meng, Y., 2010. Destruction of inorganic municipal solid waste incinerator fly ash in a DC arc plasma furnace. Journal of Hazardous Materials 181, 580–585. https://doi.org/10.1016/j.jhazmat.2010.05.052

Appendix A – Conversion Life Cycle Inventory and Energy and Carbon Efficiencies

Table A-1. Life cycle inventory for Base Case 1 (SAF-max) and Base Case 2 (Self-powered) emissions.

SAF Plant	Base Case 1	Base Case 2
Feedstock Properties		
RDF (wet basis), lb/h	83,336	83,336
Moisture content, %	7.86	7.86
Ash content (dry basis), %	11.95	11.95
Inputs		
Electricity, kW		
Total produced	10,171	31,783
Plant demand	38,036	33,359
Net electricity demand	27,865	1,576
Process water, lb/h	670,420	694,152
Hydrogen, lb/h	245	152
Outputs		
SAF, lb/h	15,388	9,541
Bio-naphtha, lb/h	1,267	785
Biodiesel lb/h	103	64
Sulfur (by-product), lb/h	162	101
Waste Streams		
Ash, lb/h	8,337	8,337
Wastewater, lb/h	86,418	63,837
Air Emissions		
CO_2 (fossil)		
Process emissions, lb/h	18,604	11,535
Process heat, lb/h	4,620	17,921
Fuel product combustion, lb/h	16,042	10,834
CO_2 (biogenic), lb/h	85,229	83,202
Carbon Efficiency (%, mass)	39.3%	24.4%
Thermal Efficiency (%, LHV, dry RDF)	36.4%	31.3%

LHV = lower heating value; RDF = refuse-derived fuel; SAF = sustainable aviation fuel.

Table A-2. Landfill emissions from organic portions of the feedstock.

	Emissions ($MTCO_2e$/MT Wet Waste)	Dry to Wet Weight Ratio [a]	Waste Composition (wt%)	Emissions ($MTCO_2e$/MT Dry Waste)
Paper products	0.40	90%	0.35	0.44
Food	0.51	29%	0.25	1.75
Leaves and grass	0.21	40%	0.075	0.51

	Emissions ($MTCO_2e$/MT Wet Waste)	Dry to Wet Weight Ratio [a]	Waste Composition (wt%)	Emissions ($MTCO_2e$/MT Dry Waste)
Branches	0.27	84%	0.075	0.32
Wood	0.27	80%	0.24	0.33
Organic waste				**0.733**

[a] Moisture content for waste categories is taken from the U.S. Environmental Protection Agency's WARM tool.
MT = metric ton.

Appendix B – Cost Factors and Financial Assumptions

Table B-1. Cost factors for direct and indirect project costs.

Direct Costs	
Item	% of total installed cost
Buildings	4.0%
Total direct cost (TDC)	104.0%
Indirect costs	
Item	% of TDC
Engineering, site development, piping, etc.	50%
Project contingency	10%
Total indirect costs	60%
Working capital	5% of fixed capital investment
Land	114 acres @ $15,000/acre

Table B-2. Financial assumptions for the economic analysis.

Assumption Description	Assumed Value
Internal rate of return	10%
Plant financing debt/equity	60%/40% of total capital investment
Plant life	30 yr
Income tax rate	21%
Interest rate for debt financing	8.0% annually
Term for debt financing	10 yr
Working capital cost	5.0% of fixed capital investment (excluding land)
Depreciation schedule	7 yr, MACRS[(a)] schedule
Construction period	3 yr (8% 1st yr, 60% 2nd yr, 32% 3rd yr)
Plant salvage value	No value
Start-up time	6 months
Revenue and costs during start-up	Revenue = 50% of normal Variable costs = 75% of normal Fixed costs = 100% of normal
On-stream factor	90% (7,884 operating hours per year)

(a) Modified accelerated cost recovery system.

Appendix C – Key Sources of Uncertainties

Table C-1. Uncertainty sources for the MSW-to-SAF conversion process.

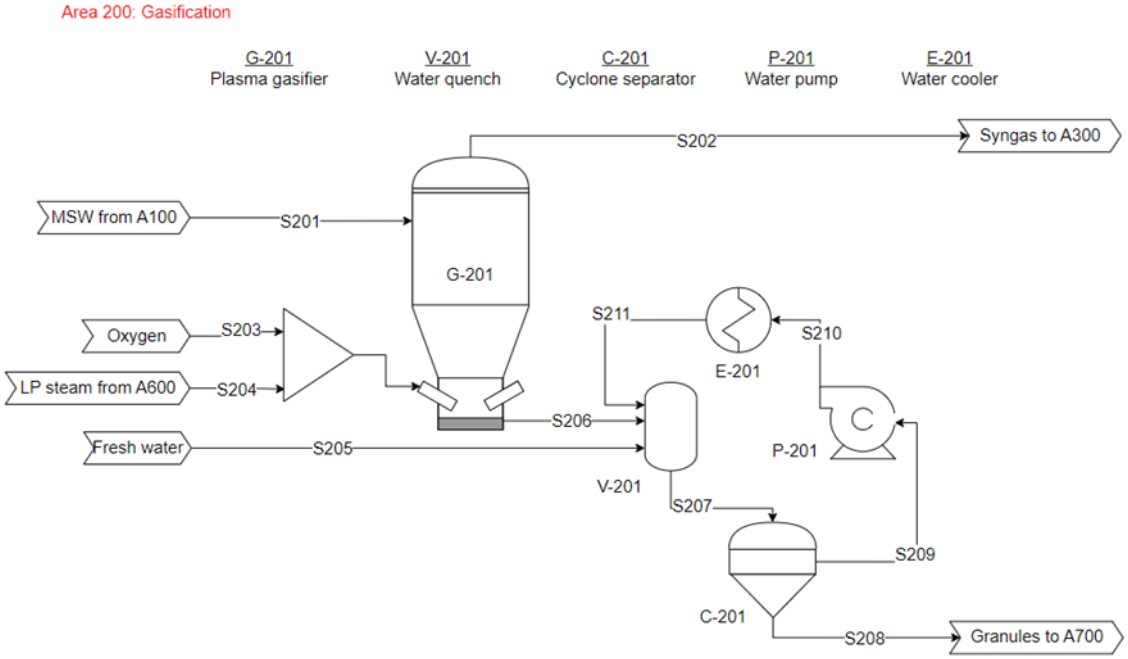
Model Input	Unit	Base Value	Uncertainty			
			Type	Alpha	Beta	Gamma
General Economic Assumptions						
Hydrogen price	$/lb	0.88	B	1.19	0.17	1.72
Electricity price	¢/kWh	6.76	T	6.76	5.83	7.66
MSW tipping fee	$/ton	0	T	15.4	0	58.3
Plant Performance						
SAF yield	Actual/predicted	1	N	1	0.05	
Utility Consumption	Actual/predicted	1	T	1	0.9	1.1
Capital Costs						
Area 100	Relative difference	0.0%	T	0.0%	−10.0%	15.0%
Area 200	Relative difference	0.0%	T	0.0%	−30.0%	50.0%
Area 300	Relative difference	0.0%	T	0.0%	−20.0%	30.0%
Area 400	Relative difference	0.0%	T	0.0%	−10.0%	15.0%
Area 500	Relative difference	0.0%	T	0.0%	−20.0%	30.0%
OSBLs (Areas 600 and 700)	Relative difference	0.0%	T	0.0%	−30.0%	50.0%

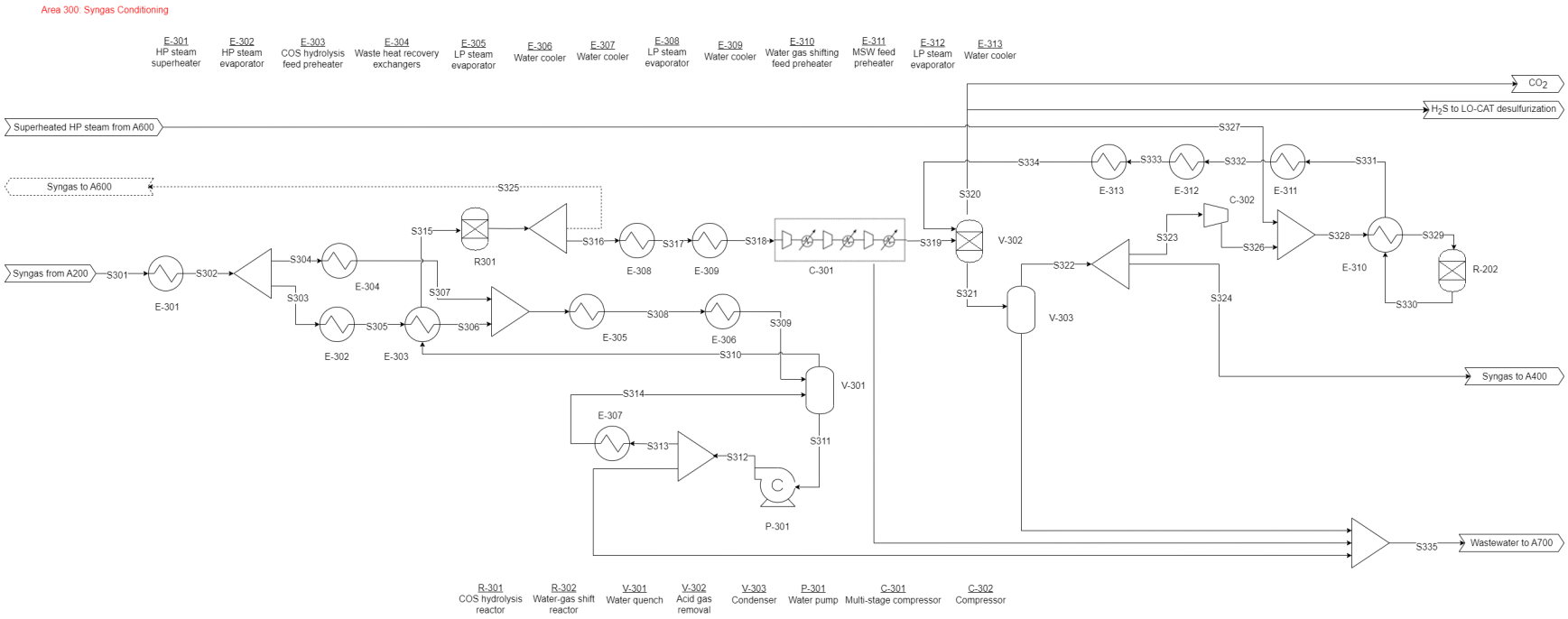
B = beta distribution (β = min ; γ = max); MSW = municipal solid waste; N = Normal distribution (α = mean; β = σ); SAF = sustainable aviation fuel; T = triangular distribution (α = likeliest; β = min; γ = max). OSBL = outside battery limits

.

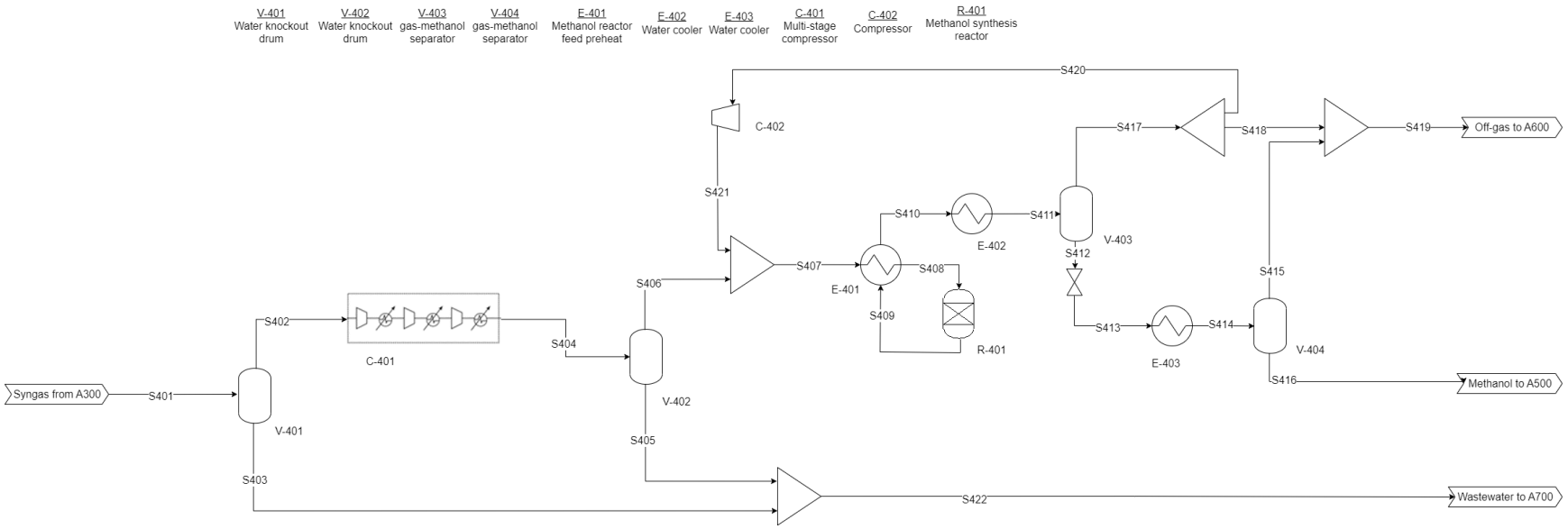
Appendix D – Detailed Process Flow Diagrams and Stream Tables

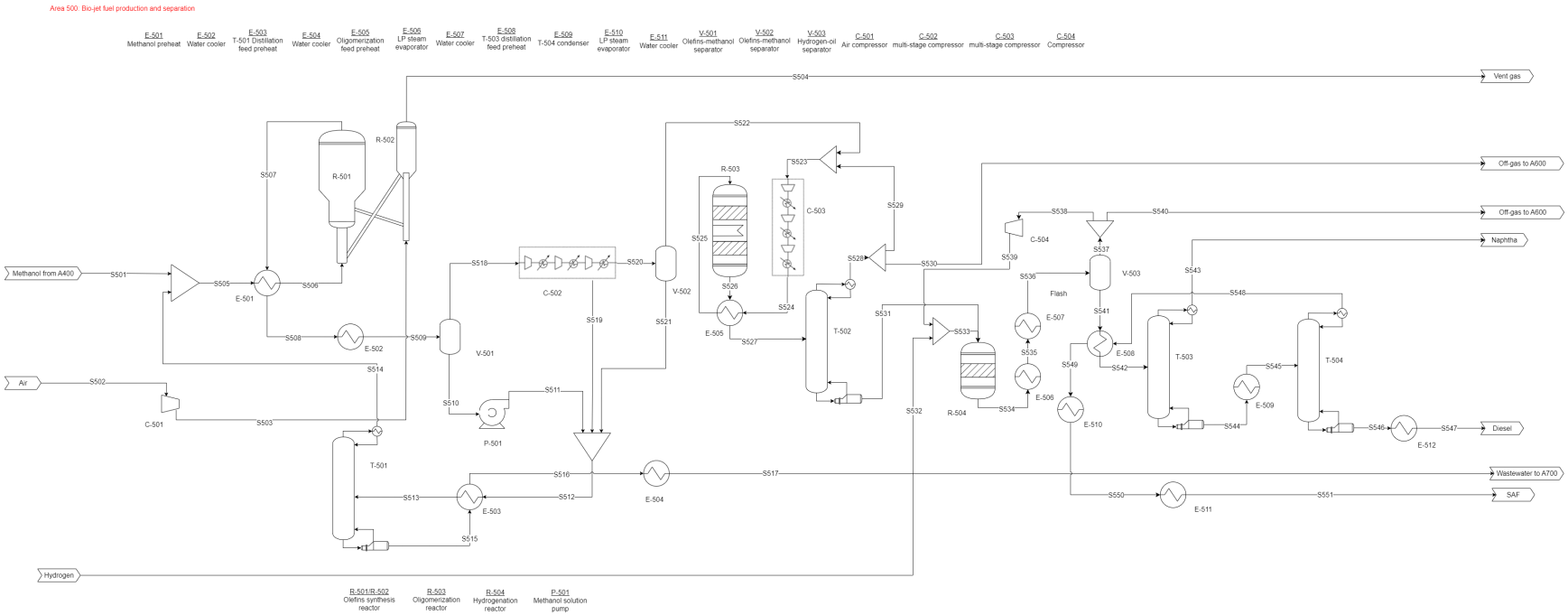
D.1 Detailed Process Flow Diagrams




Area 300: Syngas Conditioning
E-301 HP steam superheater
E-302 HP steam evaporator
E-303 COS hydrolysis feed preheater
E-304 Waste heat recovery exchangers
E-305 LP steam evaporator
E-306 Water cooler
E-307 Water cooler
E-308 LP steam evaporator
E-309 Water cooler
E-310 Water gas shifting feed preheater
E-311 MSW feed preheater
E-312 LP steam evaporator
E-313 Water cooler
Superheated HP steam from A600
Syngas to A600
Syngas from A200
CO2
H2S to LO-CAT desulfurization
Syngas to A400
Wastewater to A700
S301
S302
S303
S304
S305
S306
S307
S308
S309
S310
S311
S312
S313
S314
S315
S316
S317
S318
S319
S320
S321
S322
S323
S324
S325
S326
S327
S328
S329
S330
S331
S332
S333
S334
S335
R301
R-202
V-301
V-302
V-303
C-301
C-302
P-301
R-301 COS hydrolysis reactor
R-302 Water-gas shift reactor
V-301 Water quench
V-302 Acid gas removal
V-303 Condenser
P-301 Water pump
C-301 Multi-stage compressor
C-302 Compressor

Area 400: Methanol synthesis





D.2 Stream Tables of Base Case 1

Table D-1. Area 200: Gasification stream.

Stream	S201	S202	S203	S204	S205	S206	S207	S208	S209	S210	S211
Temperature, °F	77.0	2,389.0	77.0	287.1	77.0	4,532.0	194.0	194.0	194.0	194.0	86.0
Pressure, psia	14.7	14.7	14.7	52.9	14.7	14.7	14.7	14.7	14.7	19.7	19.7
Mass Flows, lb/h	83,335.5	130,154.8	35,918.6	25,816.0	1,322.9	11,905.7	80,216.0	13,227.7	66,988.3	66,988.3	66,987.4
O_2	0.0	0.0	35,918.6	0.0	0.0	0.0	0.0	0.0	0.0	0.0	0.0
N_2	0.0	801.8	0.0	0.0	0.0	0.0	0.0	0.0	0.0	0.0	0.0
H_2	0.0	4,156.2	0.0	0.0	0.0	0.0	0.0	0.0	0.0	0.0	0.0
CO	0.0	60,610.7	0.0	0.0	0.0	0.0	0.0	0.0	0.0	0.0	0.0
CO_2	0.0	30,239.4	0.0	0.0	0.0	0.0	0.0	0.0	0.0	0.0	0.0
H_2O	2.2	34,168.1	0.0	25,816.0	1,322.9	0.0	68,310.3	1,322.0	66,988.3	66,988.3	66,987.4
H_2S	0.0	166.3	0.0	0.0	0.0	0.0	0.0	0.0	0.0	0.0	0.0
COS	0.0	12.2	0.0	0.0	0.0	0.0	0.0	0.0	0.0	0.0	0.0

Stream	S201	S202	S203	S204	S205	S206	S207	S208	S209	S210	S211
ASH	0.0	0.0	0.0	0.0	0.0	11,905.7	11,905.7	11,905.7	0.0	0.0	0.0
MSW	83,333.3	0.0	0.0	0.0	0.0	0.0	0.0	0.0	0.0	0.0	0.0

Table D-2. Area 300: Syngas Cleanup and Conditioning stream.

Stream	S301	S302	S303	S304	S305	S306	S307	S308	S309	S310	S311
Temperature, °F	2,389.0	1,559.5	1,559.5	1,559.5	804.9	542.1	652.3	307.4	140.0	124.2	124.2
Pressure, psia	14.7	14.7	14.7	14.7	14.7	14.7	14.7	14.7	14.7	14.7	14.7
Mass Flows, lb/h	130,154.8	130,154.8	94,534.6	35,620.2	94,534.6	94,534.6	35,620.2	130,154.8	130,154.8	107,620.1	620,331.9
N_2	801.8	801.8	582.4	219.4	582.4	582.4	219.4	801.8	801.8	801.8	0.0
H_2	4,156.2	4,156.2	3,018.7	1,137.5	3,018.7	3,018.7	1,137.5	4,156.2	4,156.2	4,156.2	0.0
CO	60,610.7	60,610.7	44,023.0	16,587.7	44,023.0	44,023.0	16,587.7	60,610.7	60,610.7	60,610.6	0.1
CO_2	30,239.4	30,239.4	21,963.6	8,275.8	21,963.6	21,963.6	8,275.8	30,239.4	30,239.4	30,235.8	3.6
H_2O	34,168.1	34,168.1	24,817.1	9,351.0	24,817.1	24,817.1	9,351.0	34,168.1	34,168.1	11,637.6	620,327.7
H_2S	166.3	166.3	120.8	45.5	120.8	120.8	45.5	166.3	166.3	165.8	0.5
COS	12.2	12.2	8.9	3.3	8.9	8.9	3.3	12.2	12.2	12.2	0.0
Stream	**S312**	**S313**	**S314**	**S315**	**S316**	**S317**	**S318**	**S319**	**S320**	**S321**	**S322**
Temperature, °F	124.2	124.2	109.9	375.1	375.1	307.4	140.0	140.0	140.0	120.0	120.0
Pressure, psia	35.0	35.0	35.0	14.7	14.7	14.7	14.7	420.0	420.0	420.0	420.0
Mass Flows, lb/h	620,331.9	597,797.2	597,797.2	107,620.1	107,620.1	107,620.1	107,620.1	97,175.5	71,003.6	112,223.4	99,677.8
N_2	0.0	0.0	0.0	801.8	801.8	801.8	801.8	801.8	0.0	1,512.9	1,512.8
H_2	0.0	0.0	0.0	4,156.2	4,156.2	4,156.2	4,156.2	4,156.2	0.0	10,872.0	10,872.0
CO	0.1	0.1	0.1	60,610.6	60,610.6	60,610.6	60,610.6	60,610.6	0.0	72,256.0	72,256.0
CO_2	3.6	3.5	3.5	30,235.8	30,244.7	30,244.7	30,244.7	30,244.3	57,664.6	14,416.1	14,415.6
H_2O	620,327.7	597,793.1	597,793.1	11,637.6	11,634.0	11,634.0	11,634.0	1,189.8	13,166.3	13,166.3	621.4
H_2S	0.5	0.5	0.5	165.8	172.7	172.7	172.7	172.7	172.7	0.0	0.0
COS	0.0	0.0	0.0	12.2	0.0	0.0	0.0	0.0	0.0	0.0	0.0

Stream	S323	S324	S325	S326	S327	S328	S329	S330	S331	S332	S333
Temperature, °F	120.0	120.0	-	125.2	831.7	399.6	650.0	907.5	669.3	430.0	307.4
Pressure, psia	420.0	420.0	-	430.0	680.0	430.0	430.0	420.0	420.0	420.0	420.0
Mass Flows, lb/h	46,848.6	52,829.2	-	46,848.6	39,202.9	86,051.5	86,051.5	86,051.5	86,051.5	86,051.5	86,051.5
N_2	711.0	801.8	-	711.0	0.0	711.0	711.0	711.0	711.0	711.0	711.0
H_2	5,109.8	5,762.1	-	5,109.8	0.0	5,109.8	5,109.8	6,715.8	6,715.8	6,715.8	6,715.8
CO	33,960.3	38,295.7	-	33,960.3	0.0	33,960.3	33,960.3	11,645.4	11,645.4	11,645.4	11,645.4
CO_2	6,775.3	7,640.2	-	6,775.3	0.0	6,775.3	6,775.3	41,836.4	41,836.4	41,836.4	41,836.4
H_2O	292.1	329.4	-	292.1	39,202.9	39,495.0	39,495.0	25,142.9	25,142.9	25,142.9	25,142.9
H_2S	0.0	0.0	-	0.0	0.0	0.0	0.0	0.0	0.0	0.0	0.0
COS	0.0	0.0	-	0.0	0.0	0.0	0.0	0.0	0.0	0.0	0.0

Stream	S334	S335
Temperature, °F	140.0	127.0
Pressure, psia	420.0	28.7
Mass Flows, lb/h	86,051.5	45,524.9
N_2	711.0	0.0
H_2	6,715.8	0.0
CO	11,645.4	0.0
CO_2	41,836.4	1.1
H_2O	25,142.9	45,523.7
H_2S	0.0	0.1
COS	0.0	0.0

Table D-3. Area 400: Methanol Synthesis stream.

Stream	S401	S402	S403	S404	S405	S406	S407	S408	S409	S410	S411
Temperature, °F	120.0	118.9	118.9	140.0	140.0	140.0	124.4	440.0	500.0	213.6	105.0

Pressure, psia	420.0	420.0	420.0	925.0	925.0	925.0	925.0	925.0	875.0	875.0	870.0
Mass Flows, lb/h	52,829.2	52,780.3	48.9	52,780.3	24.6	52,755.7	259,881.4	259,881.4	259,881.4	259,881.4	259,881.4
N_2	801.8	801.8	0.0	801.8	0.0	801.8	25,945.1	25,945.1	25,945.1	25,945.1	25,945.1
H_2	5,762.1	5,762.1	0.0	5,762.1	0.0	5,762.1	18,087.9	18,087.9	12,713.6	12,713.6	12,713.6
CO	38,295.7	38,295.7	0.0	38,295.7	0.0	38,295.7	133,300.4	133,300.4	98,043.0	98,043.0	98,043.0
CO_2	7,640.2	7,640.2	0.0	7,640.2	0.0	7,640.2	79,290.3	79,290.3	77,111.7	77,111.7	77,111.7
H_2O	329.4	280.5	48.9	280.5	24.6	255.9	317.2	317.2	1,209.0	1,209.0	1,209.0
CH_4	0.0	0.0	0.0	0.0	0.0	0.0	0.2	0.2	0.2	0.2	0.2
METHANOL	0.0	0.0	0.0	0.0	0.0	0.0	2,940.3	2,940.3	44,858.8	44,858.8	44,858.8
Stream	**S412**	**S413**	**S414**	**S415**	**S416**	**S417**	**S418**	**S419**	**S420**	**S421**	**S422**
Temperature, °F	104.9	103.0	78.1	78.1	78.1	104.9	104.9	92.6	104.9	119.5	126.4
Pressure, psia	865.0	65.0	65.0	65.0	65.0	865.0	865.0	65.0	865.0	925.0	420.0
Mass Flows, lb/h	46,349.5	46,349.5	46,349.5	1,486.7	44,862.7	213,532.0	6,406.0	7,892.7	207,126.0	207,126.0	73.5
N_2	24.1	24.1	24.1	23.7	0.4	25,921.0	777.6	801.3	25,143.4	25,143.4	0.0
H_2	6.7	6.7	6.7	6.6	0.1	12,707.0	381.2	387.8	12,325.7	12,325.7	0.0
CO	99.7	99.7	99.7	97.7	2.0	97,943.3	2,938.3	3,036.0	95,005.0	95,005.0	0.0
CO_2	3,245.6	3,245.6	3,245.6	1,316.5	1,929.1	73,866.1	2,216.0	3,532.5	71,650.1	71,650.1	0.0
H_2O	1,145.8	1,145.8	1,145.8	0.9	1,144.9	63.2	1.9	2.8	61.3	61.3	73.5
CH_4	0.0	0.0	0.0	0.0	0.0	0.2	0.0	0.0	0.2	0.2	0.0
METHANOL	41,827.5	41,827.5	41,827.5	41.3	41,786.2	3,031.3	90.9	132.3	2,940.3	2,940.3	0.0

Table D-4. Area 500: Methanol to SAF stream.

Stream	**S501**	**S502**	**S503**	**S504**	**S505**	**S506**	**S507**	**S508**	**S509**	**S510**	**S511**
Temperature, °F	78.1	90.0	477.1	1,035.9	88.2	241.0	814.0	246.8	140.0	140.0	140.1
Pressure, psia	65.0	14.7	55.0	50.0	65.0	65.0	65.0	60.0	55.0	55.0	84.6
Mass Flows, lb/h	44,862.7	43,190.6	43,190.6	43,551.1	45,128.4	45,128.4	44,767.9	44,767.9	44,767.9	23,221.2	23,221.2
O_2	0.0	10,022.5	10,022.5	9,062.0	0.0	0.0	0.0	0.0	0.0	0.0	0.0
N_2	0.4	32,631.8	32,631.8	32,631.8	0.4	0.4	0.4	0.4	0.4	0.0	0.0

H_2	0.1	0.0	0.0	0.0	0.1	0.1	230.8	230.8	230.8	0.0	0.0
CO	2.0	0.0	0.0	0.0	2.0	2.0	43.9	43.9	43.9	0.0	0.0
CO_2	1,929.1	0.0	0.0	1,321.0	1,929.8	1,929.8	3,239.7	3,239.7	3,239.7	0.7	0.7
H_2O	1,144.9	0.0	0.0	0.0	1,379.4	1,379.4	23,767.3	23,767.3	23,767.3	23,190.5	23,190.5
CH_4	0.0	0.0	0.0	0.0	0.0	0.0	1.0	1.0	1.0	0.0	0.0
$C2H_4$	0.0	0.0	0.0	0.0	0.2	0.2	7,086.3	7,086.3	7,086.3	0.2	0.2
$C2H_6$	0.0	0.0	0.0	0.0	0.0	0.0	155.0	155.0	155.0	0.0	0.0
$C3H_8$	0.0	0.0	0.0	0.0	0.0	0.0	97.8	97.8	97.8	0.0	0.0
ARGON	0.0	536.2	536.2	536.2	0.0	0.0	0.0	0.0	0.0	0.0	0.0
METHANOL	41,786.2	0.0	0.0	0.0	41,816.4	41,816.4	41.8	41.8	41.8	29.8	29.8
C_3H_6	0.0	0.0	0.0	0.0	0.1	0.1	7,082.6	7,082.6	7,082.6	0.1	0.1
C_4H_8	0.0	0.0	0.0	0.0	0.0	0.0	2,174.7	2,174.7	2,174.7	0.0	0.0
C_5H_{10}	0.0	0.0	0.0	0.0	0.0	0.0	823.8	823.8	823.8	0.0	0.0
C_4H_{10}	0.0	0.0	0.0	0.0	0.0	0.0	22.8	22.8	22.8	0.0	0.0
Stream	**S512**	**S513**	**S514**	**S515**	**S516**	**S517**	**S518**	**S519**	**S520**	**S521**	**S522**
Temperature, °F	140.1	218.1	308.6	312.8	236.1	140.0	140.0	140.0	140.0	147.8	147.8
Pressure, psia	84.6	84.6	79.4	79.4	79.4	79.4	55.0	84.6	130.0	130.0	130.0
Mass Flows, lb/h	23,487.3	23,487.3	265.7	23,221.6	23,221.6	23,221.6	21,546.7	199.5	21,347.2	66.6	21,280.6
O_2	0.0	0.0	0.0	0.0	0.0	0.0	0.0	0.0	0.0	0.0	0.0
N_2	0.0	0.0	0.0	0.0	0.0	0.0	0.4	0.0	0.4	0.0	0.4
H_2	0.0	0.0	0.0	0.0	0.0	0.0	230.8	0.0	230.8	0.0	230.8
CO	0.0	0.0	0.0	0.0	0.0	0.0	43.9	0.0	43.9	0.0	43.9
CO_2	0.7	0.7	0.7	0.0	0.0	0.0	3,239.0	0.0	3,238.9	0.0	3,238.9
H_2O	23,456.0	23,456.0	234.6	23,221.4	23,221.4	23,221.4	576.9	199.1	377.8	66.5	311.3
CH_4	0.0	0.0	0.0	0.0	0.0	0.0	1.0	0.0	1.0	0.0	1.0
C_2H_4	0.2	0.2	0.2	0.0	0.0	0.0	7,086.1	0.0	7,086.1	0.0	7,086.1
C_2H_6	0.0	0.0	0.0	0.0	0.0	0.0	155.0	0.0	155.0	0.0	155.0
C_3H_8	0.0	0.0	0.0	0.0	0.0	0.0	97.8	0.0	97.8	0.0	97.8
ARGON	0.0	0.0	0.0	0.0	0.0	0.0	0.0	0.0	0.0	0.0	0.0
METHANOL	30.3	30.3	30.1	0.2	0.2	0.2	12.1	0.4	11.7	0.2	11.5
C_3H_6	0.1	0.1	0.1	0.0	0.0	0.0	7,082.5	0.0	7,082.5	0.0	7,082.5
C_4H_8	0.0	0.0	0.0	0.0	0.0	0.0	2,174.7	0.0	2,174.7	0.0	2,174.7
C_5H_{10}	0.0	0.0	0.0	0.0	0.0	0.0	823.8	0.0	823.8	0.0	823.8
C_4H_{10}	0.0	0.0	0.0	0.0	0.0	0.0	22.8	0.0	22.8	0.0	22.8
Stream	**S523**	**S524**	**S525**	**S526**	**S527**	**S528**	**S529**	**S530**	**S531**	**S532**	**S533**
Temperature, °F	117.5	140.0	482.0	589.7	344.8	83.0	83.0	83.0	609.1	77.0	113.7

Pressure, psia	130.0	350.0	345.0	250.0	250.0	235.1	235.1	235.1	245.1	147.0	140.7
Mass Flows, lb/h	27,992.9	24,431.1	24,431.1	24,431.1	24,431.1	7,896.9	6,712.3	1,184.5	16,534.3	244.9	925.5
O_2	0.0	0.0	0.0	0.0	0.0	0.0	0.0	0.0	0.0	0.0	0.0
N_2	3.0	3.0	3.0	3.0	3.0	3.0	2.5	0.4	0.0	0.0	0.0
H_2	1,538.7	1,538.7	1,538.7	1,538.7	1,538.7	1,538.7	1,307.9	230.8	0.0	244.9	790.4
CO	292.5	292.5	292.5	292.5	292.5	292.5	248.6	43.9	0.0	0.0	0.0
CO_2	3,238.9	0.0	0.0	0.0	0.0	0.0	0.0	0.0	0.0	0.0	0.0
H_2O	311.3	0.0	0.0	0.0	0.0	0.0	0.0	0.0	0.0	0.0	0.0
CH_4	6.9	6.9	6.9	6.9	6.9	6.9	5.9	1.0	0.0	0.0	0.5
C_2H_4	7,793.5	7,793.5	7,793.5	832.3	832.3	832.3	707.4	124.8	0.1	0.0	0.0
C_2H_6	1,032.7	1,032.7	1,032.7	1,032.7	1,032.7	1,032.6	877.7	154.9	0.1	0.0	1.4
C_3H_8	650.0	650.0	650.0	650.0	650.0	649.6	552.2	97.4	0.3	0.0	1.0
ARGON	0.0	0.0	0.0	0.0	0.0	0.0	0.0	0.0	0.0	0.0	0.0
METHANOL	11.5	0.0	0.0	0.0	0.0	0.0	0.0	0.0	0.0	0.0	0.0
C_3H_6	7,082.5	7,082.5	7,082.5	0.0	0.0	0.0	0.0	0.0	0.0	0.0	0.0
C_4H_8	3,001.4	3,001.4	3,001.4	974.7	974.7	972.5	826.6	145.9	2.2	0.0	0.0
C_5H_{10}	2,601.7	2,601.7	2,601.7	2,112.9	2,112.9	2,091.7	1,778.0	313.8	21.1	0.0	0.0
C_4H_{10}	149.9	149.9	149.9	149.9	149.9	149.6	127.2	22.4	0.3	0.0	2.8
C_6H_{12}	278.3	278.3	278.3	741.7	741.7	327.4	278.3	49.1	414.3	0.0	0.0
C_7H_{14}	0.0	0.0	0.0	801.5	801.5	0.0	0.0	0.0	801.5	0.0	0.0
C_8H_{16}	0.0	0.0	0.0	854.1	854.1	0.0	0.0	0.0	854.1	0.0	0.0
C_9H_{18}	0.0	0.0	0.0	2,601.6	2,601.6	0.0	0.0	0.0	2,601.6	0.0	0.0
$C_{10}H_{20}$	0.0	0.0	0.0	2,746.1	2,746.1	0.0	0.0	0.0	2,746.1	0.0	0.0
$C_{11}H_{22}$	0.0	0.0	0.0	2,369.5	2,369.5	0.0	0.0	0.0	2,369.5	0.0	0.0
$C_{12}H_{24}$	0.0	0.0	0.0	2,036.6	2,036.6	0.0	0.0	0.0	2,036.6	0.0	0.0
$C_{13}H_{26}$	0.0	0.0	0.0	1,660.0	1,660.0	0.0	0.0	0.0	1,660.0	0.0	0.0
$C_{14}H_{28}$	0.0	0.0	0.0	1,261.4	1,261.4	0.0	0.0	0.0	1,261.4	0.0	0.0
$C_{15}H_{30}$	0.0	0.0	0.0	674.5	674.5	0.0	0.0	0.0	674.5	0.0	0.0
$C_{16}H_{32}$	0.0	0.0	0.0	446.7	446.7	0.0	0.0	0.0	446.7	0.0	0.0
$C_{17}H_{34}$	0.0	0.0	0.0	337.3	337.3	0.0	0.0	0.0	337.3	0.0	0.0
$C_{18}H_{36}$	0.0	0.0	0.0	205.8	205.8	0.0	0.0	0.0	205.8	0.0	0.0
$C_{19}H_{38}$	0.0	0.0	0.0	48.2	48.2	0.0	0.0	0.0	48.2	0.0	0.0
$C_{20}H_{40}$	0.0	0.0	0.0	39.4	39.4	0.0	0.0	0.0	39.4	0.0	0.0
$C_{21}H_{42}$	0.0	0.0	0.0	13.1	13.1	0.0	0.0	0.0	13.1	0.0	0.0
C_5H_{12}	0.0	0.0	0.0	0.0	0.0	0.0	0.0	0.0	0.0	0.0	7.7
C_6H_{14}	0.0	0.0	0.0	0.0	0.0	0.0	0.0	0.0	0.0	0.0	51.2
C_7H_{16}	0.0	0.0	0.0	0.0	0.0	0.0	0.0	0.0	0.0	0.0	35.0
C_8H_{18}	0.0	0.0	0.0	0.0	0.0	0.0	0.0	0.0	0.0	0.0	13.0

C_9H_{20}	0.0	0.0	0.0	0.0	0.0	0.0	0.0	0.0	0.0	0.0	14.4
$C_{10}H_{22}$	0.0	0.0	0.0	0.0	0.0	0.0	0.0	0.0	0.0	0.0	5.4
$C_{11}H_{24}$	0.0	0.0	0.0	0.0	0.0	0.0	0.0	0.0	0.0	0.0	1.8
$C_{12}H_{26}$	0.0	0.0	0.0	0.0	0.0	0.0	0.0	0.0	0.0	0.0	0.6
$C_{13}H_{28}$	0.0	0.0	0.0	0.0	0.0	0.0	0.0	0.0	0.0	0.0	0.2
$C_{14}H_{30}$	0.0	0.0	0.0	0.0	0.0	0.0	0.0	0.0	0.0	0.0	0.1
$C_{15}H_{32}$	0.0	0.0	0.0	0.0	0.0	0.0	0.0	0.0	0.0	0.0	0.0
$C_{16}H_{34}$	0.0	0.0	0.0	0.0	0.0	0.0	0.0	0.0	0.0	0.0	0.0
$C_{17}H_{36}$	0.0	0.0	0.0	0.0	0.0	0.0	0.0	0.0	0.0	0.0	0.0
$C_{18}H_{38}$	0.0	0.0	0.0	0.0	0.0	0.0	0.0	0.0	0.0	0.0	0.0
$C_{19}H_{40}$	0.0	0.0	0.0	0.0	0.0	0.0	0.0	0.0	0.0	0.0	0.0
$C_{20}H_{42}$	0.0	0.0	0.0	0.0	0.0	0.0	0.0	0.0	0.0	0.0	0.0
$C_{21}H_{44}$	0.0	0.0	0.0	0.0	0.0	0.0	0.0	0.0	0.0	0.0	0.0
Stream	**S534**	**S535**	**S536**	**S537**	**S538**	**S539**	**S540**	**S541**	**S542**	**S543**	**S544**
Temperature, °F	853.6	307.4	109.4	109.4	109.4	129.7	109.4	109.4	337.9	190.6	364.3
Pressure, psia	135.7	135.7	132.3	128.1	128.1	140.7	128.1	128.1	128.1	15.0	17.9
Mass Flows, lb/h	17,459.8	17,459.8	17,459.8	701.6	680.6	680.6	21.0	16,758.2	16,758.2	1,266.8	15,491.3
O_2	0.0	0.0	0.0	0.0	0.0	0.0	0.0	0.0	0.0	0.0	0.0
N_2	0.0	0.0	0.0	0.0	0.0	0.0	0.0	0.0	0.0	0.0	0.0
H_2	564.6	564.6	564.6	562.3	545.4	545.4	16.9	2.3	2.3	2.3	0.0
CO	0.0	0.0	0.0	0.0	0.0	0.0	0.0	0.0	0.0	0.0	0.0
CO_2	0.0	0.0	0.0	0.0	0.0	0.0	0.0	0.0	0.0	0.0	0.0
H_2O	0.0	0.0	0.0	0.0	0.0	0.0	0.0	0.0	0.0	0.0	0.0
CH_4	0.5	0.5	0.5	0.5	0.5	0.5	0.0	0.0	0.0	0.0	0.0
C_2H_4	0.0	0.0	0.0	0.0	0.0	0.0	0.0	0.0	0.0	0.0	0.0
C_2H_6	1.6	1.6	1.6	1.5	1.4	1.4	0.0	0.1	0.1	0.1	0.0
C_3H_8	1.3	1.3	1.3	1.0	1.0	1.0	0.0	0.3	0.3	0.3	0.0
C_4H_{10}	5.5	5.5	5.5	2.9	2.8	2.8	0.1	2.5	2.5	2.5	0.0
C_5H_{12}	29.4	29.4	29.4	7.9	7.7	7.7	0.2	21.5	21.5	21.5	0.0
C_6H_{14}	475.5	475.5	475.5	52.8	51.2	51.2	1.6	422.7	422.7	422.7	0.0
C_7H_{16}	853.0	853.0	853.0	36.1	35.0	35.0	1.1	816.9	816.9	808.7	8.2
C_8H_{18}	882.4	882.4	882.4	13.4	13.0	13.0	0.4	869.0	869.0	8.7	860.3
C_9H_{20}	2,657.5	2,657.5	2,657.5	14.8	14.4	14.4	0.4	2,642.7	2,642.7	0.0	2,642.7
$C_{10}H_{22}$	2,791.0	2,791.0	2,791.0	5.6	5.4	5.4	0.2	2,785.4	2,785.4	0.0	2,785.4
$C_{11}H_{24}$	2,402.2	2,402.2	2,402.2	1.8	1.8	1.8	0.1	2,400.4	2,400.4	0.0	2,400.4
$C_{12}H_{26}$	2,061.6	2,061.6	2,061.6	0.6	0.6	0.6	0.0	2,061.0	2,061.0	0.0	2,061.0
$C_{13}H_{28}$	1,678.5	1,678.5	1,678.5	0.2	0.2	0.2	0.0	1,678.3	1,678.3	0.0	1,678.3

$C_{14}H_{30}$	1,274.4	1,274.4	1,274.4	0.1	0.1	0.1	0.0	1,274.3	1,274.3	0.0	1,274.3
$C_{15}H_{32}$	680.9	680.9	680.9	0.0	0.0	0.0	0.0	680.9	680.9	0.0	680.9
$C_{16}H_{34}$	450.8	450.8	450.8	0.0	0.0	0.0	0.0	450.8	450.8	0.0	450.8
$C_{17}H_{36}$	340.1	340.1	340.1	0.0	0.0	0.0	0.0	340.1	340.1	0.0	340.1
$C_{18}H_{38}$	207.5	207.5	207.5	0.0	0.0	0.0	0.0	207.5	207.5	0.0	207.5
$C_{19}H_{40}$	48.5	48.5	48.5	0.0	0.0	0.0	0.0	48.5	48.5	0.0	48.5
$C_{20}H_{42}$	39.7	39.7	39.7	0.0	0.0	0.0	0.0	39.7	39.7	0.0	39.7
$C_{21}H_{44}$	13.2	13.2	13.2	0.0	0.0	0.0	0.0	13.2	13.2	0.0	13.2
Stream	**S545**	**S546**	**S547**	**S548**	**S549**	**S550**	**S551**				
Temperature, °F	382.9	655.5	140.0	429.0	357.8	307.4	104.0				
Pressure, psia	17.9	17.9	17.9	15.0	15.0	15.0	15.0				
Mass Flows, lb/h	15,491.3	103.1	103.1	15,388.3	15,388.3	15,388.3	15,388.3				
C_7H_{16}	8.2	0.0	0.0	8.2	8.2	8.2	8.2				
C_8H_{18}	860.3	0.0	0.0	860.3	860.3	860.3	860.3				
C_9H_{20}	2,642.7	0.0	0.0	2,642.7	2,642.7	2,642.7	2,642.7				
$C_{10}H_{22}$	2,785.4	0.0	0.0	2,785.4	2,785.4	2,785.4	2,785.4				
$C_{11}H_{24}$	2,400.4	0.0	0.0	2,400.4	2,400.4	2,400.4	2,400.4				
$C_{12}H_{26}$	2,061.0	0.0	0.0	2,061.0	2,061.0	2,061.0	2,061.0				
$C_{13}H_{28}$	1,678.3	0.0	0.0	1,678.3	1,678.3	1,678.3	1,678.3				
$C_{14}H_{30}$	1,274.3	0.0	0.0	1,274.3	1,274.3	1,274.3	1,274.3				
$C_{15}H_{32}$	680.9	0.0	0.0	680.9	680.9	680.9	680.9				
$C_{16}H_{34}$	450.8	0.0	0.0	450.8	450.8	450.8	450.8				
$C_{17}H_{36}$	340.1	0.0	0.0	340.1	340.1	340.1	340.1				
$C_{18}H_{38}$	207.5	2.1	2.1	205.4	205.4	205.4	205.4				
$C_{19}H_{40}$	48.5	48.1	48.1	0.5	0.5	0.5	0.5				
$C_{20}H_{42}$	39.7	39.7	39.7	0.0	0.0	0.0	0.0				
$C_{21}H_{44}$	13.2	13.2	13.2	0.0	0.0	0.0	0.0				

D.3 Stream Tables of Base Case 2

Table D-5. Area 200: Gasification stream.

Stream	S201	S202	S203	S204	S205	S206	S207	S208	S209	S210	S211
Temperature, °F	77.0	2,389.0	77.0	287.1	77.0	4,532.0	194.0	194.0	194.0	194.0	86.0
Pressure, psia	14.7	14.7	14.7	52.9	14.7	14.7	14.7	14.7	14.7	19.7	19.7
Mass Flows, lb/h	83,335.5	130,154.8	35,918.6	25,816.0	1,322.9	11,905.7	80,216.0	13,227.7	66,988.3	66,988.3	66,987.4
O_2	0.0	0.0	35,918.6	0.0	0.0	0.0	0.0	0.0	0.0	0.0	0.0
N_2	0.0	801.8	0.0	0.0	0.0	0.0	0.0	0.0	0.0	0.0	0.0
H_2	0.0	4,156.2	0.0	0.0	0.0	0.0	0.0	0.0	0.0	0.0	0.0
CO	0.0	60,610.7	0.0	0.0	0.0	0.0	0.0	0.0	0.0	0.0	0.0
CO_2	0.0	30,239.4	0.0	0.0	0.0	0.0	0.0	0.0	0.0	0.0	0.0
H_2O	2.2	34,168.1	0.0	25,816.0	1,322.9	0.0	68,310.3	1,322.0	66,988.3	66,988.3	66,987.4
H_2S	0.0	166.3	0.0	0.0	0.0	0.0	0.0	0.0	0.0	0.0	0.0
COS	0.0	12.2	0.0	0.0	0.0	0.0	0.0	0.0	0.0	0.0	0.0
ASH	0.0	0.0	0.0	0.0	0.0	11,905.7	11,905.7	11,905.7	0.0	0.0	0.0
MSW	83,333.3	0.0	0.0	0.0	0.0	0.0	0.0	0.0	0.0	0.0	0.0

Table D.2. Area 300: Syngas Cleanup and Conditioning stream.

Stream	S301	S302	S303	S304	S305	S306	S307	S308	S309	S310	S311
Temperature, °F	2,389.0	1,559.5	1,559.5	1,559.5	804.9	575.5	652.3	307.4	140.0	124.2	124.2
Pressure, psia	14.7	14.7	14.7	14.7	14.7	14.7	14.7	14.7	14.7	14.7	14.7
Mass Flows, lb/h	130,154.8	130,154.8	108,070.7	22,084.1	108,070.7	108,070.7	22,084.1	130,154.8	130,154.8	107,620.1	620,331.9
N_2	801.8	801.8	665.8	136.0	665.8	665.8	136.0	801.8	801.8	801.8	0.0
H_2	4,156.2	4,156.2	3,451.0	705.2	3,451.0	3,451.0	705.2	4,156.2	4,156.2	4,156.2	0.0
CO	60,610.7	60,610.7	50,326.5	10,284.2	50,326.5	50,326.5	10,284.2	60,610.7	60,610.7	60,610.6	0.1
CO_2	30,239.4	30,239.4	25,108.5	5,130.9	25,108.5	25,108.5	5,130.9	30,239.4	30,239.4	30,235.8	3.6

H_2O	34,168.1	34,168.1	28,370.6	5,797.5	28,370.6	28,370.6	5,797.5	34,168.1	34,168.1	11,637.6	620,327.7
H_2S	166.3	166.3	138.1	28.2	138.1	138.1	28.2	166.3	166.3	165.8	0.5
COS	12.2	12.2	10.2	2.1	10.2	10.2	2.1	12.2	12.2	12.2	0.0
Stream	**S312**	**S313**	**S314**	**S315**	**S316**	**S317**	**S318**	**S319**	**S320**	**S321**	**S322**
Temperature, °F	124.2	124.2	109.9	375.1	375.1	307.4	140.0	140.0	140.0	120.0	120.0
Pressure, psia	35.0	35.0	35.0	14.7	14.7	14.7	14.7	420.0	420.0	420.0	420.0
Mass Flows, lb/h	620,331.9	597,797.2	597,797.2	107,620.1	66,724.4	66,724.4	66,724.4	60,248.8	44,022.2	69,578.5	61,800.2
N_2	0.0	0.0	0.0	801.8	497.1	497.1	497.1	497.1	0.0	938.0	938.0
H_2	0.0	0.0	0.0	4,156.2	2,576.8	2,576.8	2,576.8	2,576.8	0.0	6,740.6	6,740.6
CO	0.1	0.1	0.1	60,610.6	37,578.6	37,578.6	37,578.6	37,578.6	0.0	44,798.7	44,798.7
CO_2	3.6	3.5	3.5	30,235.8	18,751.7	18,751.7	18,751.7	18,751.5	35,752.0	8,938.0	8,937.6
H_2O	620,327.7	597,793.1	597,793.1	11,637.6	7,213.1	7,213.1	7,213.1	737.7	8,163.1	8,163.1	385.3
H_2S	0.5	0.5	0.5	165.8	107.1	107.1	107.1	107.1	107.1	0.0	0.0
COS	0.0	0.0	0.0	12.2	0.0	0.0	0.0	0.0	0.0	0.0	0.0
Stream	**S323**	**S324**	**S325**	**S326**	**S327**	**S328**	**S329**	**S330**	**S331**	**S332**	**S333**
Temperature, °F	120.0	120.0	375.1	125.2	842.0	380.7	650.0	907.5	651.1	313.5	307.4
Pressure, psia	420.0	420.0	14.7	430.0	1,305.3	430.0	430.0	420.0	420.0	420.0	420.0
Mass Flows, lb/h	29,046.1	32,754.1	40,895.6	29,046.1	24,305.8	53,351.9	53,351.9	53,351.9	53,351.9	53,351.9	53,351.9
N_2	440.8	497.1	304.7	440.8	0.0	440.8	440.8	440.8	440.8	440.8	440.8
H_2	3,168.1	3,572.5	1,579.3	3,168.1	0.0	3,168.1	3,168.1	4,163.8	4,163.8	4,163.8	4,163.8
CO	21,055.4	23,743.3	23,032.0	21,055.4	0.0	21,055.4	21,055.4	7,220.1	7,220.1	7,220.1	7,220.1
CO_2	4,200.7	4,737.0	11,493.0	4,200.7	0.0	4,200.7	4,200.7	25,938.6	25,938.6	25,938.6	25,938.6
H_2O	181.1	204.2	4,420.9	181.1	24,305.8	24,486.9	24,486.9	15,588.6	15,588.6	15,588.6	15,588.6
H_2S	0.0	0.0	65.6	0.0	0.0	0.0	0.0	0.0	0.0	0.0	0.0
COS	0.0	0.0	0.0	0.0	0.0	0.0	0.0	0.0	0.0	0.0	0.0
Stream	**S334**	**S335**									

Temperature, °F	140.0	126.3
Pressure, psia	420.0	28.7
Mass Flows, lb/h	53,351.9	36,788.6
N_2	440.8	0.0
H_2	4,163.8	0.0
CO	7,220.1	0.0
CO_2	25,938.6	0.7
H_2O	15,588.6	36,787.8
H_2S	0.0	0.0
COS	0.0	0.0

Table D-6. Area 400: Methanol Synthesis stream.

Stream	**S401**	**S402**	**S403**	**S404**	**S405**	**S406**	**S407**	**S408**	**S409**	**S410**	**S411**
Temperature, °F	120.0	118.9	118.9	140.0	140.0	140.0	124.4	440.0	500.0	213.6	105.0
Pressure, psia	420.0	420.0	420.0	925.0	925.0	925.0	925.0	925.0	875.0	875.0	870.0
Mass Flows, lb/h	32,754.1	32,723.8	30.3	32,723.8	15.3	32,708.6	161,131.7	161,131.7	161,131.7	161,131.7	161,131.7
N_2	497.1	497.1	0.0	497.1	0.0	497.1	16,086.9	16,086.9	16,086.9	16,086.9	16,086.9
H_2	3,572.5	3,572.5	0.0	3,572.5	0.0	3,572.5	11,214.5	11,214.5	7,882.4	7,882.4	7,882.4
CO	23,743.3	23,743.3	0.0	23,743.3	0.0	23,743.3	82,649.1	82,649.1	60,789.5	60,789.5	60,789.5
CO_2	4,737.0	4,736.9	0.0	4,736.9	0.0	4,736.9	49,161.1	49,161.1	47,810.4	47,810.4	47,810.4
H_2O	204.2	173.9	30.3	173.9	15.2	158.6	196.6	196.6	749.5	749.5	749.5
CH_4	0.0	0.0	0.0	0.0	0.0	0.0	0.1	0.1	0.1	0.1	0.1
METHANOL	0.0	0.0	0.0	0.0	0.0	0.0	1,823.1	1,823.1	27,812.5	27,812.5	27,812.5
C_3H_6	0.0	0.0	0.0	0.0	0.0	0.0	0.3	0.3	0.3	0.3	0.3
Stream	**S412**	**S413**	**S414**	**S415**	**S416**	**S417**	**S418**	**S419**	**S420**	**S421**	**S422**
Temperature, °F	104.9	103.0	78.1	78.1	78.1	104.9	104.9	92.6	104.9	119.5	126.4

Pressure, psia	865.0	65.0	65.0	65.0	65.0	865.0	865.0	65.0	865.0	925.0	420.0
Mass Flows, lb/h	28,736.7	28,736.7	28,736.7	921.8	27,814.9	132,395.0	3,971.8	4,893.7	128,423.1	128,423.1	45.6
N_2	15.0	15.0	15.0	14.7	0.3	16,071.9	482.2	496.8	15,589.8	15,589.8	0.0
H_2	4.1	4.1	4.1	4.1	0.0	7,878.3	236.3	240.5	7,641.9	7,641.9	0.0
CO	61.8	61.8	61.8	60.6	1.3	60,727.7	1,821.8	1,882.4	58,905.8	58,905.8	0.0
CO_2	2,012.3	2,012.3	2,012.3	816.3	1,196.0	45,798.1	1,373.9	2,190.2	44,424.1	44,424.1	0.0
H_2O	710.4	710.4	710.4	0.6	709.8	39.2	1.2	1.7	38.0	38.0	45.6
CH_4	0.0	0.0	0.0	0.0	0.0	0.1	0.0	0.0	0.1	0.1	0.0
METHANOL	25,933.1	25,933.1	25,933.1	25.6	25,907.5	1,879.4	56.4	82.0	1,823.1	1,823.1	0.0
C_3H_6	0.0	0.0	0.0	0.0	0.0	0.3	0.0	0.0	0.3	0.3	0.0

Table D-7. Area 500: Methanol to SAF stream.

Stream	**S501**	**S502**	**S503**	**S504**	**S505**	**S506**	**S507**	**S508**	**S509**	**S510**	**S511**
Temperature, °F	78.1	90.0	477.1	1,035.9	88.2	241.0	814.0	246.8	140.0	140.0	140.1
Pressure, psia	65.0	14.7	55.0	50.0	65.0	65.0	65.0	60.0	55.0	55.0	84.6
Mass Flows, lb/h	27,814.9	26,778.2	26,778.2	27,001.7	27,979.6	27,979.6	27,756.1	27,756.1	27,756.1	14,397.1	14,397.1
O_2	0.0	6,214.0	6,214.0	5,618.5	0.0	0.0	0.0	0.0	0.0	0.0	0.0
N_2	0.3	20,231.7	20,231.7	20,231.7	0.3	0.3	0.3	0.3	0.3	0.0	0.0
H_2	0.0	0.0	0.0	0.0	0.0	0.0	143.1	143.1	143.1	0.0	0.0
CO	1.3	0.0	0.0	0.0	1.3	1.3	27.2	27.2	27.2	0.0	0.0
CO_2	1,196.0	0.0	0.0	819.0	1,196.5	1,196.5	2,008.6	2,008.6	2,008.6	0.5	0.5
H_2O	709.8	0.0	0.0	0.0	855.2	855.2	14,735.7	14,735.7	14,735.7	14,378.1	14,378.1
CH_4	0.0	0.0	0.0	0.0	0.0	0.0	0.6	0.6	0.6	0.0	0.0
C_2H_4	0.0	0.0	0.0	0.0	0.1	0.1	4,393.5	4,393.5	4,393.5	0.1	0.1
C_2H_6	0.0	0.0	0.0	0.0	0.0	0.0	96.1	96.1	96.1	0.0	0.0
C_3H_8	0.0	0.0	0.0	0.0	0.0	0.0	60.6	60.6	60.6	0.0	0.0
ARGON	0.0	332.5	332.5	332.5	0.0	0.0	0.0	0.0	0.0	0.0	0.0
METHANOL	25,907.5	0.0	0.0	0.0	25,926.2	25,926.2	25.9	25.9	25.9	18.4	18.4
C_3H_6	0.0	0.0	0.0	0.0	0.1	0.1	4,391.2	4,391.2	4,391.2	0.0	0.0
C_4H_8	0.0	0.0	0.0	0.0	0.0	0.0	1,348.3	1,348.3	1,348.3	0.0	0.0
C_5H_{10}	0.0	0.0	0.0	0.0	0.0	0.0	510.7	510.7	510.7	0.0	0.0

C_4H_{10}	0.0	0.0	0.0	0.0	0.0	0.0	14.1	14.1	14.1	0.0	0.0
Stream	**S512**	**S513**	**S514**	**S515**	**S516**	**S517**	**S518**	**S519**	**S520**	**S521**	**S522**
Temperature, °F	140.1	218.1	308.6	312.8	236.1	140.0	140.0	140.0	140.0	147.8	147.8
Pressure, psia	84.6	84.6	79.4	79.4	79.4	79.4	55.0	84.6	130.0	130.0	130.0
Mass Flows, lb/h	14,562.1	14,562.1	164.7	14,397.4	14,397.4	14,397.4	13,359.0	123.7	13,235.3	41.3	13,194.0
O_2	0.0	0.0	0.0	0.0	0.0	0.0	0.0	0.0	0.0	0.0	0.0
N_2	0.0	0.0	0.0	0.0	0.0	0.0	0.3	0.0	0.3	0.0	0.3
H_2	0.0	0.0	0.0	0.0	0.0	0.0	143.1	0.0	143.1	0.0	143.1
CO	0.0	0.0	0.0	0.0	0.0	0.0	27.2	0.0	27.2	0.0	27.2
CO_2	0.5	0.5	0.5	0.0	0.0	0.0	2,008.2	0.0	2,008.1	0.0	2,008.1
H_2O	14,542.7	14,542.7	145.4	14,397.3	14,397.3	14,397.3	357.7	123.4	234.2	41.2	193.0
CH_4	0.0	0.0	0.0	0.0	0.0	0.0	0.6	0.0	0.6	0.0	0.6
C_2H_4	0.1	0.1	0.1	0.0	0.0	0.0	4,393.4	0.0	4,393.4	0.0	4,393.4
C_2H_6	0.0	0.0	0.0	0.0	0.0	0.0	96.1	0.0	96.1	0.0	96.1
C_3H_8	0.0	0.0	0.0	0.0	0.0	0.0	60.6	0.0	60.6	0.0	60.6
ARGON	0.0	0.0	0.0	0.0	0.0	0.0	0.0	0.0	0.0	0.0	0.0
METHANOL	18.8	18.8	18.7	0.1	0.1	0.1	7.5	0.2	7.2	0.1	7.1
C_3H_6	0.0	0.0	0.0	0.0	0.0	0.0	4,391.2	0.0	4,391.2	0.0	4,391.2
C_4H_8	0.0	0.0	0.0	0.0	0.0	0.0	1,348.3	0.0	1,348.3	0.0	1,348.3
C_5H_{10}	0.0	0.0	0.0	0.0	0.0	0.0	510.7	0.0	510.7	0.0	510.7
C_4H_{10}	0.0	0.0	0.0	0.0	0.0	0.0	14.1	0.0	14.1	0.0	14.1
Stream	**S523**	**S524**	**S525**	**S526**	**S527**	**S528**	**S529**	**S530**	**S531**	**S532**	**S533**
Temperature, °F	117.5	140.0	482.0	589.7	344.8	83.0	83.0	83.0	609.1	77.0	113.7
Pressure, psia	130.0	350.0	345.0	250.0	250.0	235.1	235.1	235.1	245.1	147.0	140.7
Mass Flows, lb/h	17,355.6	15,147.3	15,147.3	15,147.3	15,147.3	4,896.1	4,161.7	734.4	10,251.3	151.8	573.7
O_2	0.0	0.0	0.0	0.0	0.0	0.0	0.0	0.0	0.0	0.0	0.0
N_2	1.8	1.8	1.8	1.8	1.8	1.8	1.6	0.3	0.0	0.0	0.0
H_2	954.0	954.0	954.0	954.0	954.0	954.0	810.9	143.1	0.0	151.8	490.0
CO	181.4	181.4	181.4	181.4	181.4	181.4	154.1	27.2	0.0	0.0	0.0
CO_2	2,008.1	0.0	0.0	0.0	0.0	0.0	0.0	0.0	0.0	0.0	0.0
H_2O	193.0	0.0	0.0	0.0	0.0	0.0	0.0	0.0	0.0	0.0	0.0
CH_4	4.3	4.3	4.3	4.3	4.3	4.3	3.6	0.6	0.0	0.0	0.2
C_2H_4	4,832.0	4,832.0	4,832.0	516.0	516.0	516.0	438.6	77.4	0.0	0.0	0.0

C_2H_6	640.3	640.3	640.3	640.3	640.3	640.2	544.2	96.0	0.1	0.0	0.9
C_3H_8	403.0	403.0	403.0	403.0	403.0	402.8	342.4	60.4	0.2	0.0	0.6
ARGON	0.0	0.0	0.0	0.0	0.0	0.0	0.0	0.0	0.0	0.0	0.0
METHANOL	7.1	0.0	0.0	0.0	0.0	0.0	0.0	0.0	0.0	0.0	0.0
C_3H_6	4,391.2	4,391.2	4,391.2	0.0	0.0	0.0	0.0	0.0	0.0	0.0	0.0
C_4H_8	1,860.8	1,860.8	1,860.8	604.3	604.3	603.0	512.5	90.4	1.4	0.0	0.0
C_5H_{10}	1,613.1	1,613.1	1,613.1	1,310.0	1,310.0	1,296.9	1,102.3	194.5	13.1	0.0	0.0
C_4H_{10}	93.0	93.0	93.0	93.0	93.0	92.8	78.9	13.9	0.2	0.0	1.8
C_6H_{12}	172.5	172.5	172.5	459.9	459.9	203.0	172.5	30.4	256.9	0.0	0.0
C_7H_{14}	0.0	0.0	0.0	496.9	496.9	0.0	0.0	0.0	496.9	0.0	0.0
C_8H_{16}	0.0	0.0	0.0	529.5	529.5	0.0	0.0	0.0	529.5	0.0	0.0
C_9H_{18}	0.0	0.0	0.0	1,613.0	1,613.0	0.0	0.0	0.0	1,613.0	0.0	0.0
$C_{10}H_{20}$	0.0	0.0	0.0	1,702.6	1,702.6	0.0	0.0	0.0	1,702.6	0.0	0.0
$C_{11}H_{22}$	0.0	0.0	0.0	1,469.1	1,469.1	0.0	0.0	0.0	1,469.1	0.0	0.0
$C_{12}H_{24}$	0.0	0.0	0.0	1,262.7	1,262.7	0.0	0.0	0.0	1,262.7	0.0	0.0
$C_{13}H_{26}$	0.0	0.0	0.0	1,029.2	1,029.2	0.0	0.0	0.0	1,029.2	0.0	0.0
$C_{14}H_{28}$	0.0	0.0	0.0	782.1	782.1	0.0	0.0	0.0	782.1	0.0	0.0
$C_{15}H_{30}$	0.0	0.0	0.0	418.2	418.2	0.0	0.0	0.0	418.2	0.0	0.0
$C_{16}H_{32}$	0.0	0.0	0.0	277.0	277.0	0.0	0.0	0.0	277.0	0.0	0.0
$C_{17}H_{34}$	0.0	0.0	0.0	209.1	209.1	0.0	0.0	0.0	209.1	0.0	0.0
$C_{18}H_{36}$	0.0	0.0	0.0	127.6	127.6	0.0	0.0	0.0	127.6	0.0	0.0
$C_{19}H_{38}$	0.0	0.0	0.0	29.9	29.9	0.0	0.0	0.0	29.9	0.0	0.0
$C_{20}H_{40}$	0.0	0.0	0.0	24.4	24.4	0.0	0.0	0.0	24.4	0.0	0.0
$C_{21}H_{42}$	0.0	0.0	0.0	8.1	8.1	0.0	0.0	0.0	8.1	0.0	0.0
C_5H_{12}	0.0	0.0	0.0	0.0	0.0	0.0	0.0	0.0	0.0	0.0	4.8
C_6H_{14}	0.0	0.0	0.0	0.0	0.0	0.0	0.0	0.0	0.0	0.0	31.8
C_7H_{16}	0.0	0.0	0.0	0.0	0.0	0.0	0.0	0.0	0.0	0.0	21.7
C_8H_{18}	0.0	0.0	0.0	0.0	0.0	0.0	0.0	0.0	0.0	0.0	8.1
C_9H_{20}	0.0	0.0	0.0	0.0	0.0	0.0	0.0	0.0	0.0	0.0	8.9
$C_{10}H_{22}$	0.0	0.0	0.0	0.0	0.0	0.0	0.0	0.0	0.0	0.0	3.4
$C_{11}H_{24}$	0.0	0.0	0.0	0.0	0.0	0.0	0.0	0.0	0.0	0.0	1.1
$C_{12}H_{26}$	0.0	0.0	0.0	0.0	0.0	0.0	0.0	0.0	0.0	0.0	0.4
$C_{13}H_{28}$	0.0	0.0	0.0	0.0	0.0	0.0	0.0	0.0	0.0	0.0	0.1
$C_{14}H_{30}$	0.0	0.0	0.0	0.0	0.0	0.0	0.0	0.0	0.0	0.0	0.0
$C_{15}H_{32}$	0.0	0.0	0.0	0.0	0.0	0.0	0.0	0.0	0.0	0.0	0.0
$C_{16}H_{34}$	0.0	0.0	0.0	0.0	0.0	0.0	0.0	0.0	0.0	0.0	0.0
$C_{17}H_{36}$	0.0	0.0	0.0	0.0	0.0	0.0	0.0	0.0	0.0	0.0	0.0
$C_{18}H_{38}$	0.0	0.0	0.0	0.0	0.0	0.0	0.0	0.0	0.0	0.0	0.0

$C_{19}H_{40}$	0.0	0.0	0.0	0.0	0.0	0.0	0.0	0.0	0.0	0.0	0.0
$C_{20}H_{42}$	0.0	0.0	0.0	0.0	0.0	0.0	0.0	0.0	0.0	0.0	0.0
$C_{21}H_{44}$	0.0	0.0	0.0	0.0	0.0	0.0	0.0	0.0	0.0	0.0	0.0
Stream	**S534**	**S535**	**S536**	**S537**	**S538**	**S539**	**S540**	**S541**	**S542**	**S543**	**S544**
Temperature, °F	853.6	307.4	109.4	109.4	109.4	129.7	109.4	109.4	337.9	190.6	364.3
Pressure, psia	135.7	135.7	132.3	128.1	128.1	140.7	128.1	128.1	128.1	15.0	17.9
Mass Flows, lb/h	10,825.0	10,825.0	10,825.0	434.9	421.9	421.9	13.0	10,390.1	10,390.1	785.4	9,604.7
O_2	0.0	0.0	0.0	0.0	0.0	0.0	0.0	0.0	0.0	0.0	0.0
N_2	0.0	0.0	0.0	0.0	0.0	0.0	0.0	0.0	0.0	0.0	0.0
H_2	350.0	350.0	350.0	348.6	338.2	338.2	10.5	1.4	1.4	1.4	0.0
CO	0.0	0.0	0.0	0.0	0.0	0.0	0.0	0.0	0.0	0.0	0.0
CO_2	0.0	0.0	0.0	0.0	0.0	0.0	0.0	0.0	0.0	0.0	0.0
H_2O	0.0	0.0	0.0	0.0	0.0	0.0	0.0	0.0	0.0	0.0	0.0
CH_4	0.2	0.2	0.2	0.1	0.1	0.1	0.0	0.0	0.0	0.0	0.0
C_2H_4	0.0	0.0	0.0	0.0	0.0	0.0	0.0	0.0	0.0	0.0	0.0
C_2H_6	1.1	1.1	1.1	1.0	0.9	0.9	0.0	0.1	0.1	0.1	0.0
C_3H_8	0.8	0.8	0.8	0.6	0.6	0.6	0.0	0.2	0.2	0.2	0.0
ARGON	0.0	0.0	0.0	0.0	0.0	0.0	0.0	0.0	0.0	0.0	0.0
METHANOL	0.0	0.0	0.0	0.0	0.0	0.0	0.0	0.0	0.0	0.0	0.0
C_3H_6	0.0	0.0	0.0	0.0	0.0	0.0	0.0	0.0	0.0	0.0	0.0
C_4H_8	0.0	0.0	0.0	0.0	0.0	0.0	0.0	0.0	0.0	0.0	0.0
C_5H_{10}	0.0	0.0	0.0	0.0	0.0	0.0	0.0	0.0	0.0	0.0	0.0
C_4H_{10}	3.4	3.4	3.4	1.8	1.8	1.8	0.1	1.6	1.6	1.6	0.0
C_5H_{12}	18.3	18.3	18.3	4.9	4.8	4.8	0.1	13.3	13.3	13.3	0.0
C_6H_{14}	294.8	294.8	294.8	32.7	31.8	31.8	1.0	262.1	262.1	262.1	0.0
C_7H_{16}	528.9	528.9	528.9	22.4	21.7	21.7	0.7	506.5	506.5	501.4	5.1
C_8H_{18}	547.1	547.1	547.1	8.3	8.1	8.1	0.3	538.8	538.8	5.4	533.4
C_9H_{20}	1,647.7	1,647.7	1,647.7	9.2	8.9	8.9	0.3	1,638.5	1,638.5	0.0	1,638.5
$C_{10}H_{22}$	1,730.4	1,730.4	1,730.4	3.5	3.4	3.4	0.1	1,727.0	1,727.0	0.0	1,727.0
$C_{11}H_{24}$	1,489.4	1,489.4	1,489.4	1.1	1.1	1.1	0.0	1,488.2	1,488.2	0.0	1,488.2
$C_{12}H_{26}$	1,278.2	1,278.2	1,278.2	0.4	0.4	0.4	0.0	1,277.8	1,277.8	0.0	1,277.8
$C_{13}H_{28}$	1,040.7	1,040.7	1,040.7	0.1	0.1	0.1	0.0	1,040.5	1,040.5	0.0	1,040.5
$C_{14}H_{30}$	790.1	790.1	790.1	0.0	0.0	0.0	0.0	790.1	790.1	0.0	790.1
$C_{15}H_{32}$	422.2	422.2	422.2	0.0	0.0	0.0	0.0	422.2	422.2	0.0	422.2
$C_{16}H_{34}$	279.5	279.5	279.5	0.0	0.0	0.0	0.0	279.5	279.5	0.0	279.5
$C_{17}H_{36}$	210.9	210.9	210.9	0.0	0.0	0.0	0.0	210.9	210.9	0.0	210.9

$C_{18}H_{38}$	128.6	128.6	128.6	0.0	0.0	0.0	0.0	128.6	128.6	0.0	128.6
$C_{19}H_{40}$	30.1	30.1	30.1	0.0	0.0	0.0	0.0	30.1	30.1	0.0	30.1
$C_{20}H_{42}$	24.6	24.6	24.6	0.0	0.0	0.0	0.0	24.6	24.6	0.0	24.6
$C_{21}H_{44}$	8.2	8.2	8.2	0.0	0.0	0.0	0.0	8.2	8.2	0.0	8.2
Stream	**S545**	**S546**	**S547**	**S548**	**S549**	**S550**	**S551**				
Temperature, °F	382.9	655.5	140.0	429.0	357.8	307.4	104.0				
Pressure, psia	17.9	17.9	17.9	15.0	15.0	15.0	15.0				
Mass Flows, lb/h	9,604.7	63.9	63.9	9,540.7	9,540.7	9,540.7	9,540.7				
C_7H_{16}	5.1	0.0	0.0	5.1	5.1	5.1	5.1				
C_8H_{18}	533.4	0.0	0.0	533.4	533.4	533.4	533.4				
C_9H_{20}	1,638.5	0.0	0.0	1,638.5	1,638.5	1,638.5	1,638.5				
$C_{10}H_{22}$	1,727.0	0.0	0.0	1,727.0	1,727.0	1,727.0	1,727.0				
$C_{11}H_{24}$	1,488.2	0.0	0.0	1,488.2	1,488.2	1,488.2	1,488.2				
$C_{12}H_{26}$	1,277.8	0.0	0.0	1,277.8	1,277.8	1,277.8	1,277.8				
$C_{13}H_{28}$	1,040.5	0.0	0.0	1,040.5	1,040.5	1,040.5	1,040.5				
$C_{14}H_{30}$	790.1	0.0	0.0	790.1	790.1	790.1	790.1				
$C_{15}H_{32}$	422.2	0.0	0.0	422.2	422.2	422.2	422.2				
$C_{16}H_{34}$	279.5	0.0	0.0	279.5	279.5	279.5	279.5				
$C_{17}H_{36}$	210.9	0.0	0.0	210.9	210.9	210.9	210.9				
$C_{18}H_{38}$	128.6	1.3	1.3	127.4	127.4	127.4	127.4				
$C_{19}H_{40}$	30.1	29.8	29.8	0.3	0.3	0.3	0.3				
$C_{20}H_{42}$	24.6	24.6	24.6	0.0	0.0	0.0	0.0				
$C_{21}H_{44}$	8.2	8.2	8.2	0.0	0.0	0.0	0.0				

Appendix E – Equipment List and Costing

Table E-1. Equipment list for the Inside Battery Limits (ISBL) Area (2020$).

ID	Equipment Name	# Req'd	# Spares	Scaling Stream	Base Case 1 Scale	Base Case 1 Installed Cost ($)	Base Case 2 Scale	Base Case 2 Installed Cost ($)
				Area 100: MSW Sorting and Preprocessing				
-	Feed conveyor	1	0	MSW feed	70 short tons/h	82,391	70 short tons/h	82,391
-	Shredder VVZ 250	1	0	MSW feed	70 short tons/h	1,483,069	70 short tons/h	1,483,069
-	Overband magnet	1	0	MSW feed	70 short tons/h	123,588	70 short tons/h	123,588
-	Waste screen	1	0	MSW feed	70 short tons/h	741,533	70 short tons/h	741,533
-	Air classifier	1	0	MSW feed	70 short tons/h	1,277,085	70 short tons/h	1,277,085
-	Overband magnet	1	0	MSW feed	70 short tons/h	123,588	70 short tons/h	123,588
-	ECS separator	1	0	MSW feed	70 short tons/h	823,927	70 short tons/h	823,927
-	ECS separator	1	0	MSW feed	70 short tons/h	823,927	70 short tons/h	823,927
-	Re-shredder	1	0	MSW feed	70 short tons/h	988,712	70 short tons/h	988,712
-	Material conveyor	1	0	MSW feed	70 short tons/h	82,391	70 short tons/h	82,391
-	Two-way baler	1	0			254,546		254,546
				Area 200: Gasification				
-	Scalehouse	1	0	Plasma gasification feed (S201)	1,000 short tons/day	1,065,593	1,000 short tons/day	1,065,593
-	Utility interconnect	1	0	Plasma gasification feed (S201)	1,000 short tons/day	3,196,779	1,000 short tons/day	3,196,779

ID	Equipment Name	# Req'd	# Spares	Scaling Stream	Base Case 1 Scale	Base Case 1 Installed Cost ($)	Base Case 2 Scale	Base Case 2 Installed Cost ($)
-	Plasma arc	1	1	Plasma gasification feed (S201)	1,000 short tons/day	116,788,990	1,000 short tons/day	116,788,990
-	Heat exchanger	1	0	Plasma gasification feed (S201)	1,000 short tons/day	14,492,064	1,000 short tons/day	14,492,064
-	Air separation package unit	1	0	Oxygen flowrate (S203)	391 tonne/day	21,252,757	391 tpd	21,252,757
Area 300: Syngas Cleanup and Conditioning								
E-301	HP steam superheater	1	0	Heat duty (E-301)	55,688,540 Btu/h	1,056,991	55,688,540 Btu/h	1,056,991
E-302	HP steam evaporator	1	0	Heat duty (E-302)	33,837,326 Btu/h	464,581	38,682,394 Btu/h	579,368
E-303	COS hydrolysis feed preheater	1	0	Heat duty (E-303)	11,047,019 Btu/h	73,268	11,047,019 Btu/h	132,346
E-305	LP steam evaporator	1	0	Heat duty (E-305)	14,883,193 Btu/h	119,814	15,808,146 Btu/h	199,183
E-306	Water cooler	1	0	Heat duty (E-306)	25,527,821 Btu/h	291,830	20,252,661 Btu/h	152,459
V-301	Water quench	1	0	Flowrate (S314+S309)	765,178 lb/h	152,459	765,178 lb/h	73,268
R-301	COS hydrolysis reactor	1	0	Flowrate (S315)	113,123 lb/h	9,354	113,123 lb/h	9,354
E-308	LP steam evaporator	1	0	Heat duty (E-308)	3,017,705 Btu/h	185,586	1,870,977 Btu/h	136,019
E-309	Water cooler	1	0	Heat duty(E-309)	7,345,932 Btu/h	241,644	4,554,478 Btu/h	177,105
C-301	Compressor	1	0	Compressor work(C-301)	11,889 hp	16,686,171	7,371 hp	11,383,349
E-307	Water cooler	1	0	Heat duty(E-307)	9,647,993 Btu/h	288,489	9,647,993 Btu/h	288,489
P-301	Water pump	1	1	Flowrate (S311)	652,054 lb/h	61,751	652,054 lb/h	61,751
V-302	Amine acid gas removal system	1	0	Flowrate(S319+S334)	11,701 lbmol/h	9,627,541	7,254 lbmol/h	6,726,810
V-303	Condenser	1	0	Flowrate(S321)	117,962 lb/h	45,221	73,136 lb/h	33,143

ID	Equipment Name	# Req'd	# Spares	Scaling Stream	Base Case 1 Scale	Base Case 1 Installed Cost ($)	Base Case 2 Scale	Base Case 2 Installed Cost ($)
-	Sulfur removal, LO-CAT	1	0		8 tonnes/day	29,178	5 tonnes/day	29,178
C-302	Dry syngas compresser	1	0	Flowrate (S323)	49,244 lb/hr	94,818	30,531 lb/hr	82,150
E-310	Gas-water shift feed preheater	1	0	Heat duty(E-310)	12,728,612 Btu/h	92,565	8,487,377 Btu/h	47,428
R-202	Water-gas shift reactor, fixed-bed, catalytic	1	0	Flowrate (S329)	90,452 lb/h	15,269	56,080 lb/h	15,269
E-311	MSW feed preheater	1	0	Heat duty(E-311)	12,543,561 Btu/h	90,355	12,543,561 Btu/h	90,355
E-312	LP steam evaporator	1	0	Heat duty(E-312)	11,256,820 Btu/h	75,578	1,617,037 Btu/h	3,076
E-313	Water cooler	1	0	Heat duty(E-313)	29,995,476 Btu/h	380,802	18,597,195 Btu/h	173,040
				Area 400: Methanol Synthesis				
C-401	Synthesis Gas 2nd Compressor	1	0	Compressor work (C-401)	2,287 hp	4,463,294	1,418 hp	3,044,871
C-401	Air fin intercooler	1	0	Cooling duty (C-401)	5,168,983 Btu/h	114,441	3,204,770 Btu/h	83,876
-	Purge gas expander stage 1	1	0	-	-1,651 hp	1,588,096	-1,651 hp	1,588,096
-	Expander Gas Superheater	1	0	-	409 ft2	280,972	409 ft2	280,972
C-402	Unreacted syngas recycle compressor	1	0	Compressor work (C-402)	535 hp	1,242,235	332 hp	847,468
-	Methanol Syn Feed / Effluent Recuperator	1	0	-	14,451 ft2	2,873,676	12,043 ft2	2,552,525
R-401	Methanol Synthesis Reactor	2	0	Flowrate(S408)	273,171 lb/h	12,627,078	273,171 lb/h	12,627,078
-	Methanol Syn Feed / Effluent Recuperator2	1	0	-	107 ft2	118,325	89 ft2	105,101
-	Methanol synthesis Effluent Water Cooler	1	0	-	5,792 ft2	1,586,109	4,827 ft2	1,408,851
V-403	Methanol Gas HP V-L Separator	1	0	Flowrate(S411)	273,171 lb/h	384,138	169,371 lb/h	281,547

ID	Equipment Name	# Req'd	# Spares	Scaling Stream	Base Case 1 Scale	Base Case 1 Installed Cost ($)	Base Case 2 Scale	Base Case 2 Installed Cost ($)
-	Intermediate Methanol Day Tank	3	0	-	325,000 gpd	1,258,996	100,056 gpd	585,409
				Area 500: Jet-Fuel Production and Separation				
E-501	Methanol to olefins reactor preheater	1	0	Heat duty(E-501)	28,304,325 Btu/h	1,052,858	17,548,672 Btu/h	790,323
R-501	Methanol to olefins (UOP/Hydro)	1	0	Flowrate(S506)	47,436 lb/h	9,350,672	29,410 lb/h	6,691,413
R-502	Combustor	1	0	Flowrate(S503)	6 kg/s	409,353	4 kg/s	300,022
C-501	Air compressor	1	0	Flowrate(S502)	45,399 lb/h	92,533	28,148 lb/h	80,171
E-502	Water cooler	1	0	Heat duty(E-502)	13,826,793 Btu/h	624,452	8,572,616 Btu/h	457,671
V-501	Gas liquid separator	1	0	Flowrate(S509)	47,057 lb/h	103,094	29,175 lb/h	75,560
C-502	Compressor	1	0	Flowrate(S518)	22,649 lb/h	75,110	14,042 lb/h	65,075
V-502	Gas liquid separator	1	0	Flowrate(S520)	22,439 lb/h	63,706	13,912 lb/h	46,691
P-501	Pump	1	0	Flowrate(S510)	24,409 lb/h	11,524	15,133 lb/h	9,984
	Reboiler	1	0	Distillation reboiler duty	5,115,953 Btu/h	801,336	3,171,888 Btu/h	587,312
	Condenser-air cooled	1	0	Distillation condenser duty	2,104,778 Btu/h	382,915	1,304,961 Btu/h	280,645
	Distillation Column	1	0	Distillation feed flowrate	24,688 lb/h	1,201,499	15,307 lb/h	880,606
T-501	Reflux Drum	1	0	Distillation reflux flowrate	69 gpm	162,228	60 gpm	147,309
E-503	Wastewater cooler	1	0	Heat duty(E-503)	2,223,990 Btu/h	190,400	1,378,873 Btu/h	139,547
E-504	Water cooler	1	0	Heat duty(E-504)	2,714,672 Btu/h	216,744	1,683,095 Btu/h	158,855
C-503	Compressor	1	0	Flowrate(S523)	29,424 lb/h	81,244	18,243 lb/h	70,390
R-503	Oligomerization Reactor	1	1	Flowrate(S525)	25,680 lb/h	969,052	15,922 lb/h	693,470
E-505	Oligomerization effluent Air Fin Cooler	1	0	Heat duty(E-505)	6 mmBtu/h	59,787	4 mmBtu/h	26,526

ID	Equipment Name	# Req'd	# Spares	Scaling Stream	Base Case 1 Scale	Base Case 1 Installed Cost ($)	Base Case 2 Scale	Base Case 2 Installed Cost ($)
	Light-Heavy Olefin Splitter Reboiler	1	0	Distillation reboile duty	12,666,598 Btu/h	1,444,579	7,853,295 Btu/h	1,058,756
	Light-Heavy Olefin Splitter Condenser-air cooled	1	0	Distillation condenser duty	12,357,377 Btu/h	1,209,959	7,661,576 Btu/h	886,799
	Light-Heavy Olefin Splitter Distillation Column	1	0	Distillation feed flowrate	25,680 lb/h	1,232,663	15,922 lb/h	903,451
T-502	Light-Heavy Olefin Splitter Reflux Drum	1	0	Distillation reflux flowrate	67 gpm	158,570	60 gpm	147,309
C-504	Recycle Compressor-sgl stg centr w motor drive	1	0	Flowrate(S538)	16 lb/h	6,488	16 lb/h	20,592
R-504	Hydrogenation Reactor	1	0	Flowrate(S534)	154 mmlb/y	5,447,585	96 mmlb/y	3,716,275
E-506	Effuent LP steam evaporator	1	0	Heat duty(E-506)	9,261,281 Btu/h	481,245	5,742,025 Btu/h	352,714
E-507	Effluent Air Cooler	1	0	Heat duty(E-507)	2,800,014 Btu/h	460,970	1,735,992 Btu/h	337,850
V-503	KO drum	1	0	Flowrate(S536)	18,353 lb/h	38,328	10,921 lb/h	27,352
E-508	Heat exchanger	1	0	Heat duty(E-508)	2,340,992 Btu/h	410,325	1,451,417 Btu/h	300,735
	Naphtha/Bio-Jet Reboiler	1	0	Distillation reboile duty	1,076,500 Btu/h	224,579	667,432 Btu/h	164,598
	Naphtha/Bio-Jet Condenser	1	0	Distillation condenser duty	741,731 Btu/h	56,679	459,874 Btu/h	41,541
	Naphtha/Bio-Jet Distillation Column	1	0	Distillation feed flowrate	17,615 lb/h	458,274	10,921 lb/h	335,878
T-503	Naphtha/Bio-Jet Reflux Drum	1	0	Distillation reflux flowrate	56 gpm	112,669	49 gpm	103,866
	Bio-Jet/Diesel Reboiler	1	0	Distillation reboile duty	2,514,410 Btu/h	389,801	1,558,938 Btu/h	285,692
	Bio-Jet/Diesel Condenser	1	0	Distillation condenser duty	721,501 Btu/h	55,670	447,331 Btu/h	40,801
T-504	Bio-Jet/Diesel Distillation Column	1	0	Distillation feed flowrate	16,284 lb/h	435,458	10,096 lb/h	319,148

ID	Equipment Name	# Req'd	# Spares	Scaling Stream	Base Case 1 Scale	Base Case 1 Installed Cost ($)	Base Case 2 Scale	Base Case 2 Installed Cost ($)
	Bio-Jet/Diesel Reflux Drum	1	0	Distillation reflux flowrate	52 gpm	107,213	49 gpm	103,866
E-512	Water cooler	1	0	Heat duty(E-512)	35,816 Btu/h	7,432	22,206 Btu/h	5,447
E-510	LP steam evaporator	1	0	Heat duty(E-510)	750,420 Btu/h	93,968	465,261 Btu/h	68,870
E-511	Water cooler	1	0	Heat duty(E-511)	1,867,571 Btu/h	169,965	1,157,896 Btu/h	124,571

HP = high pressure; LP = low pressure.

Pacific Northwest National Laboratory

902 Battelle Boulevard
P.O. Box 999
Richland, WA 99354

1-888-375-PNNL (7665)

www.pnnl.gov